International PrimeNet Workshop

September, 16 – 18, 2010, Lisbon, Portugal

Summary of Contributions

Contents

Introduction	1
η and η' Decays from Experimental and Theoretical Perspectives	3
Results on η/η' With KLOE S. Giovannella	5
Possibilities for η' Physics at JLab A. Starostin	8
A Preliminary Chiral Analysis of $\eta' \to \eta \pi \pi$ P. Masjuan	9
$\pi^0,\eta o \gamma\gamma$ and $\eta o 3\pi$ at Two Loops $K.\ Kampf$	11
Towards a Better Understanding of the Slope Parameter in $\eta \to 3\pi^0$ S. Schneider	12
Determination of Quark Masses: The Contribution of $\eta \to 3\pi$ G. Colangelo	14
A new Dispersive Analysis of $\eta \to 3\pi$ S. Lanz	15
The $\eta \to \pi^+\pi^-\pi^0$ Decay with WASA-at-COSY <i>P. Adlarson</i>	17
Radiative Corrections in $K \to \pi \ell^+ \ell^-$ and Related Decays B. Kubis	20
Electromagnetic Transitions from Vectors to Pseudoscalars $S.\ Leupold$	22
New Results on the $\eta - \eta'$ Transition FF's By BaBar A. Denig	25
Meson Dalitz Decays with WASA-at-COSY $J.~Klaja$	27
Study of Anomalous η Decays T. Petri	29
Analysis of $\eta \to \pi^+\pi^-\gamma$ Measured with the WASA Facility at COSY C. F. Redmer	31

Meson Production in Photo Reactions and from Light Ion Collisions	33
η Production in Nucleon-Nucleon Collisions $C.$ Wilkin	35
Photon Induced Measurements B. Krusche	37
Meson Decays at MAMI–C - Results and Perspectives $M.\ Unverzagt$	40
HADES Results from NN Reactions and Perspectives for πN B. Ramstein	42
Comparative Studies of η and η' Mesons at COSY-11 Detector Setup $P.\ Klaja$	44
Direct Determination of the η' Meson Width E. Czerwiński	46
Some Open Issues in η and η' Photoproduction K. Nakayama	48
The $pd \rightarrow ^3 \mathrm{He} \eta \ \pi^0$ Reaction at $T_p = 1450 \ \mathrm{MeV}$ K. Schönning	50
Investigation of Double Pion Production in pp Collisions at $T_p=1400~{ m MeV}$ $T.~Tolba$	52
$\gamma\gamma$ physics with the KLOE experiment <i>C. Taccini</i>	55
A covariant formalism for the $\gamma^* N \to N^*$ transitions G. Ramalho	57
What do we learn from the ABC? H. Clement	59
Interaction of η and η' with Nucleons and Nuclei	61
Use of $\pi^+d \to \eta pp$ to Study the ηN Amplitude Near Threshold H. Garcilazo and M. T. Peña	63
Search for η -mesic nuclei at J-PARC H. Fujioka	65
Search for η Bound States in Nuclei H. Machner	67
Search for η -mesic ⁴ He with WASA-at-COSY W. Krzemień	70
List of Participants	73

Introduction

This workshop is part of the activities in the project "Study of Strongly Interacting Matter" (acronym HadronPhysics2), which is an integrating activity of the Seventh Framework Program of EU. This HP2 project contains several activities, one of them being the network PrimeNet having the focus on Meson Physics in Low-Energy QCD. This network is created to exchange information on experimental and theoretical ongoing activities on mainly η and η' physics at different European accelerator facilities and institutes.

Although by the end of the 1970's quantum chromodynamics (QCD) was established as the theory of the strong interaction, we still have only little understanding of various possible forms of confined quark states and their decays, and today there is vast area of research on hadrons, in particular mesons and their interactions, still to be explored. The talks presented at the workshop showed that experimental collaborations in this field have been crucial for recent advances. In particular, the study of η and η' decays is opening up a new era of precision to the determination of the light quark mass difference, along with information on $\pi\pi$ and $\pi\eta$ interactions. From the theoretical side, the progress achieved through Chiral Perturbation Theory (ChPT) and Large-N_c ChPT may now be tested, while lattice calculations are already providing the first ground-breaking results. On the other hand, strong and electromagnetic probing of meson-baryon interactions progressed tremendously with new and powerful detecting techniques.

The present workshop included the three general topics:

- 1. η and η' decays from experimental and theoretical perspectives.
- 2. Meson production in photo reactions and from light ion collisions.
- 3. Interaction of η and η' with nucleons and nuclei including η bound states.

The different talks covered the very recent achievements in each field from the experimental facilities KLOE at DAPHNE, Crystal Ball at MAMI, Crystal Ball and TAPS at Elsa and WASA-at-COSY as well as from different theory institutes. Viewgraphs from each talk can be found on the PrimeNet homepage http://www.fz-juelich.de/ikp/primenet

The detailed program was arranged by a program committee having the members: Reinhard Beck, Johan Bijnens, Simona Giovannella, Dieter Grzonka, Christoph Hanhart, Bo Höistad, Bastian Kubis, Andrzej Kupsc, Hartmut Machner, Pawel Moskal, Eulogio Oset, Micheal Ostrick, Teresa Peña, Susan Schadmand.

The workshop was held in Sept 16-18, 2010, at the campus of Instituto Superior Técnico, enjoying kind hospitality and support from IST, Lisboa, Portugal.

Financial support is gratefully acknowledged from the European Commission under the 7th Framework Programme through the 'Research Infrastructures' action of the 'Capacities' Programme; Call: FP7-INFRASTRUCTURES-2008-1, Grant Agreement N. 227431.

Bo Höistad, Teresa Peña and Christoph Redmer

η and η' Decays

from Experimental and Theoretical Perspectives

RESULTS ON η/η' WITH KLOE

SIMONA GIOVANNELLA* for the KLOE Collaboration

1.1 Introduction

From 2000 to 2006, the KLOE experiment collected 2.5 fb⁻¹ of e^+e^- collisions at the ϕ peak and about 240 pb⁻¹ below the ϕ resonance ($\sqrt{s}=1$ GeV). The whole data set includes 1×10^8 η 's and 5×10^5 η' 's produced through the radiative decays $\phi\to\eta\gamma/\eta'\gamma$ and tagged by means of the monochromatic recoil photon.

1.2 $\eta \to \pi\pi\pi$

The dynamics of $\eta \to \pi\pi\pi$ is sensitive to the u-d quark mass difference. A precise study of this decay can lead to a very accurate measurement of $Q^2 = (m_s^2 - \hat{m}^2)/(m_d^2 - m_u^2)$. At KLOE, the background for both charged and neutral final states is at the level of few per mil [1, 2]. The conventional Dalitz plot variables for the $\pi^+\pi^-\pi^0$ final state are $X \propto T_+ - T_-$ and $Y \propto T_0$, where T is the kinetic energy of the pions. The measured distribution is parametrized as: $|A(X,Y)|^2 = 1 + aY + bY^2 + cX + dX^2 + eXY + fY^3$. As expected from C parity conservation, the odd powers of X are consistent with zero. The other parameters are measured with an accuracy between 0.5 to 10%. C parity conservation has been tested also by measuring the left-right, quadrants and sextants charge asymmetries: all of them are consistent with zero at 10^{-3} level, thus improving existent evaluations obtained combining different experiments. In the $\eta \to \pi^0\pi^0\pi^0$ decay, the Dalitz plot density is described by a single parameter α : $|A(z)|^2 \propto 1 + 2\alpha z$, where z is related to the three pion energies in the η rest frame. Photons are paired to form π^0 's after kinematically constraining the total four-momentum to M_ϕ to improve the energy resolution. Three samples, with different efficiency and purity on photon pairing have been analyzed. The resulting value for α is: $\alpha = -0.0301 \pm 0.0035_{\rm stat} + 0.0022_{\rm colour}$

1.3 $\eta \to \pi^+\pi^-\gamma$

The $\eta \to \pi^+\pi^-\gamma$ decay provide a good tool to investigate the box anomaly, a higher term of Wess-Zumino-Witten Lagrangian. The invariant mass of the pions is a good observable to disentangle this contribution from other possible resonant ones, e.g. from the ρ -meson. Recently the CLEO collaboration published their results on the ratio $\Gamma(\eta \to \pi^+\pi^-\gamma)/\Gamma(\eta \to \pi^+\pi^-\pi^0)$, which differ more than $3\,\sigma$'s from old results [3]. From the analysis of 1.2 fb⁻¹, the preliminary KLOE measurement of the same ratio is: $\Gamma(\eta \to \pi^+\pi^-\gamma)/\Gamma(\eta \to \pi^+\pi^-\pi^0) = 0.2014 \pm 0.0004_{\rm stat} \pm 0.0060_{\rm stat}$. The final systematic error, under evaluation, is expected to be less than 1%. Our number is in agreement with the old results and differs significantly from recent CLEO measurement.

1.4
$$\eta \to \pi^+\pi^-e^+e^-/e^+e^-e^+e^-$$

The $\eta \to \pi^+\pi^-e^+e^-$ decay allows to probe the structure of the η meson, to compare the predictions of the branching ratio value based on Vector Meson Dominance model and Chiral Perturbation

^{*}Laboratori Nazionali di Frascati dell'INFN, via Enrico Fermi 40, 00044 Roma, Italy, si-mona.giovannella@lnf.infn.it

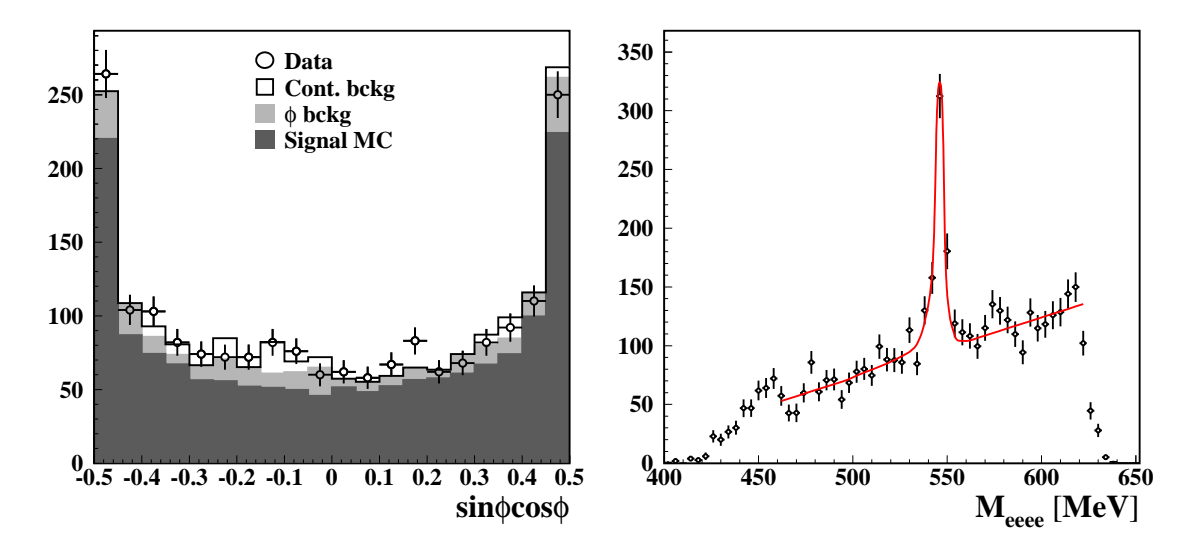


Figure 1.1: Left: angular asymmetry between pions and electrons decay planes for $\eta \to \pi^+\pi^-e^+e^-$ events. Data (dots) are compared with the expected distribution in case of null A_{ϕ} value for the signal. Right: fit to the four electron invariant mass for events $\eta \to e^+e^-e^+e^-$.

Theory and to study CP violation beyond the prediction of the Standard Model by measuring the angular asymmetry between pions and electrons decay planes [4]. The analysis has been performed on 1.73 fb⁻¹ [5]. Background contribution is evaluated performing a fit on the sidebands of the $\pi^+\pi^-e^+e^-$ invariant mass with background shapes. For the signal estimate the η mass region ([535, 555] MeV) is considered, performing the event counting after background subtraction. The resulting number of signal events, $N_{\pi\pi ee}=1555\pm52$, is used to extract the branching ratio: BR($\eta \to \pi^+\pi^-e^+e^-\gamma$) = (26.8 ± 0.9_{stat} ± 0.7_{syst}) × 10⁻⁵. The decay plane asymmetry A_ϕ is defined as the sign asymmetry of the quantity $\sin\phi \cdot \cos\phi$, ϕ being the angle between the pion and the electron planes in the η rest frame. It has been evaluated for the events in the signal region after background subtraction. The value obtained is: $A_\phi = (-0.6 \pm 2.5_{\rm stat} \pm 1.8_{\rm syst}) \times 10^{-2}$. This is the first measurement of this asymmetry. The distribution of the $\sin\phi\cos\phi$ variable is shown in the left panel of Fig. 1.1.

With the same data sample, the $\eta \to e^+e^-e^+e^-$ decay has been studied. Events with four electrons are selected using time of flight information provided by the calorimeter. The number of signal events is obtained by fitting the data distribution of the four electron invariant mass, M_{eeee} , with signal and background shapes (Fig. 1.1-right). From the fit we extract $N_{\eta \to e^+e^-e^+e^-} = 413 \pm 31$. This constitutes the first observation of this decay.

1.5 Search for gluonium in η'

The η' meson, being almost a pure SU(3) singlet, is a good candidate for a sizeable gluonium content. In this hypothesis, the η and η' wave functions can be written in terms of the u,d quark wave function the strange component and the gluonium [6]. From the study of $\phi \to \eta' \gamma \to \pi^+ \pi^- 7 \gamma$'s and $\phi \to \eta \gamma \to 7 \gamma$'s decays, the ratio $R_\phi = BR(\phi \to \eta' \gamma)/BR(\phi \to \eta \gamma)$ has been measured [7]: $R_\phi = (4.77 \pm 0.09_{\rm stat} \pm 0.19_{\rm syst}) \times 10^{-3}$. Combining our result with other experimental constraints and using the corresponding SU(3) relations between decay modes, we found a 3σ evidence for gluonium content in η' [8].

1.6 $\phi \rightarrow \eta e^+ e^-$

Pseudoscalar production at the ϕ factory associated to internal conversion of the photon into a lepton pair allows the measurement of the form factor $\mathcal{F}_P(q_1^2 = M_\phi^2, q_2^2 > 0)$ of pseudoscalar mesons P in the kinematical region of interest for the VMD model. The only existing data on

 $\phi \to \eta e^+ e^-$ come from the SND experiment at Novosibirsk which has measured the M_{ee} invariant mass distribution on the basis of 213 events [9]. At KLOE, a preliminary study of this decay has been performed on 213 pb⁻¹ (about 1/10 of the total luminosity) using the $\eta \to \pi^+\pi^-\pi^0$ final state. Simple analysis cuts provide ~ 2000 signal events with very small residual background contamination (Fig. 1.2). The extraction of the branching fraction and the study of the form factor is under way. The analysis will be extended to the whole data set.

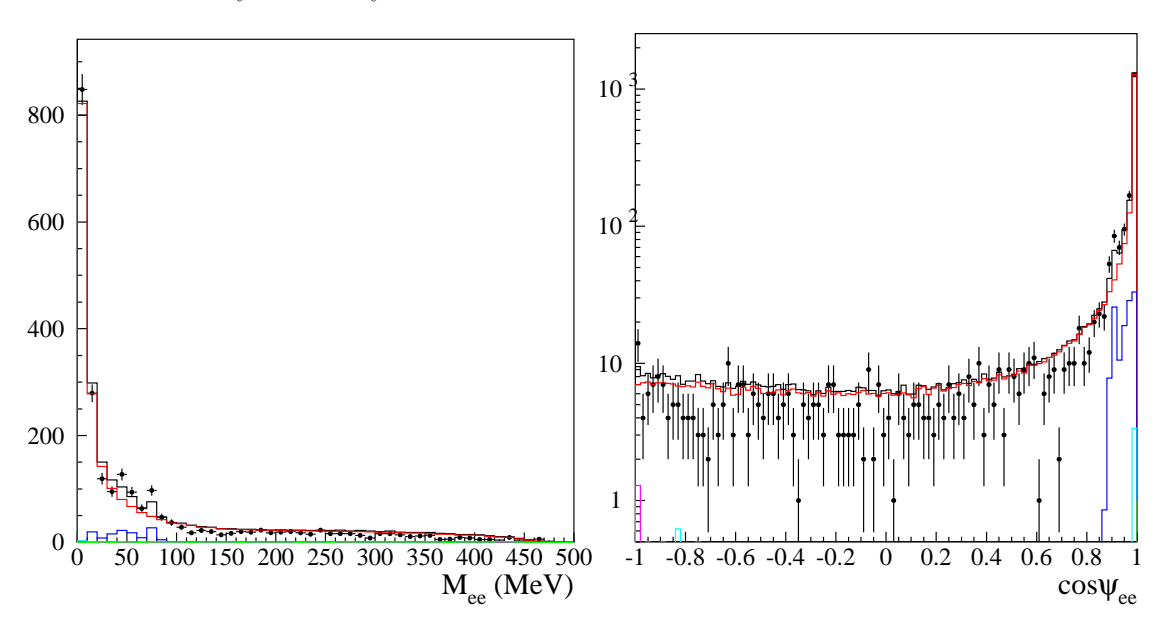


Figure 1.2: Invariant mass (left) and 3-dimensional opening angle (right) of e^+e^- pairs for $\phi \to \eta e^+e^-$ events. Dots: data, black: total MC shape, red: MC signal, other colours: residual background.

- [1] F. Ambrosino et al. [KLOE Collaboration], JHEP 05 (2008) 006.
- [2] F. Ambrosino et al. [KLOE Collaboration], arXiv:1004.1319, to be published on Phys. Lett. B.
- [3] A. Lopez et al [CLEO Collaboration], Phys. Rev. Lett. 99 (2007) 122001.
- [4] D. N. Gao, Mod. Phys. Lett. A 17 (2002) 1583.
- [5] F. Ambrosino et al. [KLOE Collaboration], Phys. Lett. B 675 (2009) 283.
- [6] J. L. Rosner, Phys. Rev. D 27 (1983) 1101.
- [7] F. Ambrosino et al. [KLOE Collaboration], Phys. Lett. B 648 (2007) 267.
- [8] F. Ambrosino et al. [KLOE Collaboration], JHEP 07 (2009) 105.
- [9] M. N. Achasov et al. [SND Collaboration], Phys. Lett. B 504 (2001) 275.

POSSIBILITIES FOR η' PHYSICS AT JLab

ALEKSANDER STAROSTIN*

Decay $\eta' \to \eta \pi \pi$ is a unique source of information on $\eta - \pi$ interactions; $\eta' \to e^+ e^- \gamma$ gives access to the electromagnetic transition form factor of η' , which is an essential contribution to the value of the muon anomalous magnetic moment, g-2, predicted by the Standard Model. There is a long list of η' decays allowing to test discrete symmetries C, P and CP in search for physics beyond the Standard Model. Our present knowledge of η' decays is based on experimentas with very limited statistics, therefore new high statistics measurements will be important.

The η' photoproduction cross section has a strong maximum between 1.6 GeV and 2.3 GeV photon beam energy. A high intensity tagged photon beam in this energy range is available at the JLab Hall-B, where the CLAS detector is installed [1]. Currently, CLAS is a magnetic spectrometer with toroidal field equipped with high resolution time-of-flight system, several layers of drift chambers, forward electromagnetic calorimeter and a gas Cerenkov detector in front of the calorimeter. It provides good acceptance and excellent momentum resolution for charged particles and some acceptance for photons. Electrons and positrons can be separated from π^-/π^+ only for forward angles covered by the Cerenkov detector. There are two CLAS data sets which can be used to extract information on some decay modes of η' . The g11 and g12 runs were taken by the CLAS collaboration in 2004 and 2009 using the high intensity beam of tagged photons. In these two runs the beam with maximum energy about 5.7 GeV was incident on 40 cm long liquid hydrogen target installed slightly upstream in respect to the center of the CLAS detector. The data allow reliable identification of $\eta' \to \eta \pi^+ \pi^-$, $\eta' \to \pi^0 \pi^+ \pi^-$, $\eta' \to \pi^+ \pi^- \pi^+ \pi^-$ and some other decay modes. In the cases when one neutral particle is involved this particle can be identified by its missing mass. A preliminary analysis of the g11 data set indicates that about $10^5 \eta'$ were produced with about $2\times10^5 \eta' \to \eta\pi^+\pi^-$ and $5000 \eta' \to \pi^0\pi^+\pi^-$ events reconstructed. This statistics potentially allows to investigate the Dalitz plot of the decays although the detector acceptance is highly asymmetric in respect to the positively and the negatively charged particles. A substantial drawback of the g11 data set is that the gas Cerenkov detector was switched off for the run. This problem was fixed in the g12 run allowing identification of the η' Dalitz decays, specifically $\eta' \to e^+e^-\gamma$. The statistical accuracy of the existing data for this decay mode is extremely poor so the new CLAS data can improve the existing data sample substantially allowing a detailed investigation of the transition from factor of η' . The analysis of the data is underway.

A new experimental hall, Hall-D, will be available at JLab after completion of the 12 GeV upgrade in 2015. The hall will be equipped with GlueX detector and a beam of tagged photons with maximum energy up to 12 GeV. The detector will provide high acceptance and resolution for both, charged and neutral particles, and will be used as a universal setup for meson spectroscopy at JLab. This setup can also be used for η/η' physics and we anticipate that significant amount of new data will became available once the GlueX will start its operation.

Bibliography

[1] B. A. Mecking et al. (CLAS), Nucl. Instrum. Meth. **A503**, 513 (2003).

 $^{^*}$ University of California Los Angeles, starost@ucla.edu

A PRELIMINARY CHIRAL ANALYSIS OF

$\eta' o \eta \pi \pi$.

The Role of Final State Interactions.

PERE MASJUAN*

1.1 Introduction

The decays $\eta' \to \eta \pi \pi$ are interesting because, due to the quantum numbers of the pseudoscalar mesons involved, if the decay proceeds through resonances these can be mostly of scalar nature, G-parity prevents vectors to contribute, intended for the analysis of the properties of the $f_0(600)$ (or σ) resonance (even though the $a_0(980)$ is also present and indeed dominant) [1]. Also, the presence of η and η' in this reaction is ideal for studying the mixing properties of both mesons. Finally, this decay allows to test Chiral Perturbation Theory (ChPT) and its possible extensions such as Large- N_c ChPT and Resonance Chiral Theory (RChT). For all that, precision measurements on η and η' would be very helpful and provide useful information in our understanding of low energy QCD.

Chiral Perturbation Theory (ChPT) [2] is the low energy effective theory of Quantum Chromodynamics (QCD). It is described in terms of an octet of pseudoscalar bosons appearing in the theory as a result of the spontaneous breaking of the chiral symmetry of QCD which are identified with the lightest hadronic states (π, K, η) . To include the pseudoscalar singlet η_1 one should apply the large N_c limit. Then, a simultaneous expansion in p^2 , m_q and $1/N_c$ is possible and the interactions among the (π, K, η, η') mesons are in principle well described [3]. In addition, large N_c ChPT does not include resonances as external states. The effects of these resonances are then virtual and encoded in the low energy constants (LECs) of the chiral Lagrangian. However, when the energy of the process is of the order of the resonance mass, the perturbative expansion of ChPT fails and the resonant effects must be taken explicitly. This is accounted for in Resonance Chiral Theory (RChT) [4], where the interactions of the pseudoscalar mesons are supplemented with new interactions among these and nonets of vectors, axials, scalars, representing the ρ , a_1 , σ , etc., in a minimal way.

From the experimental side, large effort has been done to obtain an accurate value for the Branching ratio of this decay [5] and also the Dalitz plot parameters are of interest, see Table 1.1.

1.2 The Role of Final State Interactions

At Leading Order (LO) in large– N_c ChPT, the prediction of the Branching ratio is completely off the experimental value: the LO predicts 0.9% to be compared with the PDG value 43.2%, [5]. This result can be improved by studying the Next to Leading Order (NLO) that predicts 64.4%, still off but in the right direction. It turns out that at NLO, the amplitude is basically dominated by a certain LECs combination, $3L_2 + L_3$. This combination can be predicted by using the experimental Branching ratio and then, reexpanding, obtain the Dalitz plot parameters. One could estimate what is missing when computing the amplitude only at NLO by a unitarization process, [1]. This process evaluates the role of final state interactions indicating the presence of the σ meson in the s-channel. The N/D unitarization method [8] for this decay produces very accurate results for the Dalitz plot parameters, shown in Table 1.2.

1.2.1 Acknowledgments

I would like to thank the organizers for the nice atmosphere during the conference. This work has been supported by the EU contract MRTN-CT-2006-035482 (FLAVIAnet), by MICINN, Spain (FPA2006-05294) and the Spanish Consolider-Ingenio 2010 Programme CPAN (CSD2007-00042) and by Junta de Andalucía (Grants P07-FQM 03048 and P08-FQM 101).

^{*}Departamento de Física Teórica y del Cosmos, Universidad de Granada. masjuan@udg.es

Parameter	Exp. $[\eta' \to \eta \pi^0 \pi^0]$	Exp. $[\eta' \to \eta \pi^+ \pi^-]$
	GAMS- 4π [6]	VES [7]
a	$-0.066 \pm 0.016 \pm 0.003$	$-0.127 \pm 0.016 \pm 0.008$
b	$-0.063 \pm 0.028 \pm 0.004$	$-0.106 \pm 0.028 \pm 0.014$
c	$-0.107 \pm 0.096 \pm 0.003$	$+0.015 \pm 0.011 \pm 0.014$
d	$+0.018 \pm 0.078 \pm 0.006$	$-0.082 \pm 0.017 \pm 0.008$

Table 1.1: Experimental Dalitz slope parameters for $\eta' \to \eta \pi^0 \pi^0$ (second column) and $\eta' \to \eta \pi^+ \pi^-$ (fourth column), respectively.

	$large-N_cChPT$	$large-N_cRChT$	$large-N_cRChT$
	N/D method	N/D method	J = 2 reson. $+N/D$ method
${\mathfrak B}_{\eta' o\eta\pi^+\pi^-}$	$43.2\%^{\dagger}$	$43.2\%^{\dagger}$	$43.2\%^{\dagger}$
a[Y]	$-0.098(48)^{\dagger}$	$-0.098(48)^{\dagger}$	$-0.098(48)^{\dagger}$
b $[Y^2]$	-0.047(8)	-0.0297(8)	- 0.0332(5)
$d[X^2]$	-0.093(5)	-0.0573(4)	-0.0718(3)
$\kappa_{21} [X^2 Y]$	0.002(3)	-0.010(1)	-0.009(2)
$\kappa_{40} [X^4]$	0.0023(2)	0.0009(1)	0.0013(1)
$(3L_2 + L_3) \times 10^3$	1.03(5)	_	_
$c_d \; (\mathrm{MeV})$		26.6(7)	24.8(8)
C-constant	$-1.24 \le C \le -0.12$	$2.06 \le C \le 3.37$	$1.38 \le C \le 2.74$

Table 1.2: Dalitz parameters of the decay $\eta' \to \eta \pi^+ \pi^-$ for the N/D-unitarization of the large- N_c χ PT (second column) and large- N_c R χ T amplitude (third and fourth columns). $3L_2 + L_3$, c_d and C are fixed using the experimental Branching Ratio and the Dalitz plot parameter a, marked with \dagger . The last column shows the result if one also takes into account the the impact of J=2 resonances in the R χ T framework. To compare with experimental data, see Table 1.1.

- [1] R. Escribano, P. Masjuan and J.J. Sanz-Cillero, [arXiv:152708 [hep-ph,nucl-th]; P. Masjuan, PoS C **D09** (2009) 117 [arXiv:0910.0140 [hep-ph]].
- [2] J. Gasser and H. Leutwyler, Nucl. Phys. B **250** (1985) 465.
- [3] R. Kaiser and H. Leutwyler, Eur. Phys. J. C 17, 623 (2000) [hep-ph/0007101].
- [4] G. Ecker, J. Gasser, A. Pich and E. de Rafael, Nucl. Phys. B 321 (1989) 311.
- [5] C. Amsler et al. [Particle Data Group], Phys. Lett. B 667 (2008) 1.
- [6] A. M. Blik et al., Phys. Atom. Nucl. 72 (2009) 231 [Yad. Fiz. 72 (2009) 258].
- [7] V. Dorofeev et al., Phys. Lett. B 651 (2007) 22 [arXiv:hep-ph/0607044].
- [8] J.A. Oller and E. Oset, Phys. Rev. D **60** (1999) 074023 [arXiv:hep-ph/9809337].

π^0 , $\eta \to \gamma \gamma$ AND $\eta \to 3\pi$ AT TWO LOOPS

KAROL KAMPF*, JOHAN BIJNENS*

All three presented processes $\pi^0 \to \gamma\gamma$, $\eta \to \gamma\gamma$ and $\eta \to 3\pi$ (in fact four processes if we distinguish $\pi^0\pi^0\pi^0$ and $\pi^0\pi^+\pi^-$ in the latter) represent important tools for studying basic phenomena of the underlying theory: quantum chromodynamics (QCD). The first two played an important role in understanding a symmetry pattern of the theory as they are directly connected with the so-called $U(1)_A$ anomaly. QCD enlarged by photons possesses, however, two such anomalies. The first one, internal, connected with QCD only, proportional to gluonic term $G_{\mu\nu}\tilde{G}^{\mu\nu}$, dubbed U(1)problem and the resulting strong CP problem is still an open issue. As a remnant of the anomaly, the η' plays a more important role than naively expected and has to be included in a theoretical consideration. The second anomaly, external, in our case connected with electromagnetic interaction (or $F_{\mu\nu}\tilde{F}^{\mu\nu}$) explains why $\pi^0 \to \gamma\gamma$ can decay so quickly even it should be suppressed due to Sutherland's theorem. On the other hand, the two last processes represent 95% of all η -decay modes and are thus perfectly suited to study directly properties of η which is one of the main tasks of PrimeNet. Simultaneous treatment of two-photon π^0 and η decays, apart from testing or fixing our understanding of η' , can provide valuable information on the decay constants F_{π} and F_{η} or quark mass ratios (e.g. $R = \frac{m_d - m_u}{m_s - \hat{m}}$). It is well known that there are no chiral logarithms for these decays generated by one-loop diagrams [1] which motivate the necessity to go to two-loop order [2]. This order is also inevitable for $\eta \to 3\pi$ as was performed in the framework of chiral perturbation theory (ChPT) in [3]. The discrepancy with present measurements [4] is a motivation for a new dispersive study (see [5] and references therein). There are two remarks to make. The first, connected with the fact that $\eta \to 3\pi$ as forbidden in isospin limit is a good candidate for extracting of $m_d - m_u$ parameter (e.g. R). The dispersive method, however powerful based only on very general assumptions, has to rely at some point on ChPT to extract such a parameter. First analyses show that how we perform this matching is very crucial and has big impact on R(or other physical parameters). Another remark concerns the absolute value of the partial decay width for $\eta \to 3\pi$. Experimentally it is obtained via normalization to $\eta \to \gamma\gamma$. Change in one decay width has thus influence in other (a change by 1\% in $\Gamma(\eta \to \gamma \gamma)$ input shifts R by ≈ 0.2).

To summarize all three decay modes of π^0 and η are important for basic properties of QCD and as they are closely interconnected it is desirable to study them simultaneously at appropriate order. First results of these calculations were presented.

- J. F. Donoghue, B. R. Holstein and Y. C. R. Lin, Phys. Rev. Lett. 55 (1985) 2766 [Erratumibid. 61 (1988) 1527];
 J. Bijnens, A. Bramon and F. Cornet, Phys. Rev. Lett. 61 (1988) 1453.
- [2] K. Kampf and B. Moussallam, Phys. Rev. D 79 (2009) 076005 [arXiv:0901.4688 [hep-ph]];
 J. Bijnens and K. Kampf, arXiv:1009.5493 [hep-ph] and in prep.
- [3] J. Bijnens and K. Ghorbani, JHEP **0711** (2007) 030 [arXiv:0709.0230 [hep-ph]].
- [4] see e.g. contributions by M. Unverzagt and S. Giovannella
- [5] M. Zdrahal, K. Kampf, M. Knecht and J. Novotny, PoS C D09 (2009) 122 [arXiv:0910.1721 [hep-ph]] and in prep.; G. Colangelo, S. Lanz and E. Passemar, PoS C D09 (2009) 047 [arXiv:0910.0765 [hep-ph]] and contribution of S. Lanz here.

^{*}Department of Astronomy and Theoretical Physics, Lund University, Sölvegatan 14A, SE 223-62 Lund, Sweden

TOWARDS A BETTER UNDERSTANDING OF THE SLOPE PARAMETER IN $\eta \to 3\pi^0$

SEBASTIAN P. SCHNEIDER*, BASTIAN KUBIS AND CHRISTOPH DITSCHE

The isospin-breaking decay $\eta \to 3\pi$ is an ideal tool to extract information on light quark mass ratios from experiment. For precise determinations, however, a detailed theoretical and experimental understanding of the Dalitz plot distribution is essential. While experimentally agreed upon, the slope parameter α of the neutral decay channel raises some question marks from a theoretical point of view. Chiral perturbation theory (ChPT) at next-to-leading [1] (one loop, $\mathcal{O}(p^4)$) and next-to-next-to-leading [2] (two loops, $\mathcal{O}(p^6)$) predicts a positive sign, in strong disagreement with the world average [3] of $\alpha = -0.0317 \pm 0.0016$ (see also Fig. 1). A dispersive approach [4] predicts the correct sign, but still misses the experimental value substantially. We use the modified non-relativistic effective field theory (NREFT) approach [5] as a diagnostic tool in order to understand these discrepancies [6].

In Dalitz plot analyses experimental data is fitted to the squared amplitude, which for the charged and neutral $\eta \to 3\pi$ decay channels is expanded in polynomial terms according to

$$|\mathcal{M}_{c}(x,y)|^{2} = |\mathcal{N}_{c}|^{2} \left\{ 1 + ay + by^{2} + dx^{2} + \dots \right\}, \qquad |\mathcal{M}_{n}(z)|^{2} = |\mathcal{N}_{n}|^{2} \left\{ 1 + 2\alpha z + \dots \right\},$$

$$x = \frac{\sqrt{3}(u-t)}{2M_{\eta}Q_{\eta}}, \qquad y = \frac{3(s_{n}-s)}{2M_{\eta}Q_{\eta}}, \qquad z = x^{2} + y^{2}, \qquad Q_{\eta} = M_{\eta} - 3M_{\pi}, \quad (1)$$

where the amplitudes are related by isospin symmetry (in Condon-Shortley phase convention),

$$\mathcal{M}_n(s,t,u) = -\mathcal{M}_c(s,t,u) - \mathcal{M}_c(t,u,s) - \mathcal{M}_c(u,s,t) . \tag{2}$$

In order to determine the coefficients of the polynomial in Eq. (1), we use NREFT, which is ideally suited to describe final-state interactions among the pions and has been applied to the precise extraction of $\pi\pi$ scattering lengths from experiment [5]. One of the great advantages of NREFT is the fact that the decay amplitude can be parameterized directly in terms of $\pi\pi$ threshold parameters, so that we can implement physical scattering lengths, effective ranges, etc., instead of expanding them in terms of quark masses (as is the case in ChPT). Furthermore, we obtain fully covariant results with the correct thresholds in the physical region. In that respect the term "non-relativistic" only summarizes the fact that we neglect inelasticities outside the physical region.

The low-energy coupling constants of the non-relativistic theory are not determined a priori and have to be determined otherwise. For the tree-level decay constants this is done by matching to ChPT at $\mathcal{O}(p^4)$. To fix the $\pi\pi$ final-state interactions we match to the low-energy representation of the $\pi\pi$ scattering amplitude. Numerically we thus obtain for the slope parameter [6],

$$\alpha = -0.025 \pm 0.005 \;, \tag{3}$$

where the error stems from varying between two sets of threshold parameters from phenomenological analyses [7] and from estimating higher-order contributions by partial unitarization. Our result is considerably closer to the experimental determination than previous analyses and it is interesting to note that while tree-level and one-loop diagrams give a positive contribution to α , a large negative shift is induced by the inclusion of the two-loop bubble diagrams. Our result is compared to several other theoretical and experimental determinations in Fig. 1.

Within our approach it is also possible to understand the ChPT determination of α . For that we "simulate" the ChPT result by inserting $\pi\pi$ rescattering vertices only up to $\mathcal{O}(p^2)$ in the two-loop graphs and up to $\mathcal{O}(p^4)$ in the one-loop graphs. We find $\alpha_{\text{ChPT}} = -0.0011$, which is

^{*}Helmholtz-Institut für Strahlen- und Kernphysik and Bethe Center for Theoretical Physics, Universität Bonn, e-mail: schneider@hiskp.uni-bonn.de

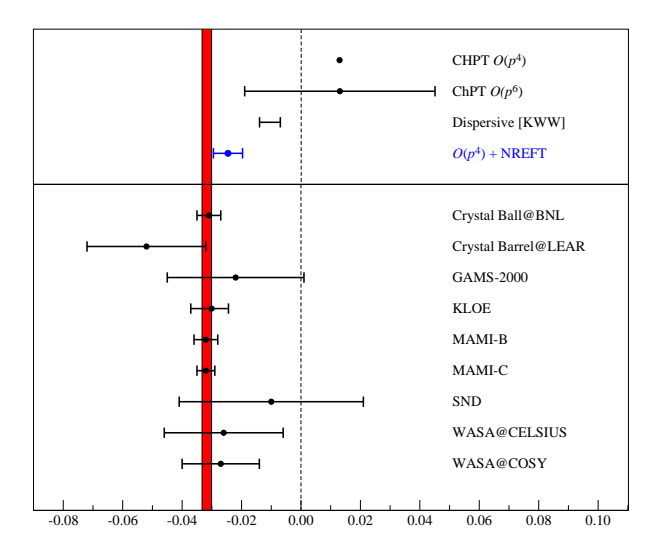


Figure 1: Comparison of values for the slope parameter α . Top: theoretical predictions. Bottom: experimental determinations. The red shaded area is the particle data group average [3].

very close to zero and shifted strongly from our initial result in Eq. (3). This discrepancy can be attributed to the significantly weaker $\pi\pi$ rescattering.

By means of the isospin relation (2), one can relate charged and neutral Dalitz plot parameters,

$$\alpha = \frac{Q_n^2}{4Q_c^2} \left(b + d - \frac{a^2}{4} \right) - \zeta_1 (1 + \zeta_2 a)^2 , \qquad Q_{c(n)} = M_\eta - M_{\pi^0} - 2M_{\pi(\pi^0)} , \tag{4}$$

where the coefficients $\zeta_{1/2}$ are exclusively determined by $\pi\pi$ phases and therefore not subject to uncertainties from matching to ChPT at $\mathcal{O}(p^4)$. Using the precise KLOE determinations for the charged Dalitz plot parameters as input [8], we find

$$\alpha_{\rm KLOE}^{\rm theo} = -0.062 \pm 0.003 ({\rm stat})^{+0.004}_{-0.006} ({\rm stat}) \pm 0.003 (\pi\pi) ,$$
 (5)

which strongly disagrees with the world average and the collaboration's own experimental finding. The $\Delta I = 1$ determination of α from a fit of the charged data in [8], which is in agreement with the world average, can be understood using chiral one-loop phases. An ongoing dispersive analysis [9] indicates that the discrepancy in Eq. (5) might be slightly overpredicted.

- [1] J. Gasser and H. Leutwyler, Nucl. Phys. B 250 (1985), 539.
- $[2] \ \ J. \ Bijnens \ and \ K. \ Ghorbani, \ \textit{JHEP 0711} \ (2007), \ 030 \ [arXiv:0709.0230 \ [hep-ph]].$
- [3] K. Nakamura [Particle Data Group], J. Phys. G 37, 075021 (2010).
- [4] J. Kambor et al., Nucl. Phys. B 465, 215 (1996) [arXiv:hep-ph/9509374].
- [5] G. Colangelo et al., Phys. Lett. B 638, 187 (2006) [arXiv:hep-ph/0604084].
- [6] S. P. Schneider, B. Kubis and C. Ditsche, arXiv:1010.3946 [hep-ph].
- $[7] \ B. \ Ananthanarayan et al., Phys. \ Rept. \ \textbf{353}, 207 \ (2001) \ [arXiv:hep-ph/0005297].$ R. Kamiński et al., Phys. Rev. D \textbf{77}, 054015 (2008) [arXiv:0710.1150 [hep-ph]].
- [8] F. Ambrosino et al. [KLOE Collaboration], JHEP 0805, 006 (2008) [arXiv:0801.2642 [hep-ex]].
- [9] G. Colangelo, S. Lanz and E. Passemar, arXiv:0910.0765 [hep-ph], and these proceedings.

DETERMINATION OF QUARK MASSES: THE CONTRIBUTION OF $\eta \to 3\pi$

GILBERTO COLANGELO*

In this talk I have discussed the current status of the determination of the light quark masses, concentrating in particular on those based on lattice calculations. I have presented a summary of the available lattice calculations, as it has now appeared in the FLAG (FLAVIAnet Lattice Averaging Group) review [1]. Current lattice determinations have reached a remarkable level of precision: about 10% for m_s and the average of the up and down quark masses m_{ud} , and about 4% for the ratio m_s/m_{ud} . Including isospin breaking effects on the lattice, and in particular photons, is however still problematic. A first calculation with two dynamical flavours (but with photons still treated in the quenched approximation) has recently appeared [2], but the precision is not yet comparable to what has been achieved in the isospin limit. In particular the control of systematic effects is not yet fully satisfactory.

The analysis of the process $\eta \to 3\pi$, on the other hand, allows one to extract clean information about the isospin-violating mass ratio Q:

$$\frac{1}{Q^2} = \frac{m_d^2 - m_u^2}{m_s^2 - \hat{m}^2} \ ,$$

as it has already been shown by dispersive analyses of this process [3, 4]. The current experimental activity aiming at a better measurement of the decay rate and the Dalitz plot of this process, which has been extensively reported at this Workshop, and recent as well as forthcoming theoretical analyses [5, 6, 7] will indeed allow a precision determination of this quark mass ratio. This information is complementary to the one provided by the lattice in the isospin limit and will lead to a precise determination of all three light quark masses.

- [1] G. Colangelo et al., arXiv:1011.4408 [hep-lat].
- [2] T. Blum, R. Zhou, T. Doi, M. Hayakawa, T. Izubuchi, S. Uno and N. Yamada, arXiv:1006.1311 [hep-lat].
- [3] A. V. Anisovich and H. Leutwyler, Phys. Lett. B 375 (1996) 335 [arXiv:hep-ph/9601237].
- [4] J. Kambor, C. Wiesendanger and D. Wyler, Nucl. Phys. B 465 (1996) 215 [arXiv:hep-ph/9509374].
- [5] Stefan Lanz, these proceedings.
- [6] Sebastian Schneider, these proceedings.
- [7] S. P. Schneider, B. Kubis and C. Ditsche, arXiv:1010.3946 [hep-ph].

^{*}Albert Einstein Center for Fundamental Physics, Institut für Theoretische Physik, Universität Bern, Sidlerstr. 5, CH-3012 Bern, Switzerland. gilberto@itp.unibe.ch

A NEW DISPERSIVE ANALYSIS OF $\eta \to 3\pi^*$

STEFAN LANZ

Albert Einstein Center for Fundamental Physics, Institut für Theoretische Physik, Universität Bern, Sidlerstr. 5, CH-3012 Bern, Switzerland

The decay $\eta \to 3\pi$ is of particular theoretical interest because it can only proceed through isospin breaking. If the strongly suppressed electromagnetic contributions are neglected, the decay amplitude is proportional to $(m_u - m_d)$ or, alternatively, to the quark mass double ratio

$$\frac{1}{Q^2} = \frac{m_d^2 - m_u^2}{m_s^2 - \hat{m}^2} , \quad \text{with} \quad \hat{m} = \frac{m_u + m_d}{2} . \tag{1}$$

Furthermore, this process involves two theoretical puzzles. The first one is the fact that the results for the decay width from current algebra, but also from one-loop chiral perturbation theory (ChPT) fail to reproduce the experimental value. It is understood that this is due to large final state rescattering effects that can be ideally treated using dispersion relations. The second puzzle is related to the slope parameter α in the neutral channel, where ChPT, but also an older dispersive analysis [1] fail to reproduce the experimental finding.

In 1996 two dispersive analyses of $\eta \to 3\pi$ have been published [1, 2]. Our analysis follows closely the method proposed in the second reference, where a detailed description can be found. Many developments in recent years, as well as current activity by many groups, have made a new analysis worthwhile. Several groups provide accurate descriptions of the $\pi\pi$ scattering phase shifts [3, 4, 5]. Non-relativistic effective field theories allow for yet another way of treating this process and, in particular, explicitly including isospin breaking in the pion masses [6]. There is a lot of experimental activity that will lead to several precise measurements of the Dalitz plot in the near future. In ChPT, the decay amplitude has been calculated to two-loop order [7] and effects of $O(e^2m)$ have been completely analysed [8]. In addition to our work, there is a second on-going dispersive analysis following a somewhat different approach [9].

We rely on a decomposition of the amplitude into isospin amplitudes $M_I(s)$ that are functions of one variable only [10],

$$M(s,t,u) = M_0(s) + (s-u)M_1(t) + (s-t)M_1(u) + M_2(t) + M_2(u) - \frac{2}{3}M_2(s).$$
 (2)

From unitarity and analyticity follow dispersion relations for the function $M_I(s)$,

$$M_0(s) = \Omega_0(s) \left\{ \alpha_0 + \beta_0 s + \gamma_0 s^2 + \frac{s^2}{\pi} \int_{4m_\pi^2}^{\infty} \frac{ds'}{|\Omega_0(s')|(s'-s-i\epsilon)|} \right\},$$
(3)

and similarly for $M_1(s)$ and $M_2(s)$. The functions $M_I(s)$ are angular averages over all of the M_I such that the dispersion relations are coupled. The Omnès function is given by

$$\Omega_I(s) = \exp\left\{\frac{s}{\pi} \int_{4m_{\pi}^2}^{\infty} \frac{\delta_I(s')}{s'(s'-s)} ds'\right\}. \tag{4}$$

The dispersion relations contain a total number of four subtractions constants: α_0 , β_0 and γ_0 in the equation for M_0 and one more, β_1 , in the equation for M_1 . These are left free by the dispersion relations and have to be determined otherwise. The dispersion relations are solved numerically by an iterative procedure, starting at some initial configuration for the $M_I(s)$. If the subtraction constants are determined by a matching to the one-loop result from ChPT (as in Ref. [2]), it turns out that there is some deviation from the experimental result in Ref. [11]

^{*}in collaboration with G. Colangelo, H. Leutwyler and E. Passemar

[†]Email: slanz@itp.unibe.ch

for large s (see Fig. 1). Alternatively, we can determine the subtraction constants by a combined fit to the measured Dalitz plot and to one-loop ChPT around the Adler zero, where the series is expected to converge best. Because the amplitude is proportional to Q^{-2} , the normalisation from experiment can not be used. Instead, it has to be taken from ChPT. The results from a preliminary fit are also shown in Fig. 1.

Comparing the decay width that is calculated from our dispersive amplitude with the present PDG value of $\Gamma_{\pi^0\pi^+\pi^-}=295\pm20$ eV, we can extract a value for Q. Using the subtraction constants from the matching to one-loop we get $Q=22.6\pm0.4$, thus updating the analysis from Ref. [2]. The preliminary result using the subtraction constants from the fit to the KLOE data is $Q=22.0\pm0.4$. In both cases the given error comes from the uncertainty on the decay width only and does not yet include an estimate for the theoretical uncertainty. We plan to extend our analysis to include additional contributions as well as a complete error analysis, resulting in an accurate estimate for Q and other physical quantities.

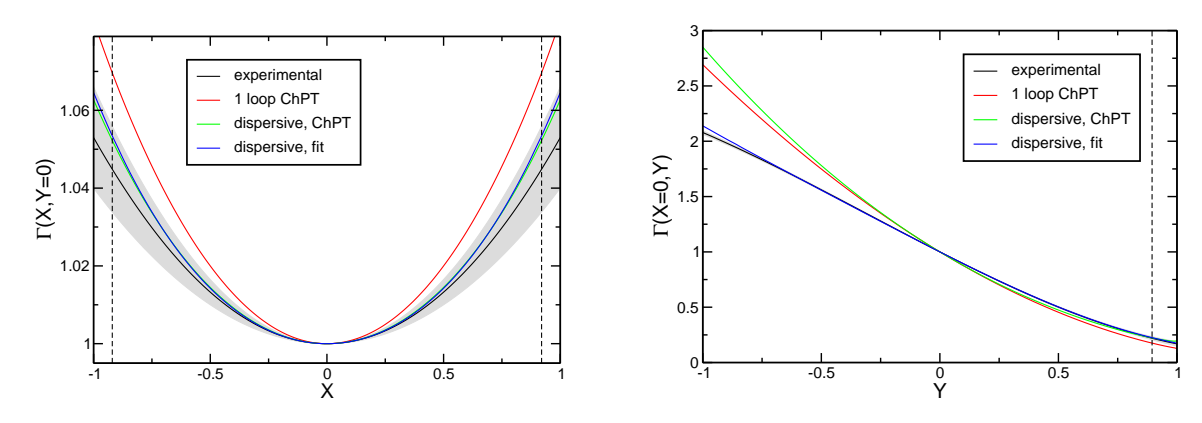


Figure 1: The squared amplitude for the decay $\eta \to \pi^0 \pi^+ \pi^-$ along the lines Y=0 (left) and X=0 (right). X and Y are the usual Dalitz plot variables, the dashed lines represent the limits of the physical region. One can clearly see the disagreement between the dispersive result and experiment for Y<0 (which corresponds to large s).

- [1] J. Kambor et al., Nucl. Phys. **B465** (1996) 215–266, [hep-ph/9509374].
- [2] A. V. Anisovich and H. Leutwyler, *Phys. Lett.* B375 (1996) 335–342, [hep-ph/9601237].
- [3] B. Ananthanarayan et al., Phys. Rept. 353 (2001) 207–279, [hep-ph/0005297].
- [4] S. Descotes-Genon et al., Eur. Phys. J. C24 (2002) 469–483, [hep-ph/0112088].
- [5] R. Kaminski et al., arXiv:0905.2139.
- [6] C. Ditsche, B. Kubis, S. Schneider, to be published. Talk by S. Schneider in this workshop.
- [7] J. Bijnens and K. Ghorbani, JHEP 11 (2007) 030, [arXiv:0709.0230].
- [8] C. Ditsche et al., Eur. Phys. J. C60 (2009) 83-105, [arXiv:0812.0344].
- [9] K. Kampf et al., PoS(CD09)122, [arXiv:0910.1721]. Talk by K. Kampf in this workshop.
- [10] J. Stern et al., Phys. Rev. **D47** (1993) 3814–3838, [hep-ph/9301244].
- [11] **KLOE** Collaboration, F. Ambrosino et. al., JHEP **05** (2008) 006, [arXiv:0801.2642].

THE $\eta \to \pi^+\pi^-\pi^0$ DECAY WITH WASA-AT-COSY

 $PATRIK\ ADLARSON^*$ on behalf of the WASA-at-COSY Collaboration

1.1 Introduction

The isospin violating strong decay $\eta \to \pi^+\pi^-\pi^0$ is an important decay since it allows access to light quark mass ratios. At lowest order of chiral perturbation theory (ChPT) the amplitude is given by

$$A \propto \frac{m_d - m_u}{F_\pi^2} \left(1 + \frac{3(s - s_0)}{m_\eta^2 - m_\pi^2} \right),$$
 (1.1)

where F_{π} is the pion decay constant, $s=(p_{\pi^+}+p_{\pi^-})^2=(p_{\eta}-p_{\pi^0})^2$, $s_0=\frac{1}{3}(m_{\eta}^2+3m_{\pi}^2)$ and $m_{\pi^+}=m_{\pi^0}=m_{\pi}$. Electromagnetic corrections are small [1]. The tree level decay width, $\Gamma_{tree}\approx 70~{\rm eV}$ [2], deviate more than a factor of four from the PDG value $\Gamma=296\pm 16$ [3]. Higher order diagrams are needed which, among other things, take into account $\pi\pi$ final state pion interactions [4, 5, 6]. Alternatively, $\pi\pi$ final state re-scattering can be implemented in dispersive approaches [7, 8, 9, 10]. The decay width scales as

$$\Gamma = \left(\frac{Q_D}{Q}\right)^4 \bar{\Gamma},\tag{1.2}$$

where $Q^2 = (m_s^2 - \hat{m}^2)/(m_d^2 - m_u^2)$, $\hat{m} = \frac{1}{2}(m_u + m_d)$, and the decay width $\bar{\Gamma}$ and $Q_D = 24.2$ are calculated in the Dashen limit [11]. Q gives access to light quark mass ratios and serves also as an important input for lattice QCD [12]. To derive Q, $\bar{\Gamma}$ has to be known reliably from theory which can be tested by comparing with the experimental Dalitz plot distributions. As Dalitz plot variables

$$x = \sqrt{3} \frac{T_{+} - T_{-}}{Q_{\eta}}, \ y = \frac{3T_{0}}{Q_{\eta}} - 1.$$
 (1.3)

are used. Here T_+ , T_- and T_0 denote the kinetic energies of π^+ , π^- and π^0 in the η rest frame, and $Q_{\eta} = m_{\eta} - 2m_{\pi^+} - m_{\pi^0}$. The standard way to parametrize the Dalitz plot density is a polynomial expansion around x = y = 0

$$|A(x,y)|^2 \propto 1 + ay + by^2 + dx^2 + fy^3 + gx^2y + \dots$$
 (1.4)

where a,b,...,g are called the Dalitz Plot parameters. The most precise experimental result is based on a Dalitz plot containing $1.34\cdot 10^6$ events obtained by KLOE [13]. Parameters b and f in [13] deviate significantly from ChPT predictions. Independent measurements are therefore important and WASA-at-COSY aims at providing two independent data sets with η produced in pp and in pd-reactions.

1.2 Experiment

In 2008 and 2009 WASA-at-COSY [14] collected $1\cdot 10^7$ and $2\cdot 10^7$ η mesons respectively, in the reaction $pd\to{}^3{\rm He}X$ at a kinetic beam energy of 1 GeV. The missing mass with respect to ${}^3{\rm He}$ is used to tag the η in the reaction $pd\to{}^3{\rm He}X$ (Fig. 1.1 left). In addition, two tracks of opposite charge in the central drift chamber and two photons with an invariant mass close to π^0 in the electromagnetic calorimeter are required. Background from $pd\to{}^3{\rm He}\pi\pi$ reactions is reduced by imposing conditions on the missing mass calculated for ${}^3{\rm He}\pi^+\pi^-$ and for ${}^3{\rm He}\pi^0$. The preliminary analysis gives 149 000 $\eta\to\pi^+\pi^-\pi^0$ candidates from the 2008 data, shown in Fig. 1.1 right.

^{*}Institute for Physics and Astronomy, Uppsala University, Uppsala, 751 20, Sweden, patrik.adlarson@fysast.uu.se

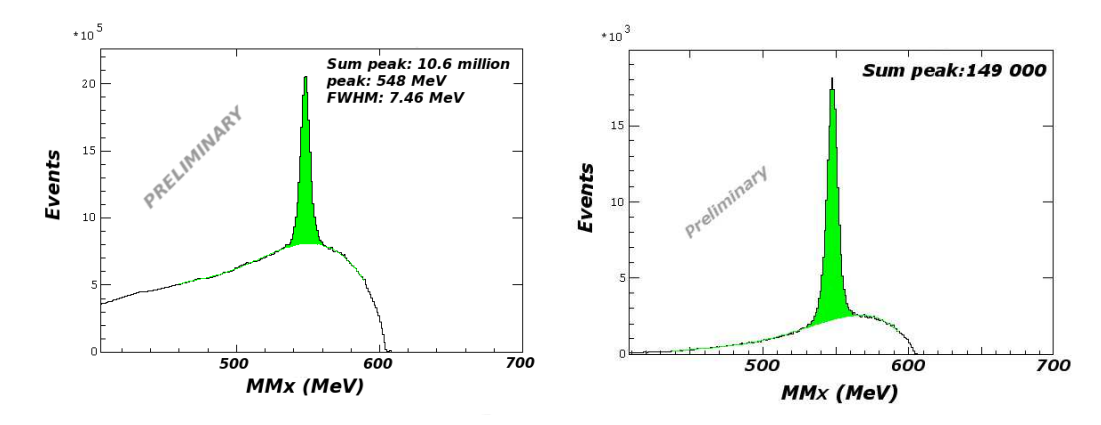


Figure 1.1: Results from 2008 data. (left) The missing mass calculated from the identified 3 He $MM(^3$ He) shows a distinct peak at the η mass. (right) Same after selecting $\pi^+\pi^-\pi^0$ signature in the central detector and including a cut on the missing masses with respect to 3 He $\pi^+\pi^-$ and 3 He π^0 .

The experimental resolution is better for the η four-momenta from ³He compared to the information derived from the η decay products. To improve the resolution for the four-momenta of the η decay products, a kinematical fit for the reaction $pd \to {}^3\text{He}\pi^+\pi^-\gamma\gamma$ has been used with ³He observables fixed and a cut on the 1% level of the probability density function. The η content in each Dalitz Plot bin is derived by performing a four-degree polynomial fit over the background region and the fitted polynomial is subtracted from the signal region. The preliminary experimental results for the x,y projections of the Dalitz Plot are compared in Fig. 1.2 to Monte Carlo simulations of the $\eta \to \pi^+\pi^-\pi^0$ weighted with the tree-level prediction (equation 1).

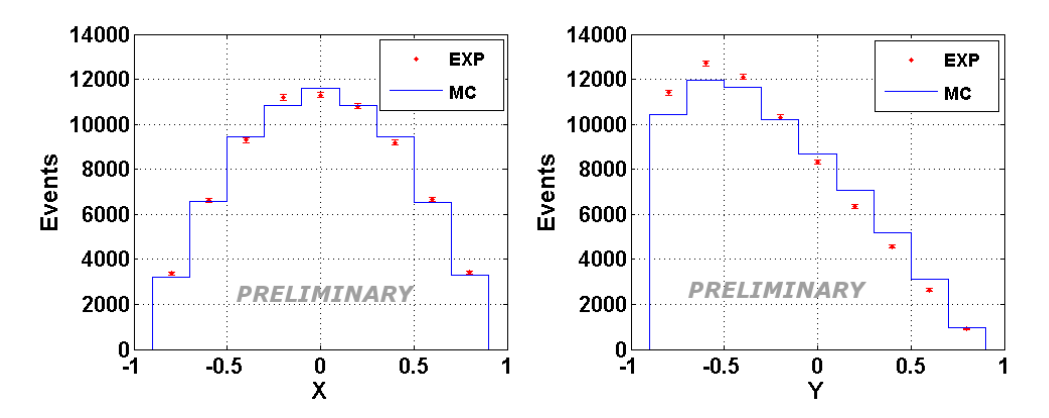


Figure 1.2: Dalitz Plot projection from 2008 data, not corrected for acceptance. The error bars represent only statistical errors of the experimental data on x (left) and y (right) for MC (solid line) and experimental data.

In 2008 and 2010 measurements have been performed using the tagging reaction $pp \to ppX$ at a beam kinetic energy of 1.4 GeV. From the 2010 data approximately $10^7~\eta \to \pi^+\pi^-\pi^0$ are recorded on disk and the analysis of this reaction is in progress [15].

1.3 Outlook

The work for both pd and pp data will be continued in order to obtain two independent determinations of the Dalitz plot parameters for $\eta \to \pi^+\pi^-\pi^0$. Further improvements include the acceptance correction of the experimental data and an assessment of systematical errors.

- [1] D.G. Sutherland, Phys Lett 23, 384, (1966).
- [2] W.A. Bardeen, et al., Phys Rev Lett 18, 1170, (1967).
- [3] K.Nakamura et al., J Phys G 37, 075021, (2010).
- [4] C. Roiesnel, T. Truong, Nucl Phys B 187, 293, (1981).
- [5] J. Gasser, H. Leutwyler, Nucl Phys B 250, 539, (1985).
- [6] J.Bijnens, K.Ghorbani, *JHEP* 11, 030, (2007).
- [7] A.Anisovich, H.Leutwyler, *Phys Lett B* **375**, 335, (1996).
- [8] J.Kambor, C.Wiesendanger, D.Wyler, Nucl Phys B 465, 215, (1996).
- [9] J.Bijnens, J.Gasser, *Phys Scripta* **T99**, 34, (2002).
- [10] S.Lantz, contribution to these proceedings.
- [11] R. Dashen, Phys Rev 183, 1245, (1969).
- [12] G.Colangelo, contribution to these proceedings.
- [13] F. Ambrosini et al (KLOE Collab.), JHEP 05, 006, (2008).
- [14] H. H. Adam et al., arXiv:0411038 [nucl-ex].
- [15] P.Adlarson, M.Zielinski, arXiv:1009.5508v1 [hep-ex].

RADIATIVE CORRECTIONS IN $K \to \pi \ell^+ \ell^-$ AND RELATED DECAYS

BASTIAN KUBIS* AND REBEKKA SCHMIDT

We calculate radiative corrections to the flavor-changing neutral current processes $K \to \pi \ell^+ \ell^-$ [1]. Such transitions are suppressed to the one-loop level in the Standard Model and therefore rare; the CP-allowed K^\pm and K_S decays are expected to be dominated by one-photon exchange. Furthermore these processes are also suppressed to one loop in the effective-theory description of chiral perturbation theory [2].

The process is characterized by the form factor F(s), which can be extracted from the spectrum with respect to the squared invariant mass of the dilepton pair s,

$$\frac{d\Gamma}{ds} = \frac{\alpha^2 |F(s)|^2}{3(4\pi)^5 M_K^7} \lambda^{3/2} (M_K^2, s, M_\pi^2) \sqrt{1 - \frac{4m_\ell^2}{s}} \left(1 + \frac{2m_\ell^2}{s} \right) (1 + \Omega) . \tag{1}$$

 $\lambda(a,b,c) \doteq a^2 + b^2 + c^2 - 2(ab + ac + bc)$ is the Källén function. Radiative corrections are included in the factor Ω , which is of the order of the fine structure constant α . Ω is given as a simple sum of corrections to the hadronic and the leptonic current, both of which are ultraviolet finite without requiring a counterterm. The correction $\Omega_{K\pi}$ to the hadronic current, which only applies to the charged kaon decays $(K^{\pm} \to \pi^{\pm})$, is a smooth function of s that increases the spectrum by only 1%–1.5%. We therefore only discuss the leptonic part $\Omega_{\ell^+\ell^-}$ in the following. The infrared divergences that occur due to the effects of (massless) virtual photons are canceled by the inclusion of real-photon radiation (bremsstrahlung), which is integrated up to a maximal photon energy cut $E_{\rm max}$. The calculation of the bremsstrahlung contribution is often simplified by applying the "soft-photon approximation", which accurately reproduces terms $\propto \log E_{\rm max}$ as well as constant parts, but differs from the exact result by terms of $\mathcal{O}(E_{\rm max})$.

For the muon final state, the correction factor $\Omega_{\mu^+\mu^-}$ is dominated by the Coulomb singularity $\propto \alpha (s-4m_\mu^2)^{-1/2}$ close to threshold; apart from this enhancement it is small, on the 1%–2% level. The soft-photon approximation with a cut on the additional photon energy in the bremsstrahlung contribution is very accurate compared to the exact result. Employing the same expression for the electron final state leads to apparently huge electromagnetic corrections of the order of 10% or more, with furthermore a significant deviation of the soft approximation from the exact result. The reason can be seen when expanding $\Omega_{e^+e^-}$ in the electron mass,

$$\Omega_{e^+e^-} = \frac{\alpha}{\pi} \left\{ \frac{1}{4} - 2 \left[\log \epsilon + \frac{(1-\epsilon)(3-\epsilon)}{4} \right] \log \delta + \frac{1-\epsilon}{2} \left[(3-\epsilon) \log (1-\epsilon) - \frac{11-3\epsilon}{2} \right] - 2 \log \epsilon + \frac{\pi^2}{3} - 2 \operatorname{Li}(\epsilon) \right\} + \mathcal{O}(m_e) , \qquad \operatorname{Li}(z) = -\int_0^z \frac{\log(1-t)}{t} dt , \qquad (2)$$

with $\epsilon = 2E_{\rm max}/\sqrt{s}$ and $\delta = m_e^2/s$. The appearance of mass singularities $\propto \log \delta$ in Eq. (2), so-called Sudakov logarithms, is only seemingly in contradiction with the Kinoshita–Lee–Nauenberg theorem [3, 4], which guarantees the absence of such terms only in total or *inclusive* transition probabilities. Indeed, in the inclusive limit $\epsilon \to 1$, the $\log \delta$ term in Eq. (2) vanishes. This cancellation, however, does obviously *not* hold in the soft-photon approximation, in which terms of $\mathcal{O}(\epsilon)$ are neglected.

The origin of these mass singularities is to be found in the collinear radiation of photons off very light particles (here: electrons). However, much as the inclusion of soft photons in a realistic measurement is an experimental requirement due to finite detector energy resolution, so is the inclusion of collinear photons due to finite angular resolution. It is therefore the (unphysical) excision of hard collinear bremsstrahlung photons that leads to the survival of logarithmic mass singularities in the electron channels. In realistic experiments, this requires the introduction of

^{*}Helmholtz-Institut für Strahlen- und Kernphysik and Bethe Center for Theoretical Physics, Universität Bonn, e-mail: kubis@hiskp.uni-bonn.de

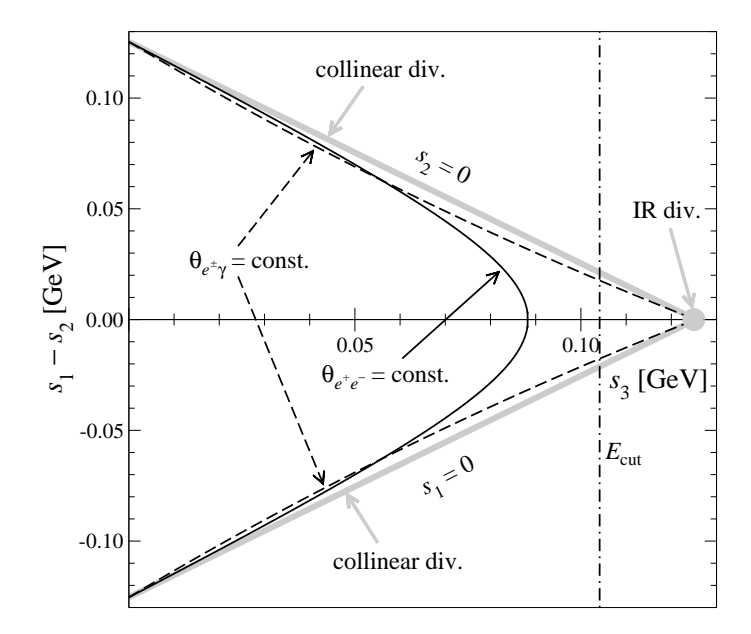


Figure 1: Dalitz plot for $\gamma^* \to e^+e^-\gamma$ at maximal $s = (M_K - M_\pi)^2$. Shown are the positions of the collinear singularities for $s_1 = 0$ and $s_2 = 0$ (broad grey bands) as well as the infrared singularity at their intersection (thick grey dot). Drawn relative to those are various cut positions in $\theta_{e^{\pm}\gamma}$ (dashed line), E_{max} (vertical dash-dotted), and $\theta_{e^+e^-}$ (full black). Figure taken from Ref. [1].

additional angular cuts in the leptonic radiative corrections, either between bremsstrahlung photon and electron/position, or on the electron-positron angle. The position of the various infrared and collinear singularities in the Dalitz plot of the sub-decay process $\gamma^* \to e^+e^-\gamma$ is depicted in Fig. 1, together with the various energy and angular cuts. Only a correction factor $\Omega_{e^+e^-}$ inclusive with respect to all singular regions of the bremsstrahlung contribution is physically reasonable. We provide closed analytic results for the cut dependence of these correction factors in the limit of the electron mass going to zero, which is shown to be a very good approximation [1]. The mass singularities of Eq. (2) are translated into phase space singularities therein.

Finally, we show that the universal correction factors for the dilepton spectra can be directly used also for other decays such as π^0 or η Dalitz decays or vector meson conversion decays like $\omega \to \pi^0 \ell^+ \ell^-$ [5], despite a totally different form of the hadronic vector current involved. The consequences of our results in particular for existing high-precision studies of the Dalitz decay $\pi^0 \to \gamma e^+ e^-$ [6] ought to be investigated.

- [1] B. Kubis and R. Schmidt, Eur. Phys. J. C (2010) [arXiv:1007.1887 [hep-ph].
- [2] G. Ecker, A. Pich and E. de Rafael, Nucl. Phys. B 291, 692 (1987).
- [3] T. Kinoshita, J. Math. Phys. 3, 650 (1962).
- [4] T. D. Lee and M. Nauenberg, Phys. Rev. 133, B1549 (1964).
- [5] C. Terschlüsen and S. Leupold, *Phys. Lett. B* **691**, 191 (2010) [arXiv:1003.1030 [hep-ph]].
- [6] K. Kampf, M. Knecht and J. Novotný, Eur. Phys. J. C 46, 191 (2006) [arXiv:hep-ph/0510021].

ELECTROMAGNETIC TRANSITIONS FROM VECTORS TO PSEUDOSCALARS

STEFAN LEUPOLD *, ** AND CARLA TERSCHLÜSEN *

1.1 Introduction

Electromagnetic form factors are regarded as interesting quantities to learn about the structure of hadrons. In the following we will apply a recently proposed effective field theory [1, 2] to determine the transition form factors of vector to pseudoscalar mesons [3]. In the present section we will motivate why an effective field theory can give a more reliable answer than a hadronic model. We focus in particular on the vector-meson-dominance model (see , e.g., [4]). A form factor is a decay or reaction rate normalized to the corresponding process for point-like particles. For the decay of a vector meson into a pseudoscalar meson and a dilepton the form factor, F, is a function of q^2 which is the four-momentum squared of the lepton-antilepton pair. It is normalized to the photon point, i.e. $F(q^2 = 0) = 1$. In the following we will discuss three cases: a) a model for F, b) a very general field theory, c) an effective field theory.

In the vector-meson-dominance model (VMD) the form factor is given by

$$F(q^2) = \frac{m^2}{m^2 - q^2} \tag{1.1}$$

with the mass m of the intermediate vector meson. (We assume for simplicity that there is only one contributing vector meson.) The good thing about a model is that it has predictive power. In the present case, the only quantity which enters is the mass of the intermediate vector meson which ideally can be obtained from another experiment. On the other hand, if the model fails to describe the data, it is unclear how to improve it in a systematic way.

In contrast to (1.1) a general field theory yields for the form factor

$$F(q^2) = \frac{c_0 m^2}{m^2 - q^2} + (1 - c_0) + c_1 \frac{q^2}{m^2} + c_2 \frac{q^4}{m^4} + \dots$$
 (1.2)

It is assumed here that this general field theory contains vector mesons and arbitrary point interactions between the initial hadron, the final hadron(s) and the virtual photon. The general-field-theory expression (1.2) has infinitely many parameters c_i . Some of them might be related to other processes and therefore could be fixed. But, having infinitely many parameters, such an approach does not have any predictive power. It is rather ineffective.

An effective field theory formally yields the same expression (1.2). However, it assigns different degrees of importance to the various parameters c_i . For example, one might get c_0 , $c_2 \sim O(1)$, $c_1 \sim O(q^2/\Lambda^2)$ and all other $c_i \sim O(q^4/\Lambda^4)$ or higher. Here we have introduced two scales: a) The "small" scale which characterizes the energies and momenta at which the effective field theory is supposed to work. We have implicitly assumed here that we work in the energy regime of the vector mesons. Thus the small scale is $\sim m \sim \sqrt{q^2}$. b) The "large" breakdown scale Λ which describes the energy regime where new degrees of freedom become active which are not considered in the effective field theory. As long as the energy regime of interest is sufficiently far away from the breakdown scale we can determine the form factor in the following way: In our example, the leading-order approximation involves only c_0 and c_2 . This is a finite number of parameters and we assume that one can determine them from other experiments. Then we gain predictive power for the form factor. If we want to get a more accurate description, we can include the c_1 term. In the energy regime where the effective field theory works, this latter term is less important than the c_0 and c_2 terms, i.e. it provides a correction to the leading-order result. Still it is more important than all the other c_i terms with i > 2. In general, an effective field theory provides predictive

^{*}Division of Nuclear and Particle Physics, Uppsala University, Uppsala, Sweden

^{**}stefan.leupold@fysast.uu.se

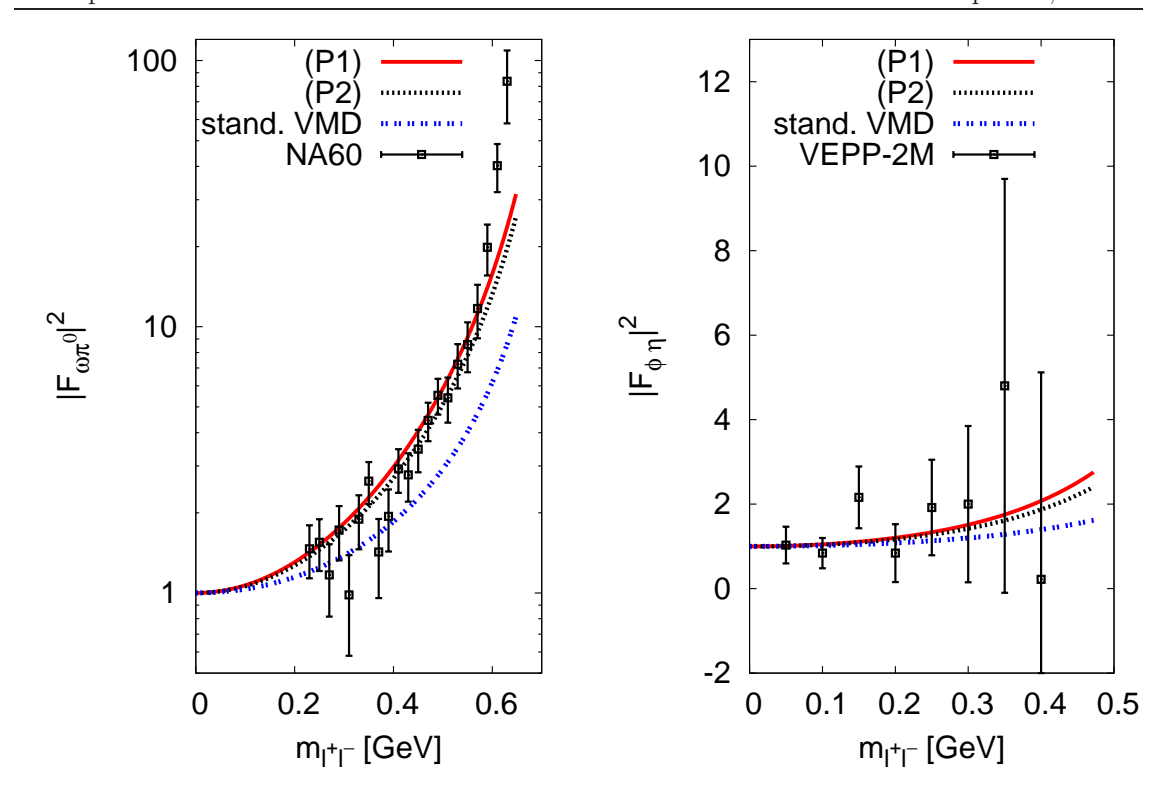


Figure 1.1: Transition form factors $\omega \to \pi$ (left) and $\phi \to \eta$ (right) calculated in VMD and in the effective field theory (full line) as compared to data from [5] and [6], respectively. See [3] for details.

power, because for a given accuracy only a finite number of terms are needed. In addition, it yields a systematic way how to improve the results.

Of course, the previous example did not tell how to get such an effective field theory. In practice, the challenge is a) to construct a theory which includes all relevant degrees of freedom, b) to devise a power counting scheme which assigns the respective degrees of importance to the interaction terms, and c) to figure out for which energy regime the scheme works. From the example above one can see that the breakdown scale is roughly located at the energy where the next-to-leading-order terms become as important as the leading-order terms. Thus, to determine the breakdown scale one has to perform at least a next-to-leading-order calculation.

1.2 Transition form factors for vector mesons

In [1, 2] an effective field theory has been proposed which treats the light pseudoscalar and vector mesons as active/relevant degrees of freedom. So far only leading-order calculations have been performed. Therefore, it not clear yet for which energy regime the scheme works. Nonetheless from a phenomenological point of view the results are very encouraging [1, 2, 3].

For the transition form factor of the ω meson to the pion the proposed effective field theory yields that only the parameter c_0 in (1.2) is of leading order. All other parameters are subleading (and have not been determined yet). In addition, it turns out that c_0 can be completely determined from the decays of vector mesons into pseudoscalar mesons and real photons. Thus, the scheme has predictive power for the form factor. Numerically one finds that c_0 is very close to 2. Therefore, to a good approximation the form factor can be written as

$$F(q^2) \approx \frac{m^2 + q^2}{m^2 - q^2} \tag{1.3}$$

which should be compared to the standard VMD formula (1.1). Obviously the results are rather different. Both the results from the effective field theory [3] and from VMD are compared to data from NA60 [5] in Fig. 1.1, left. One observes that the effective field theory provides a much better description of the experimental data. On the right hand side of Fig. 1.1 the transition form factors for $\phi \to \eta$ are compared. Here the experimental data are not accurate enough to discriminate

between the different theoretical results (and the results are much closer together as compared to the ω -meson case). The KLOE2 collaboration will study this ϕ decay with much better statistics in the near future.

To summarize: The leading-order calculation within the proposed effective field theory provides a parameter-free and much better description of the ω transition form factor than standard vector-meson dominance. This provides a solution for a long-standing puzzle [4]. In the future the impact of the vector mesons on the pseudoscalar decays into two real or virtual photons will be examined. In addition, next-to-leading-order calculations must be carried out to get an idea about the breakdown scale of the proposed effective field theory.

- [1] M. F. M. Lutz and S. Leupold, Nucl. Phys. A 813, 96 (2008) [arXiv:0801.3821 [nucl-th]].
- [2] S. Leupold and M. F. M. Lutz, Eur. Phys. J. A 39, 205 (2009) [arXiv:0807.4686 [hep-ph]].
- [3] C. Terschlüsen and S. Leupold, *Phys. Lett. B* **691**, 191 (2010) [arXiv:1003.1030 [hep-ph]].
- [4] L. G. Landsberg, Phys. Rept. 128, 301 (1985).
- [5] R. Arnaldi *et al.* [NA60 Collaboration], *Phys. Lett. B* **677**, 260 (2009) [arXiv:0902.2547 [hep-ph]].
- [6] M. N. Achasov et al., Phys. Lett. B 504, 275 (2001).

NEW RESULTS ON MESON TRANSITION FORM FACTORS AT BABAR

ACHIM DENIG* for the BaBar Collaboration

1.1 Introduction

Meson transition form factors can be accessed at electron-positron colliders in $\gamma\gamma$ -processes, in which both incoming beam particles are emitting a t-channel photon. In this paper we present recent BaBar results, in which a pseudoscalar mesons - either a π^0 , η or η' - is produced in a $\gamma\gamma$ -fusion reaction, where one of the photons is required to be quasi-real, while for the second photon a four-momentum-transfer $Q^2>3~{\rm GeV}^2$ is required. As a consequence, the electron (or positron) emitting the quasi-real photon will have a very small scattering angle and will not be detected by the BaBar detector, while the second positron (or electron) will be tagged at large polar angles.

The $\gamma\gamma^*$ production cross section in such a so-called single-tag measurement is proportional to the transition form factor $F(Q^2)$, which theoretically can be written as the convolution of the hard scattering process into quarks $(\gamma\gamma^* \to q\bar{q})$ with the meson distribution amplitude (DA) $\Phi(x,Q^2)$ after integration over x, where x is the fraction of the meson momentum carried by one of the two valence quarks. At present only phenomenological models exist for the meson DAs, such that precision measurements can shed new light on this important quantity in meson structure physics. Measurements of the Q^2 dependence of the transition form factor can also be used to test models, which are used in computations of the hadronic light-by-light scattering process for the standard model prediction of the muon anomaly $(g-2)_{\mu}$.

1.2 π^0 transition form factor

BaBar results on the π^0 transition form factor [1], multiplied by Q^2 , are shown in Fig. 1(a). BaBar is in reasonable agreement with previous measurements by CELLO and CLEO, covering however a much wider Q^2 range up to 40 GeV². In total ca. 140.000 events of the kind $e^+e^- \to e^+e^-\pi^0$ could be selected in a total data sample of 500 fb⁻¹. The plot shows also the theory prediction for $F(Q^2)$ of three different models for the pion DA: (i) ASY: asymptotic DA [2]; (ii) CZ: Chernyak-Zhinitsky DA [3]; (iii) BMS: Bakulev-Mikhailov-Stefanis DA [4]. None of the models shows agreement with the BaBar experimental data. Especially, data exceed the asymptotic limit $Q^2F(Q^2) = \sqrt{2}f_\pi$ above 10 GeV², which was previously thought to be the plateau value for this quantity. It can be concluded, that the pion DA is poorly known at present.

1.3 η and η' transition form factors

BaBar preliminary results on the $\gamma\gamma^* \to \eta$ and η' transition form factors, measured in the $e^+e^- \to e^+e^-\eta^{(\prime)}$ reactions, are shown in Figs.1 (b) and 1(c) in comparison with previous CLEO measurements. Presented is again the meson transition form factor multiplied with Q^2 . The BaBar spectra contain in total 2.760 η events and ca. 5.000 η' events from a 500 fb⁻¹ data sample. BaBar data significantly improve the precision and extend the Q^2 region for these form factor measurements. In the case of η' , results from BaBar and CLEO are in good agreement; for the η transition form factor the agreement is worse. Shown are also the asymptotic limits for the η and η' transition form factors, as calculated in Ref. [5]. We observe a completely different Q^2 behaviour compared to the π^0 transition form factor. While for the π^0 transition form factor a significant slope even at high Q^2 is observed, for the η and η' cases, BaBar data is flattening at or below the asymptotic limit. An analysis, in which also high- Q^2 measurements timelike form factors have been taken into account, and in which in a flavour decomposition, the non-strange and strange form factors have been mapped out, do also not show conclusive results.

^{*}Institute for Nuclear Physics, Johannes Gutenberg University Mainz, 55099 Mainz, Germany

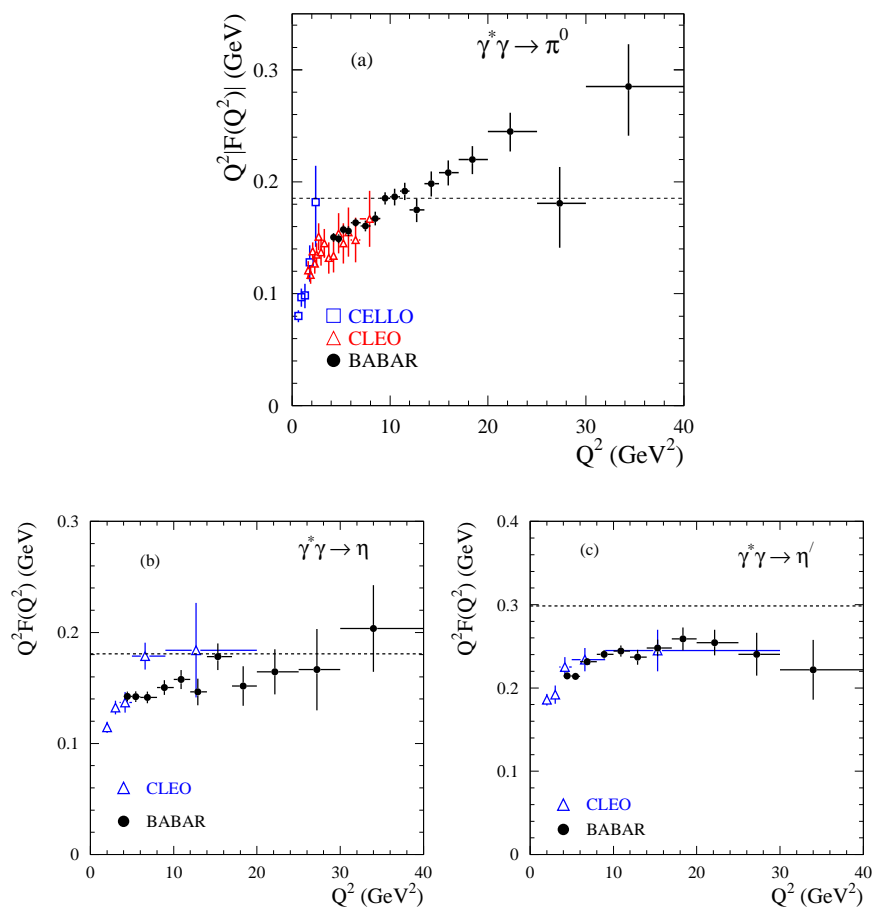


Figure 1.1: BaBar results on the Q^2 dependence of meson transition form factors for 8a) π^0 , (b) η and (c) η' in comparison with previous measurements and several models for the meson distribution amplitudes; results (b) and (c) are preliminary.

- [1] B. Aubert et al., BaBar collaboration Phys. Rev., **D80**, 052002, (2009).
- [2] G. P. Lepage and S. J. Brodsky Phys. Lett., B87, 359, (1979).
- [3] V. L. Chernyak and A. R. Zhitnitsky Nucl. Phys., **B201**, 492, (1982).
- [4] A. P. Bakulev, S. V. Mikhailov, and N. G. Stefanis *Phys. Lett.*, **B508**, 279, (2001).
- [5] T. Feldmann and P. Kroll Phys. Rev., **D58**, 057501, (1998).

MESON DALITZ DECAYS WITH WASA-AT-COSY

JOANNA KLAJA*, on behalf of the WASA-at-COSY Collaboration

1.1 Introduction

The 4π detector facility WASA [1] - an internal experiment at the COoler SYnchrotron COSY in Jülich, Germany - is designed for studies of light mesons decays, in particular (rare) η decays. Due to the unique capability of detecting neutral as well as charged particles a large number of the important decays modes can be measured in order to study symmetries and symmetry breaking, hadron structure and hadron dynamics.

Here, we report the investigation of the electomagnetic transition form factor, studied in meson Dalitz decays.

1.2 Meson Dalitz Decays

Electromagnetic decay modes of light unflavored mesons include Dalitz decays $A \to B \ \gamma^* \to B l^+ l^-$. Here, meson A decays into an object B (another meson or photon) and a lepton pair, formed by internal conversion of an intermediate virtual photon with invariant mass M. If the particles A and B were point-like, then calculations for mass distributions and decay widths would be straightforward using standard quantum electrodynamics (QED). However, the decay rate of this process is modified by the electromagnetic structure arising at the vertex of the transition. Deviations of measured quantities from the QED predictions are described by a transition form factor. Vector mesons have the same quantum numbers ($J^P=1^-$) as the photon, and couple directly to real and virtual photons (the latter can be converted into dileptons). A virtual photon can interact with hadrons not only directly but also after a transition to a virtual vector meson—this type of interaction is called vector-meson dominance. The transition form factor is extracted by comparing the measured dilepton invariant mass spectrum with the point-like QED predictions. The form factor can be parameterized with a pole approximation (Λ):

$$F = \frac{1}{1 - \frac{q^2}{\Lambda^2}} \approx 1 + \frac{q^2}{\Lambda^2}.$$
 (1.1)

to get the parameter Λ which can be then compared with theoretical model predictions.

Until now, significant results on transition form factors have been obtained by the Lepton-G experiment [2]. For the η meson the Λ^{-2} value has been found to be (1.9±0.4) GeV⁻², which is compatible with standard VMD. Experimental measurement of the transition form factor for $\omega \to \pi^0 e^+ e^-$ decay reveal a significant deviation with the fitted $\Lambda^{-2} = (2.36 \pm 0.21) \text{ GeV}^{-2}$ exceeding the VMD calculation by 3 standard deviations.

Recently, the heavy ion experiment NA60 has measured the electromagnetic transition form factors of η and ω mesons [3]. The values for Lambda agree with older data, comfirming the strong enhancement of the ω form factor beyond the expectation from VMD. However, NA60 is a heavy-ion experiment and some additional assumptions enter in the analysis. On the theoretical side, a new counting scheme for the theory of pseudoscalar and vector mesons has recently been introduced to go beyond ChPT to include the vector mesons in a systematic way [4]. A leading-order calculations for the $\omega\pi$ transition form factor yield an improvement in the descrition of the experimental data [5]. However, the available experimental data is still too scarce and additional data are needed. In this context, forthcoming data from WASA-at-COSY will contribute to understanding the problem.

^{*}Institute for Nuclear Physics and Jülich Center for Hadron Physics, Research Center Jülich, Germany; j.klaja@fz-juelich.de

1.2.1 η meson decay

Before investigating the ω decays, it is relevant to study the η Dalitz decay by measuring electron-positron pairs. The $\eta \to \gamma e^+ e^-$ decays are studied with WASA-at-COSY both in proton-proton [6] and proton-deuteron [7] collisions. A thirty thousand $\eta \to \gamma e^+ e^-$ events are expected from the combined pp and pd data sets. Dilepton pairs are selected by using the reconstructed momentum and charge state of the particle from the tracking detectors. The main difficulty in selecting e^+e^- pairs is the discrimination against the dominant pion background. For the higher invariant masses of e^+e^- pairs, the main source of the background comes from multipion production, like the $\eta \to \pi^+\pi^-\gamma$ and $\eta \to \pi^+\pi^-\pi^0$ decay channels. Also, the $\eta \to \gamma\gamma$ decay channel has a significant contribution where one of the photons undergoes external conversion. Applying particle identification and restrictions based on the $\eta \to \gamma e^+e^-$ kinematics, the amount of background is significantly reduced.

In the pp case, the analysis for the determination the transition form factor is in progress.

In the pd case, the background coming from channels with pions in the final state is still dominant. The double Dalitz decay $\eta \to e^+e^-e^+e^-$ is studied using the $pd \to {}^3He\eta$ reaction at a beam energy of 1.0 GeV, with the goal to establish the branching ratio and to determine the η transition form factor $F(q_1^2, q_2^2)$. 30 events candidates are identified being consistent with the current upper limit of $< 6.9 \times 10^{-5}$ [8].

1.2.2 ω meson decay

The WASA-at-COSY Collaboration has begun the program for ω decays. The first beam time, using the $pd \to {}^3He\omega$ reaction with beam momentum 2.196 GeV/c, is scheduled for four weeks in spring 2011. The $\omega \to \pi^+\pi^-\pi^0$ Dalitz plot will be investigated. Futhermore, the $\omega \to \pi^0e^+e^-$ Dalitz decay will be studied as well as $\omega \to \pi^0\gamma$ as reference channel.

In a separate one week of experiment, the $pp \to pp\omega$ reaction will be measured. We will test the possibility of studying ω decays with smaller branching ratios, in particular the conversion decays $\omega \to \pi^0 e^+ e^-$ and $\omega \to \eta e^+ e^-$. By comparing the data quality of the pp and pd data sets we will choose the better reaction for the determination of the $\omega \pi$ transition form factor.

- [1] WASA-at-COSY Collaboration, proposal for WASA-at-COSY, nucl-ex/0411038.
- [2] L. G. Landsberg, Phys. Rept. 128, 301 (1985).
- [3] R. Arnaldi et al., Phys. Lett. B 677, 260 (2009).
- [4] S. Leupold and M. F. M. Lutz, Eur. Phys. J. A 39, 205 (2009).
- [5] C. Terschluesen and S. Leupold, *Phys. Lett. B* **691**, 191 (2010).
- [6] H. Bhatt, AIP Conf. Proc., (2010) in print.
- [7] M. Hodana, Int. J. Mod. Phys. A, (2010) in print.
- [8] K. Nakamura et al., J. Phys. G 37, 075021 (2010).

STUDY OF ANOMALOUS η DECAYS

THIMO PETRI* AND ANDREAS WIRZBA†

1.1 Introduction and Agenda

We report about a study [1] of all anomalous η decays and the corresponding decays of the η' and, if kinematically allowed, π^0 mesons in the framework of vector meson dominance (VMD) models of the 'hidden gauge' class [2, 3]. These decays are interrelated by the Wess-Zumino-Witten action and mostly belong to the group of rare or even very rare decays. While in the workshop we also discussed the double-Dalitz decays of the above-mentioned pseudoscalar mesons into two dilepton pairs, in this presentation we focus on the decay of the η meson into $\pi^+\pi^-e^+e^-$ pairs. This process is governed by the box anomaly in the chiral limit, whereas in the framework of the socalled hidden gauge VMD the decay amplitude features a subtle interplay of a triangle-anomaly term involving two virtual vector mesons and contact interactions of box-anomaly type, see, e.g., Refs. [4, 5, 6]. Moreover, these decays are remarkable since a measurement of an asymmetry of the dihedral angle ϕ between the pion- and the lepton-pair planes would signal the presence of an unconventional flavor-conserving CP violating mechanism of electric-dipole type. Note that the latter is sensitive to the electromagnetic coupling to the s-quark- \bar{s} -antiquark content of the decaying meson and is therefore neither tested by flavor changing transitions in the kaon or Bmeson sectors of the Standard Model nor by the empirical upper bound on the electric dipole moment of the neutron, see Refs. [7, 8].

1.2 Results and Discussion

In Table 1.1 we list our results for the branching ratio BR($\eta \to \pi^+\pi^-e^+e^-$) that we calculated in the framework of the hidden gauge VMD model [2] and the modern refinement of Ref. [3] together with the prediction of unitarized chiral perturbation theory (UChPT) of Ref. [9] and the most recent measurement by the KLOE collaboration [10]. Furthermore, by comparing our predictions of the asymmetry A_ϕ of the hidden gauge model [2] and the modified VMD model [3] with the KLOE measurement [10] (listed in the 2nd row of Table 1.1), we can constrain the free parameter G of the unconventional CP-violating mechanism of Refs. [7, 8] as -0.9 < G < 1.2. Finally, given the constrained G values, the row BR $_{E_1}$ of Table 1.1 shows that the contribution of the electric dipole amplitudes of Refs. [7, 8] is by far too small to alter the value of the tabulated branching ratio(s) substantially.

		hidden gauge	modified VMD	UChPT [9]	KLOE@DAΦNE [10]
BR	(10^{-4})	3.14 ± 0.17	3.02 ± 0.12	$2.99^{+0.08}_{-0.11}$	$2.68 \pm 0.09 \pm 0.07$
A_{ϕ}	(10^{-2})	$(-3.88 \pm 0.11) G$	$(-3.95 \pm 0.08) G$		$-0.6 \pm 2.5 \pm 1.8$
BR_{E_1}	(10^{-6})	$1.6 G ^2$ independent on VMD			

Table 1.1: Theoretical values and experimental data of the branching ratio and asymmetry A_{ϕ} in the decay $\eta \to \pi^+\pi^-e^+e^-$ and the contribution of the electric terms to the branching ratio.

Note that the KLOE measurement of the branching ratio is two standard deviations below the theoretical results listed in Table 1.1, which are all compatible. By normalizing the branching ratio $\mathrm{BR}(\eta \to \pi^+\pi^-e^+e^-)$ to the branching ratio $\mathrm{BR}(\eta \to \pi^+\pi^-\gamma)$ most of the systematical errors in the calculations drop out. In fact, in the reported VMD calculations only the sensitivity to the ρ meson mass and to the relative strengths of vector meson dominance and contact terms

^{*}Institut für Kernphysik, Forschungszentrum Jülich, D-52425 Jülich, Germany and t.petri@fz-juelich.de

[†] JCHP and IAS, Forschungszentrum Jülich, D-52425 Jülich, Germany and a.wirzba@fz-juelich.de

remains – see the reduced errors for the relative branching ratios listed in the first three columns of Table 1.2. The comparison with the fourth row of Table 1.2 that lists the relative ratio of the measured KLOE BR($\eta \to \pi^+\pi^-e^+e^-$) to the BR($\eta \to \pi^+\pi^-\gamma$)_{PDG} = $(4.60 \pm 0.16) \times 10^{-2}$ of the PDG [11, 12] is thus a problem for theory or for experiment or for both.

hidden gauge	modified VMD	UChPT [9]			$\frac{\text{PDG}(2008)[11]}{\text{PDG}[11, 12]}$
6.32 ± 0.01	6.33 ± 0.01	$6.39^{+0.08}_{-0.11}$	5.83 ± 0.31	6.77 ± 0.44	9.13 ± 2.63

Table 1.2: The relative branching ratio $\Gamma(\eta \to \pi^+\pi^-e^+e^-)/\Gamma(\eta \to \pi^+\pi^-\gamma)$ times 10³.

Therefore, in Ref. [10] it was argued that the KLEO branching ratio, if normalized to the smaller BR($\eta \to \pi^+\pi^-\gamma$)_{CLEO} = $(3.96 \pm 0.14 \pm 0.14) \times 10^{-2}$ of the CLEO collaboration [13] than to the above-mentioned PDG value, would be compatible with the theoretical result of Ref. [9], see the fifth column of Table 1.2. Only for completeness, we have also listed the rather inaccurate ratio of the 2008 PDG value [11] for BR($\eta \to \pi^+\pi^-e^+e^-$) to the above mentioned BR($\eta \to \pi^+\pi^-\gamma$)_{PDG} [11, 12]. Note, however, that the preliminary result of the KLOE collaboration for the relative branching ratio $\Gamma(\eta \to \pi^+\pi^-\gamma)/\Gamma(\eta \to \pi^+\pi^-\pi^0)$, which was reported in this workshop [14], is compatible with the PDG average [12], such that the above mentioned problem remains.

Further details – also on the other $\eta, \eta' \to \pi^+ \pi^- l^+ l^-$ decays and the double Dalitz decays – can be found in the Diplom thesis [1] and, partially, in the upcoming paper [15].

- [1] T. Petri, Diplomarbeit, University of Bonn, July 2010, arXiv:1010.2378v1 [nucl-th].
- [2] M. Bando et al., Phys. Rev. Lett., 54, 1215, (1985); T. Fujiwara et al, Prog. Theo. Phys., 73, 926, (1985); M. Harada and K. Yamawaki, Phys. Rep., 381, 1, (2003).
- [3] M. Benayoun, P. David, L. DelBuono and O. Leitner, Eur. Phys. J. C, 65, 211, (2009).
- [4] J. Bijnens, A. Bramon and F. Cornet, Phys. Lett. B, 237, 488, (1990).
- [5] C. Picciotto and S. Richardson, Phys. Rev. D, 48, 3395, (1993).
- [6] B. R. Holstein, Phys. Scr. T, 99, 55, (2002).
- [7] C.Q. Geng, J.N. Ng and T.H. Wu, Mod. Phys. Lett. A, 17, 1489, (2002).
- [8] D.-N. Gao, Mod. Phys. Lett. A, 17, 1583, (2002).
- [9] B. Borasov and R. Nißler, Eur. Phys. J. A, 33, 95, (2007).
- [10] F. Ambrosino et al. (KLOE Collaboration), Phys. Lett. B, 675, 283, (2009).
- [11] C. Amsler et al. (Particle Data Group), Phys. Lett. B, 667, 1, (2008).
- [12] K. Nakamura et al. (Particle Data Group), J. Phys. G, 37, 075021, (2010).
- [13] A. Lopez et al. (CLEO Collaboration), Phys. Rev. Lett., 99, 122001, (2007).
- [14] S. Giovannella, this workshop.
- [15] T. Petri and A. Wirzba, in preparation.

ANALYSIS OF $\eta \to \pi^+\pi^-\gamma$ MEASURED WITH THE WASA FACILITY AT COSY

 $CHRISTOPH\ F.\ REDMER^*$ on behalf of the WASA-at-COSY Collaboration

1.1 Introduction

In the chiral limit the process $\eta \to \pi^+\pi^-\gamma$ is described by the box-anomaly term of the Wess-Zumino-Witten Lagrangian [1, 2]. Meanwhile, the dynamic range of the decay, $4m_\pi^2 \le s_{\pi\pi} \le m_\eta^2$, is well above the chiral limit, giving rise to a significant difference between the predicted and the experimental value of the decay rate. Higher order terms of the chiral Lagrangian become important in order to achieve a correct description. Corrections at the one-loop level [3] can reduce the discrepancy between theory and experiment, however, they are not sufficient to reproduce experimental results. Efforts have been made to incorporate final state interactions by unitarized extensions to the box anomaly term [4, 5, 6, 7]. The validity of the models has to be tested with differential distributions of the Dalitz plot variables, but experimental data are scarce. Moreover, the two statistically most significant measurements [8, 9] have been published without efficiency corrections. Instead, the model descriptions presented along with the data have been folded with the detector efficiency. Recent attempts to interpret the data [6, 10] yield ambiguous results from the two data sets. The missing efficiency corrections are held responsible for the ambiguities. A new high statistics measurement is described in the following.

1.2 Experiment

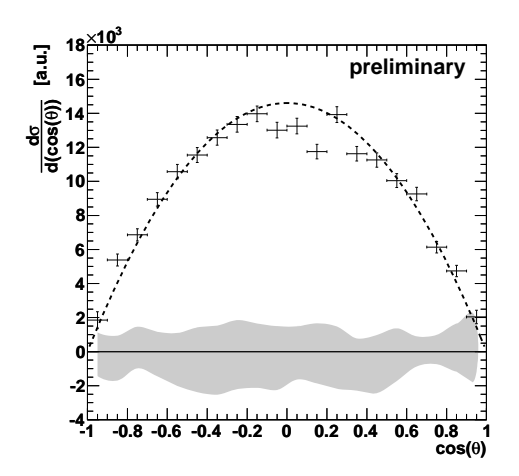
The measurement was carried out with the WASA facility at COSY [11]. η mesons have been produced in the fusion reaction pd \to^3 He X at a proton beam momentum of 1.7 GeV/c. The meson production is tagged by the identification of the helium ions in the detection system. To reconstruct the decay $\eta \to \pi^+\pi^-\gamma$, signals from one neutral and two charged particles are required in coincidence with the 3 He, which can be associated with pion and photon candidates. Further conditions are applied to reduce contributions from two and three pion production, including the decay $\eta \to \pi^+\pi^-\pi^0$, which are the major background reactions. Finally, a kinematic fit has been performed using energy and momentum conservation as the only constraints. Remaining background is subtracted bin-wise by determining the number of η mesons from the corresponding invariant mass distribution of the $\pi^+\pi^-\gamma$ system. The resulting 13740 \pm 140 events of the decay $\eta \to \pi^+\pi^-\gamma$ form the largest sample taken in an exclusive measurement so far.

Fig. 1.1 shows the background subtracted and efficiency corrected angular distribution of the π^+ relative to the photon in the two-pion rest frame and the photon energy distribution in the η rest frame. The systematic uncertainties, indicated in gray, are currently dominating the total error.

The angular distribution can be described by the function $\frac{d\sigma}{d\cos(\theta)} = A \cdot \sin^2(\theta)$, which is shown with the dashed curve in Fig. 1.1. The dependence corresponds to a relative p- wave of the pions. Evidence for angular momenta other than l=1 has not been found.

The line shape of the photon energy distribution cannot be described by the simplest gauge invariant matrix element (dot-dashed curve), which confirms the observations of previous experiments [8, 9]. A combination of the box-anomaly term with a VMD model to describe final state interactions [4] achieves a considerably better agreement. The line shape prediction (solid curve) reproduces the measured distribution within the combined statistical and systematical error.

^{*}Institute for Physics and Astronomy, Uppsala University, 75120 Uppsala, Sweden, christoph.redmer@fysast.uu.se



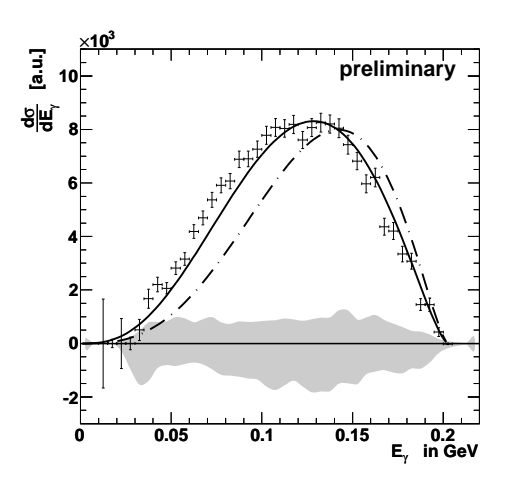


Figure 1.1: The background subtracted and efficiency corrected angular distribution of the pions (left) and the photon energy distribution (right). The shaded areas indicate the systematic uncertainties. The angular distribution agrees with a relative p - wave of the pions (dashed curve). The line shape of the photon energy distribution is compared to predictions of the simplest gauge invariant matrix element (dot-dashed curve) and a VMD-based calculation [4] (solid curve).

1.3 Outlook

In order to perform more precise studies of the box-anomaly in the decay $\eta \to \pi^+\pi^-\gamma$ the total error needs to be decreased. In recent production runs with the WASA facility at COSY, further high statistics data sets on η decays have been acquired. The data will not only reduce the statistical error, but also help to reduce the systematic uncertainties.

- [1] J. Wess and B. Zumino, *Phys. Lett.*, **B37**, 95, (1971).
- [2] E. Witten, Nucl. Phys., **B223**, 422, (1983).
- [3] J. Bijnens, A. Bramon and F. Cornet Phys. Lett., B237, 488, (1990).
- [4] C. Picciotto, Phys. Rev., **D45**, 1569, (1992).
- [5] B. R. Holstein, Phys. Scripta, **T99**, 55, (2002).
- [6] M. Benayoun et al., Eur. Phys. J., C31, 525, (2003).
- [7] B. Borasoy and R. Nissler, Nucl. Phys., A740, 362, (2004).
- [8] M. Gormley et al., Phys. Rev., **D2**, 501, (1970).
- [9] J. G. Layter et al., Phys. Rev., D7, 2565, (1973).
- [10] B. Borasoy and R. Nissler, Eur. Phys. J., A33, 95, (2007).
- [11] WASA-at-COSY Collaboration, arXiv:nucl-ex/0411038, (2004).

Meson Production

in Photo Reactions and from Light Ion Collisions

η PRODUCTION IN NUCLEON-NUCLEON COLLISIONS

COLIN WILKIN*

Preliminary results are reported on three new experiments that measured the production of the η meson in nucleon-nucleon collisions near threshold. In addition, greater insight on the existence of the 3_n He quasibound state is provided by recent photoproduction data.

The ηd interaction was studied at CELSIUS in two different kinematical regimes, viz quasifree $pd \to p_{\rm sp} d\eta$ [1] and the same reaction at much lower energies, *i.e.* well below the threshold in nucleon-nucleon collisions [2]. A consistent FSI description of both data sets was achieved by dividing the ηd invariant mass distribution by the corresponding phase space.

New data have been taken on $dp \to p_{\rm sp} dX$ at the maximum COSY deuteron beam energy of 2.27 GeV and the meson X identified from the missing mass [3]. Here $p_{\rm sp}$ denotes a spectator proton. Since the central neutron energy is below the $d\eta$ threshold, only the higher Fermi momenta contribute to η production. Below-threshold data provide a robust method for background subtraction and the resulting η signal is very clean and the whole η angular domain sampled. The analysis, which is still in progress, suggests an ηd FSI that is not as strong as that found at CEL-SIUS. The prime reason for the difference is the question whether the data should be compared to phase space [2] or to a pure spectator model [3]. Theoretical work [4] suggest that the truth lies between these two extremes and this will have to be incorporated in the ongoing analysis.

In order to study the effects of s-wave rescattering of the η meson from a proton pair, and hence investigate the ηpp FSI, it is important to know at what point higher partial waves are needed for the description of the $pp \to pp\eta$ reaction. The production of the η in proton-proton collisions was investigated by the CELSIUS-WASA collaboration at Q=40 and 72 MeV by detecting the η through its $3\pi^0$ decay [5]. However, the data from the two-photon decay branch have been subjected to a much more refined analysis, which is now approaching completion [6].

The $pp \to pp\eta$ Dalitz plots look similar when the meson is detected through its $3\pi^0$ [5] or 2γ decay [6]. The distributions at both 40 and 72 MeV show a deep valley along the diagonal where $m_{\eta p_1} \approx m_{\eta p_2}$. This is probably due to the η being able to form the $N^*(1535)$ with only one nucleon at a time. The valley implies that there must be higher partial waves in both the pp and ηpp systems, at least $L_{pp}\ell_{\eta} = Pp$. In order to unfold the acceptance, a partial wave fit was made to the combined 40 and 72 MeV data with constant amplitudes. Although the $N^*(1535)$ is not explicitly included, factors arising from the angular momentum barriers and the pp FSI are.

The pp and ηp invariant mass distributions are well reproduced at 40 MeV but for the 72 MeV data, where the statistics are higher, the description in the FSI region is poorer. The better description of the data at 40 MeV persists also for the η angular distributions. In the simple approach used, deviations from isotropy arise from Ss-Sd interference and these must be too small in the model at 72 MeV. This suggests that even higher partial waves are required at this energy.

With parameters tuned to describe the 40 and 72 MeV data, the shapes of the COSY-11 data at 15.5 MeV [7] are well described. In the analysis, higher partial waves in the pp system are vital for the description of the data at the largest m_{pp} ; it the significant contribution from the Ps wave that gives more events at high m_{pp} and hence low $m_{p\eta}$. Since there is no associated angular dependence, this is NOT a proof and an unambiguous separation of Ps from Ss would require a measurement of the initial spin-spin correlation parameter.

Although the poorer description of the η angular distribution at 72 MeV is probably a signal for the influence of even higher partial waves, the constant amplitude ansatz overestimates the increase in the total cross section with energy. This was to be expected and, despite this, the methodology is quite sufficient for its primary purpose of performing acceptance corrections, which are relatively small at WASA.

To study the s-wave $\eta pp\ FSI$ experimentally, we need to control the higher partial waves; the ηd case is simpler because it is a two-body system. The ANKE spectrometer has only limited

^{*}Physics & Astronomy Dept., UCL, London WC1E 6BT, U.K. (cw@hep.ucl.ac.uk)

acceptance, but it can measure well $pp \to \{pp\}_S X$, where the diproton $\{pp\}_S$ has an excitation energy below 3 MeV, so that it is dominantly in the 1S_0 state. Results have already been published for η production in quasi-two-body kinematics at $Q \approx 55$ MeV [8] and similar data have been taken at ANKE for the η' , where about 500 events are expected. Under such conditions, only the Ss and Sd partial waves are important and so many uncertainties are removed.

Although outside the remit of the title, the new data on γ^3 He $\rightarrow \eta^3$ He [9, 10] are too interesting for me not to mention them. The COSY data on $dp \rightarrow \eta^3$ He show clearly that there is a pole in the η^3 He sector for an excess energy Q at |Q| < 1 MeV [11, 12], though whether this is quasi-bound or anti-bound remains ambiguous. The sign of the angular asymmetry changes as a function of Q and this probably reflects the phase variation in the s-wave amplitude associated with the pole.

Analogous results on $\gamma^3 {\rm He} \to \eta^3 {\rm He}$ confirm the pole interpretation since the cross section jumps to one third of its maximum within the first energy bin [9, 10]. Even more convincing evidence comes from a study of the angular dependence. Away from threshold the data are described well by impulse approximation, where the kinematics strongly favour the η emerging in the beam direction. In the first two energy bins this tendency is reversed, as it is for $dp \to \eta^3 {\rm He}$, and the reason is the same. The strong s-wave $\eta^3 {\rm He}$ FSI changes the s-p interference and, using the same parameters as employed for the COSY data [13], the energy variation of the slope in $\gamma^3 {\rm He} \to \eta^3 {\rm He}$ can be understood. It is therefore important to investigate the interaction of the η with other light nuclei to track more precisely how the pole moves with nucleon number A. It is in this context that studies in the two-nucleon sector assume an even greater importance.

- [1] H. Calén et al., Phys. Rev. Lett. 79, 2642 (1997), ibid 80, 2069 (1998).
- [2] R. Bilger et al., Phys. Rev. C 65, 044608 (2002).
- [3] S. Dymov, private communication (2010).
- [4] U. Tengblad, G. Fäldt, C. Wilkin, Eur. Phys. J. A 25, 267 (2005).
- [5] C. Pauly, PhD thesis, University of Hamburg (2006).
- [6] H. Petrén, PhD thesis, University of Uppsala (2009) and article in preparation.
- [7] P. Moskal et al., Phys. Rev. C 69, 025203 (2004); idem Eur. Phys. J. A 43, 131 (2010).
- [8] S. Dymov et al., Phys. Rev. Lett. 102, 192301 (2009).
- [9] F. Phéron, PhD thesis, University of Basel (2010).
- [10] B. Krusche (these proceedings) (2010).
- [11] T. Mersmann et al., Phys. Rev. Lett. 98, 242301 (2007).
- [12] J. Smyrski et al., Phys. Lett. B 649, 258 (2007).
- [13] C. Wilkin et al., Phys. Lett. B 654, 92 (2007).

PHOTOPRODUCTION OF MESONS OFF LIGHT NUCLEI

BERND KRUSCHE*

Photoproduction of mesons has been studied in a series of experiments at the Bonn ELSA and the Mainz MAMI accelerators. Both sets of experiments use very efficient 4π electromagnetic calorimeters (Crystal Barrel and TAPS in Bonn, Crystal Ball and TAPS in Mainz) for the detection of meson decay photons as well as neutral (neutrons) and charged (protons, charged pions) particles. These setups allow for example the measurement of the production of neutral mesons (e.g. η , η') or even pairs of neutral mesons such as $\pi^o\pi^o$, $\pi^o\eta$ in coincidence with recoil neutrons, which is unique and nicely complements the experimental program at other facilities like the CLAS experiment at Jlab, which is more focused on (at least partly) charged final states.

So far, only very few precise experimental data are available for the photoproduction of mesons off the neutron. However, it is clear that this is the only direct access to the iso-spin dependence of the electromagnetic excitation of N* resonances and due to SU(3) selection rules [1] at least for some states the electromagnetic coupling to the proton is strongly suppressed. The non-availability of free neutrons as a target requires of course the study of quasi-free photoproduction reactions off neutrons bound in light nuclei, in particular the deuteron. Apart from the technical complications stemming from the coincident detection of recoil neutrons, also nuclear effects like e.g. Fermi motion and final state interaction (FSI) processes have to be considered. However, fortunately both types of problems can be systematically investigated. This has been demonstrated in detail for our results for quasi-free photoproduction of η and η' mesons off the neutron. The technical problem of controlling the notoriously difficult detection efficiency of recoil neutrons can be solved by a comparison of cross section data measured in coincidence with recoil neutrons (σ_n) to the difference of the inclusive cross section (σ_{np}) (without any condition for recoil nucleons) and the cross section with coincident recoil protons (σ_p) . Since for both reactions coherent photoproduction is negligible, the simple relation $\sigma_{np} = \sigma_p + \sigma_n$ must hold as long as proton and neutron detection efficiencies are correct. Agreement was indeed found within statistical uncertainties, demonstrating that no significant systematic problems are involved. Nuclear effects can be tested via a comparison of quasi-free proton cross sections with free proton cross sections. Here, it was found for η and η' production that no significant effects beyond Fermi motion must be considered. This is not too surprising since the momentum miss-match of participant and spectator nucleons is large and the overlap of the final state wave function of the two-nucleon system with the deuteron wave function is small (both reactions have dominant contributions from S_{11} resonances excited via the E_{0+} spin-flip multipole). In case of the η' channel even Fermi motion does not cause large effects since the excitation functions have no fast varying structures. The results for this channel, which have been already accepted for publication [2] show some difference between the proton and neutron data in particular at intermediate incident photon energies around $E_{\gamma} \approx 1.8$ GeV, which might point to different resonance contribution. However, so far model analyses of both the proton as well as the neutron data are inconclusive since they are not sufficiently constrained by the angular distributions alone. The measurement of polarization observables is clearly necessary.

So far, the most interesting results are related to the $n\eta$ final state, which has been studied in much detail. Already the results reported in [3] have confirmed, that the neutron excitation function shows a narrow structure of unknown nature around incident photon energies of 1 GeV. These data have now been further analyzed using a different concept [4]. The excitation functions for protons and neutrons have been constructed in dependence on the final state invariant mass rather than the incident photon energy. The advantage of this analysis is, that it does not suffer from Fermi smearing. This analysis was possible since although the kinetic energy of the recoil neutrons was not directly measured, the neutron angular information (together with incident

^{*}Department of Physics, University of Basel, Ch-4056 Basel, Switzerland, Bernd.Krusche@unibas.ch

photon energy and measured four-momentum of the η) is sufficient for a full reconstruction of the final state kinematics. The proton data reconstructed this way agree excellently with free proton data. The neutron data show now an even much more pronounced structure with a width around 25 MeV (still including some contribution from experimental resolution). New data from MAMI show this structure with even much better statistical quality [5] and even in an experiment using ³He target nuclei, it is clearly seen in the excitation function with coincident neutrons [6]. Altogether, the existence of this structure is by now established beyond any doubt but it's nature is still controversially discussed. Currently, experiments with polarized deuteron targets (frozen spin deuterated buthanol) and polarized photon beams at MAMI and ELSA try to identify the responsible partial waves via the measurement of double polarization observables.

Finally it should be mentioned, that the analysis of many other channels for quasi-free photoproduction off the deuteron is almost finished and results will be published soon. These are for example data for single π^o -, $2\pi^o$ -, $\pi^o\pi^{\pm}$ -, $\pi^o\eta$ -, $\pi^{\pm}\eta$ -, and $K^o\Lambda$ -production. In case of the double meson channels, not only results for differential cross sections but also for the helicity asymmetry I^o (circularly polarized photon beam, unpolarized target) have been already obtained. Also here it could be demonstrated by a comparison to free proton results that the effects from nuclear Fermi smearing can be well controlled in the analysis. This observable promises very interesting additional information of the reaction dynamics. First measurements of it for double pion production off the free proton [7] had demonstrated it's large sensitivity but also an almost complete failure of available reactions models.

More recently, we started also with an investigation of coherent photoproduction of light nuclei, which can be used to extract additional information for the iso-spin dependence of reaction cross sections. This channel is strongly suppressed for η and η' , however, larger cross sections have been found not only for single π^o but also for multiple meson final states like $\eta\pi^o$, $2\pi^o$ and $3\pi^o$. These reactions can be used as iso-spin filters. For example, in single π^o production off the deuteron only Δ -resonances contribute, while coherent double π^o production projects out the N^* states. Of particular interest is the $\eta\pi^o$ channel, which might also give a new way of access to the search for η -mesic states.

The other important topic in meson photoproduction off nuclei is the meson - nucleus interaction, and for light nuclei in particular the search for meson - nucleus bound states like η -mesic nuclei. Here the question is, whether the properties of the strong interaction allow the formation of meson - nucleus bound states, which depend very sensitively on the strength of the interaction. Pionic atoms are well established and deeply bound pionic states [8] yielded important results [9], directly related to the predicted decrease of the chiral condensate in nuclear matter. In this case the superposition of the repulsive s-wave π^- - nucleus interaction with the attractive Coulomb interaction gives rise to bound states. Neutral mesons on the other hand can form bound states only in case of a sufficiently attractive strong meson - nucleus interaction. Due to the strong s-wave η -nucleus interaction at threshold (caused by the coupling to the $S_{11}(1535)$ nucleon resonance) η -mesic states are among the best candidates for such systems.

The investigation of the threshold behavior of η -photoproduction off light nuclei is one promising approach for the search for η -mesic states. Previous experiments have investigated quasi-free and coherent photoproduction off ²H, ^{3,4}He in the threshold region. In the case of ³He Pfeiffer et al. [10] found a very strong threshold enhancement, although the experiment was somewhat limited in counting statistics. Once a (quasi-)bound state has been formed the η -meson may also be recaptured by a nucleon, exciting it to the S₁₁-state which decays with a \approx 50 % branching ratio to a nucleon - pion pair. This decay channel should result in a peak-like structure in the excitation function of nucleon - pion pairs, emitted back-to-back in the photon - ³He center-of-momentum (cm) system. Some indication for this effects had also been reported by Pfeiffer et al. [10].

A new experiment at MAMI using the Crystal Ball/TAPS detector setup covering almost 4π of the solid angle [11] has confirmed the extremely strong rise of the coherent η -production reaction at threshold with much better statistical quality. However, it has also shown, that the weak signal observed in [10] for the peak-like structure in the π^o-p excitation function, although existent, can be attributed to contributions from N^\star resonances to single π^o production and is not related to an η -mesic state.

- [1] R.G. Moorehouse, Phys. Rev. Lett. 16, 772 (1966).
- [2] I. Jaegle et al., Eur. Phys. J. A, accepted
- [3] I. Jaegle et al., Phys. Rev. Lett. 100, 252002 (2008).
- [4] I. Jaegle et al., in preparation
- [5] D. Werthmüller et al., in preparation
- [6] L. Witthauer et al., in preparation
- [7] D. Krambrich et al., Phys. Rev. Lett. 103, 052002 (2009).
- [8] H. Geissel et al., Phys. Rev. Lett. 88, 122301 (2002).
- [9] P. Kienle and T. Yamazaki Prog. Part. Nucl. Phys. 52, 85 (2004).
- [10] M. Pfeiffer et al., Phys. Rev. Lett. 92, 252001 (2004).
- [11] F. Pheron et al., in preparation

MESON DECAYS AT MAMI-C - RESULTS AND PERSPECTIVES

 $MARC\ UNVERZAGT^*$ for the A2-Collaboration

1.1 Experimental Setup

The electron accelerator MAMI–C [1, 2] provides a very stable electron beam (energy drift $\delta E < 100~{\rm keV}$) with a maximum energy of $E_0 = 1604~{\rm MeV}$. Within the A2 collaboration, experiments are performed with a real photon beam. The photon beam for the production of the light mesons is derived from the production of Bremsstrahlung photons during the passage of the MAMI electron beam through a thin radiator. The Glasgow photon tagging spectrometer [3, 4] at Mainz provides energy tagging of the photons, through $E_{\gamma} = E_0 - E_{e^-}$, by detecting the post–radiating electron energy.

The central 4π -detector system, surrounding the liquid hydrogen target, consists of the Crystal Ball calorimeter (CB) [5, 6] combined with a barrel of scintillation counters for particle identification and two layers of Multi-Wire Proportional-Chambers (MWPC). At forward polar angles the TAPS detector [7, 8] made of BaF₂-crystals provides acceptance for particle detection.

1.2 Recent Results

The experimental setup at MAMI–C is ideally suited for studying the neutral decays of the lightest mesons. The key–investigation in this field was the determination of the Dalitz Plot Parameter α from the isospin–breaking decay $\eta \to 3\pi^0$. Two MAMI results for α were obtained from different data sets with different electron beam energies, $E_{e^-}=883\,\mathrm{MeV}$ [9] and $E_{e^-}=1508\,\mathrm{MeV}$ [10], respectively. Thus, they can be considered as independent measurements. These results, with $1.8\cdot 10^6$ and $3\cdot 10^6$ events, represent the two world highest statistics for the $\eta\to 3\pi^0$ decay. The two totally independent values, $\alpha=-0.032\pm 0.002_{\mathrm{stat}}\pm 0.002_{\mathrm{syst}}$ and $\alpha=-0.032\pm 0.003_{\mathrm{tot}}$, from MAMI agree perfectly with each other and are consistent with other experiments. Recently, an analysis of MAMI–C data from 2009 confirmed these results.

The rare, double–radiative decay $\eta \to \pi^0 \gamma \gamma$ has been investigated as there are contradictions in its experimental decay width and its theoretical predictions. Although the statistics gained at MAMI so far is lower than in the recently published result of the Crystal Ball at AGS [11], a much better signal to background ratio could be achieved. Nevertheless, a preliminary branching ratio $BR(\eta \to \pi^0 \gamma \gamma) = (2.25 \pm 0.46_{stat} \pm 0.17_{syst}) \cdot 10^{-4}$ was determined. The Crystal Ball at MAMI result agrees with the value obtained at BNL within one standard deviation. Both are presently the most precise data for this decay.

Another work was dedicated to the investigation of the Dalitz decays $\pi^0 \to e^+e^-\gamma$ and $\eta \to e^+e^-\gamma$ [12]. The aim was to determine the electromagnetic transition form factors, which provides significant information on the electromagnetic properties of the mesons and is of crucial importance for testing hadronic models used in light–by–light contributions to $(g-2)_\mu$. In the exclusive analysis of $\eta \to e^+e^-\gamma$ 827 events were reconstructed, which is an improvement by a factor 8 with respect to an old measurement by the SND collaboration, the slope parameter of the associated transition form factor was determined to be consistent with other experiments. The analysis of the π^0 –Dalitz decay showed no deviation from the QED prediction, as expected. This work also showed that it is possible with the A2–setup at MAMI to investigate charged channels including electrons and positrons.

New upper limits for the C-violating decays $\omega \to \eta \pi^0$ and $\omega \to 3\pi^0$ were calculated [13]. Also for the first time a value for the upper limit of the branching ratio of the $\omega \to 2\pi^0$ was determined.

^{*}Institute of Nuclear Physics, University of Mainz, Email: unvemarc@kph.uni-mainz.de

1.3 Detector Developments

Since the η' photoproduction threshold is at $E_{thr}\approx 1447\,\mathrm{MeV}$, almost the full photon energy range accessible at MAMI for η' production is not covered by the Glasgow photon tagging spectrometer. Therefore, a new tagging device (End–point tagger) is currently constructed. At the maximum electron beam energy, $E_0=1604\,\mathrm{MeV}$, photon energies between $E_\gamma\approx 1590\,\mathrm{MeV}$ and $E_\gamma\approx 1450\,\mathrm{MeV}$ can be tagged with the End–point tagger. To study the decays of the η' meson, the End–point tagger is essential for a clean trigger. The assembly of the End–point tagger is underway and mid of 2011 first tests will be performed.

The MWPCs integrated in the Crystal Ball–setup have problems to work at high-rates meson–decay experiments. Therefore, a Time Projection Chamber (TPC) with GEM read–out is currently investigated as central tracking device. Not only the rate capability will be improved, but also the resolution and the track reconstruction. In addition, the TPC could contribute to the particle identification. First tests with an old TPC from Karlsruhe, Germany, were successful and 2011 a first prototype will be constructed.

1.4 Perspectives at MAMI–C

The A2–collaboration will continue to study light meson decays, especially the η' , after the assembly of the End–point tagger. Within 600 hours of beam time, 9 million η' will be produced. With the roughly 400,000 $\eta' \to \eta \pi^0 \pi^0$ and 4,000 $\eta' \to 3\pi^0$ events expected after analysis of these data, we will investigate the Dalitz plot parameters, the cusp effect and the $\pi\pi$ –scattering lengths. Within 800 hours of beam time, we will produce 250 million η –mesons. This will allow us to improve our results on the $\eta \to 3\pi^0$ and $\eta \to \pi^0 \gamma \gamma$ decays by at least one order of magnitude. Furthermore, as the Crystal Ball at MAMI setup could also be considered as an ω –factory, we will investigate the transition form factor of the $\omega \to e^+e^-\pi^0$ with improved statistics.

1.5 Conclusions

The Crystal Ball at MAMI–C experiment is ideally suited for meson–decay physics with high rates. The worlds most precise results on $\eta \to 3\pi^0$ and $\eta \to \pi^0 \gamma \gamma$ already come from this experiment. Other results as the $\eta \to e^+e^-\gamma$ transition form factor will be published soon. The construction of the new detector devices (End–point tagger, TPC) will provide high–rate production of η' –mesons and an efficient detection of charged decay channels. In near future many results on the light mesons will be improved by the Crystal Ball at MAMI–C experiment.

- [1] H. Herminghaus et al., IEEE Trans Nucl. Sci. 30, 3274, (1983).
- [2] K.-H. Kaiser et al., Nucl. Instrum. Meth. A 593, 159, (2008).
- [3] I. Anthony, J.D. Kellie, S.J. Hall, G.J. Miller, J. Ahrens. Nucl. Instrum. Meth. A 301, 230, (1991).
- [4] S.J. Hall, G.J. Miller, R. Beck, P. Jennewein, Nucl. Instrum. Meth. A 368, 698, (1996).
- [5] M. Oreglia et al., Phys. Rev. D 25, 2259, (1982).
- [6] A. Starostin et al., Phys. Rev. C 64, 055205, (2001).
- [7] R. Novotny, *IEEE Trans. Nucl. Sci.* **38**, 379, (1991).
- [8] A.R. Gabler et al., Nucl. Instrum. Meth. A346, 168, (1994).
- [9] M. Unverzagt et al., Eur. Phys. J. A 39, 169 (2009).
- [10] S. Prakhov et al., Phys. Rev. C 79, 035204 (2009).
- [11] S. Prakhov et al., Phys. Rev. C 78, 015206 (2008).
- [12] H. Berghuser, PhD thesis, Gieen, Germany, 2010.
- [13] A. Starostin et al., Phys. Rev. C 79, 065201 (2009).

HADES RESULTS FROM NN REACTIONS AND PERSPECTIVES FOR πN

B. RAMSTEIN for the HADES Collaboration *

Experiments with the High Acceptance Dielectron Spectrometer (HADES) [1] explore hadronic matter at high densities ($\rho \sim 2$ -3 ρ_0) and moderate temperatures (T \leq 80 MeV) using the dilepton probe in heavy-ion reactions. These studies aim at testing predictions of in-medium modifications of vector meson spectral functions [2]. This requires as a prerequisite a detailed understanding of dilepton production in the 1-2 AGeV range, which motivates the HADES experimental program with elementary reactions. Baryonic resonances play an important role in dilepton emission. This is first due to their mesonic decays and the subsequent direct dilepton (e.g. $\rho/\omega \to e^+e^-$) or Dalitz (also called conversion) decay ($\pi^0/\eta \to \gamma e^+e^-$ or $\omega \to \pi^0 e^+e^-$) modes of these mesons. Baryonic resonances are also expected to contribute directly to dilepton emission via their Dalitz decay modes (N*/ $\Delta \to$ Ne⁺e⁻). All these baryonic transitions involve Time-Like electromagnetic form-factors which are of fundamental interest in the context of electromagnetic structure of hadrons in the non-perturbative regime. Following the vector dominance model (VDM), the Dalitz decay of baryonic resonances is intimately connected to off-shell (ρ , ω and ϕ) meson production, which is an important issue for the description of dilepton production in heavy-ion collisions.

In the last years, the HADES collaboration has measured dilepton production in C+C collisions at 1 and 2 AGeV [3], Ar+KCl at 1.75 AGeV and p+Nb at 3.5 GeV [4]. In parallel, pp (at 1.25 GeV, 2.2 GeV and 3.5 GeV) and dp reactions at 1.25 AGeV have been studied. The analysis tool for these studies is the PLUTO event generator[7], which allows the implementation of different hadronic physics models, and can take into account the experimental conditions (resolution, acceptance) in a very flexible way. Similarly to transport model calculations, dilepton cocktails can be built up from different processes added incoherently. Differential cross-sections provided by theoretical calculations can also be used to generate the events.

The inclusive pp \rightarrow e⁺e⁻X dilepton production in pp reactions at 1.25 GeV (i.e. just below the η threshold) can be described quantitatively using only two dilepton sources: the π^0 and the Δ Dalitz decays, which have known cross-sections. An improvement of the description of the e⁺e⁻ invariant mass spectra is obtained when a VDM-like N- Δ transition form factor is used, which shows the sensitivity of our data to the electromagnetic structure of hadrons. In addition, the exclusive pp \rightarrow ppe⁺e⁻ measurement reveals the excitation of the Δ resonance, which confirms that the contribution of pp bremsstrahlung is small. These results can therefore be considered as the first direct measurement of the Δ Dalitz decay; the branching ratio is found to be in agreement with QED calculations (4.2×10⁻⁵ within 20 %). At higher energies, other resonances are contributing and the issue is to get a consistent description of dilepton emission including Dalitz decays of baryonic resonances with corresponding electromagnetic form-factors and vector meson decays. The π^0 and η Dalitz decays could be isolated in exclusive pp \rightarrow ppe⁺e⁻channels at 2.2 GeV, but the sensitivity to form-factors is small. More significant results should be obtained at 3.5 GeV.

Using "quasi-free" pn reactions at 1.25 GeV, a very strong isospin dependence of the inclusive dilepton emission could be observed [5]. Calculations within the One Boson Exchange model [6], which take into account graphs involving nucleons and baryonic resonances in a coherent way, were used to describe the data obtained in pp and pn reactions. In pn interactions, graphs involving only nucleons have a more important contributions than in pp interactions, but the dilepton production at large invariant mass is still underestimated by the calculations. As shown recently in [8], an improvement of the description can be achieved by using time-like pion electromagnetic form-factors for the in-flight emission graph, which hints again to the sensitivity of dilepton emission to hadronic electromagnetic structure.

Exclusive meson (π^0, π^+) and η) production in the pp reactions at 1.25 GeV and 2.2 GeV was also analysed. In addition to detector and analysis efficiency tests, these channels are very useful to check that the production of meson and baryonic resonances is consistent with the inputs of the

^{*}I.P.N. Orsay ramstein@ipno.in2p3.fr

PLUTO event generator used for the analysis of dilepton channels. In these reactions, the Delta resonance is dominating although N(1440), N(1535) and N(1520) are also contributing.

HADES has just been upgraded to increase the granularity at forward angles and the data acquisition rate. Heavy systems (Au+Au, Ni+Ni) are planned to be studied. We are also preparing pion beam experiments ($p_{\pi^-} \sim 0.6\text{-}1.5~\text{GeV/c}$) with nuclear and hydrogen targets. Simultaneous studies of hadronic and dilepton channels in the π^-+p reaction with HADES should allow dedicated investigations of resonances heavier than $\Delta(1232)$ and give a unique opportunity to probe their time-like electromagnetic structure.

- [1] G. Agakichiev et al. (HADES Collaboration), Eur. Phys. J. A41, 243 (2009).
- [2] S. Leupold et al., Int. J. Mod. Phys. E19, 147 (2010).
- [3] G. Agakichiev et al. (HADES Collaboration), Phys. Rev. Lett. 98, 052302 (2007); Phys. Lett. B663, 43 (2008).
- [4] T. Galatyuk et al. (HADES Collaboration), to appear in INPC conference proceedings, (2010).
- [5] G. Agakichiev et al. (HADES Collaboration), Phys. Lett., B690, 118 (2010).
- [6] L. P. Kaptari and B. Kämpfer, Phys. Rev. C80, 064003(2009). R. Shyam and U. Mosel, Phys. Rev. C79, 035203 (2009).
- [7] http://www-hades.gsi.de/computing/pluto/html/PlutoIndex.html; I. Fröhlich et al., J. Phys. Conf. Ser. 219, 032039 (2010); I. Fröhlich et al. Eur. Phys. J.A45, 401, (2010).
- [8] R. Shyam and U. Mosel, arXiv:1006.3873[hep-ph] (2010).

COMPARATIVE STUDIES OF η AND η' MESONS AT COSY-11 DETECTOR SETUP*

 $PAWEŁ\ KLAJA^{\dagger}$ for the COSY-11 Collaboration

The proton-proton and proton- η' invariant mass distributions have been determined for the $pp \to pp\eta'$ reaction at an excess energy of Q = 16.4 MeV. The shapes of the determined invariant mass distributions presented in Figure 1 are similar to those of the $pp \to pp\eta$ reaction and reveal an enhancement for large relative proton-proton momenta. This result, together with the fact that the proton- η interaction is much stronger that the proton- η' interaction, excludes the hypothesis that the observed enhancement is caused by the interaction between the proton and the meson. Calculations assuming a significant contribution of P-wave in the final state, and models including energy dependence of the production amplitude, reproduce the data within error bars equally well. Therefore, on the basis of the presented in Figure 1 invariant mass distributions, it is not possible to disentangle univocally which of the discussed models is more appropriate. Future measurements of the spin correlation coefficients should help disentangle these two model results in a model independent way.

For the very first time, the correlation femtoscopy method is applied to a kinematically complete measurement of meson production in the collisions of hadrons. A two-proton correlation function was derived from the data for the $pp \to ppX$ reaction, measured near the threshold of η meson production. A technique developed for the purpose of this analysis permitted to establish the correlation function separately for the production of the $pp + \eta$ and of the pp + pions systems. The shape of the two-proton correlation function shown in left panel of Figure 2 for the $pp\eta$ differs from that for the pp(pions) and both do not show a peak structure opposite to results determined for inclusive measurements of heavy ion collisions.

At present it is not possible to draw a solid quantitative conclusion about the size of the system since it would require to solve a three-body problem where pp and $p\eta$ interactions are not negligible and both contribute significantly to the proton-proton correlation. However, based on semi-quantitative predictions one can estimate that the system must be unexpectedly large with a radius in the order of 4 fm. This makes the result interesting in context of the predicted quasi-bound ηNN state and in view of the hypothesis that at threshold for the $pp \to pp\eta$ reaction the proton-proton pair may be emitted from a large Borromean like object whose radius is about 4 fm.

The upper limit of the total cross section for the $pn \to pn\eta'$ reaction has been determined near the kinematical threshold in the excess energy range from 0 to 24 MeV. The measurement was performed using a deuteron cluster target, and the proton beam with a momentum of 3.35 GeV/c. The energy dependence of the upper limit of the cross section was extracted exploiting the Fermi momenta of nucleons inside the deuteron. The comparison of the determined upper limit of the ratio $R_{\eta'} = \sigma(pn \to pn\eta')/\sigma(pp \to pp\eta')$ with the corresponding ratio for η meson production is presented in right panel of Figure 2 and disvafours the dominance of the $N^*(1535)$ resonance in the production process of the η' meson and suggests non-identical production mechanisms for the η and η' mesons. To pin down the detailed reaction mechanism further theoretical as well as experimental investigations with better statistics are required.

^{*}Text and figures reffer to: P. Klaja et al., Phys. Lett. B 684 11 (2010), P. Klaja and P. Moskal et al., J. Phys. G 37 055003 (2010) and J. Klaja et al., Phys. Rev. C 81 035209 (2010).

[†]Institut für Kernphysik, FZ-Jülich, Jülich, Germany, p.klaja@fz-juelich.de

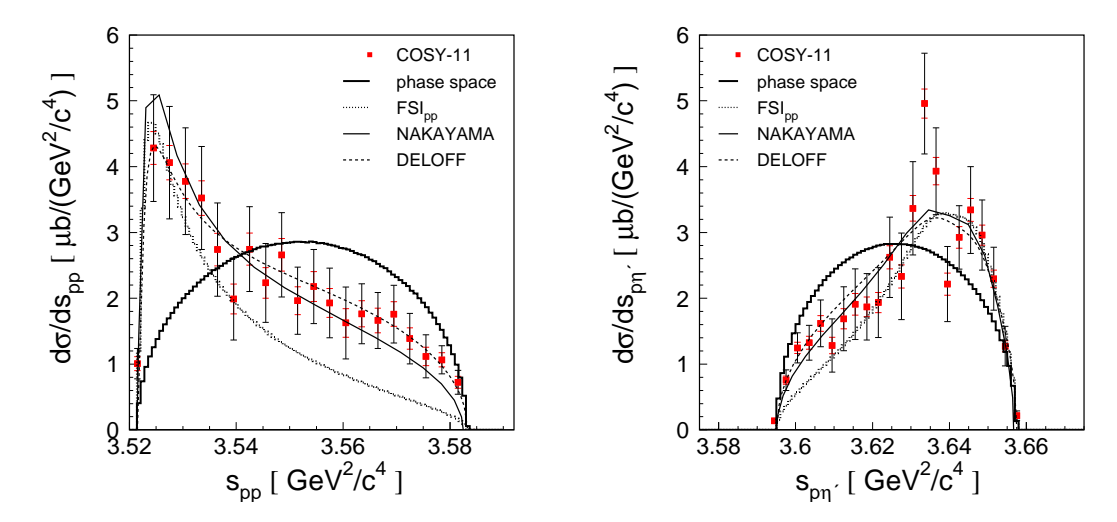


Figure 1: Distributions of the squared proton-proton (s_{pp}) and proton- η' $(s_{p\eta'})$ invariant masses, for the $pp \to pp\eta'$ reaction at the excess energy of Q = 16.4 MeV. The experimental data (closed squares) are compared to the expectation under the assumption of a homogeneously populated phase space (thick solid lines) and the integrals of the phase space weighted by the proton-proton scattering amplitude - FSI_{pp} (dotted histograms). The solid and dashed lines correspond to calculations when taking into account contributions from higher partial waves and allowing for a linear energy dependence of the $^3P_0 \to ^1S_0s$ partial wave amplitude, respectively.

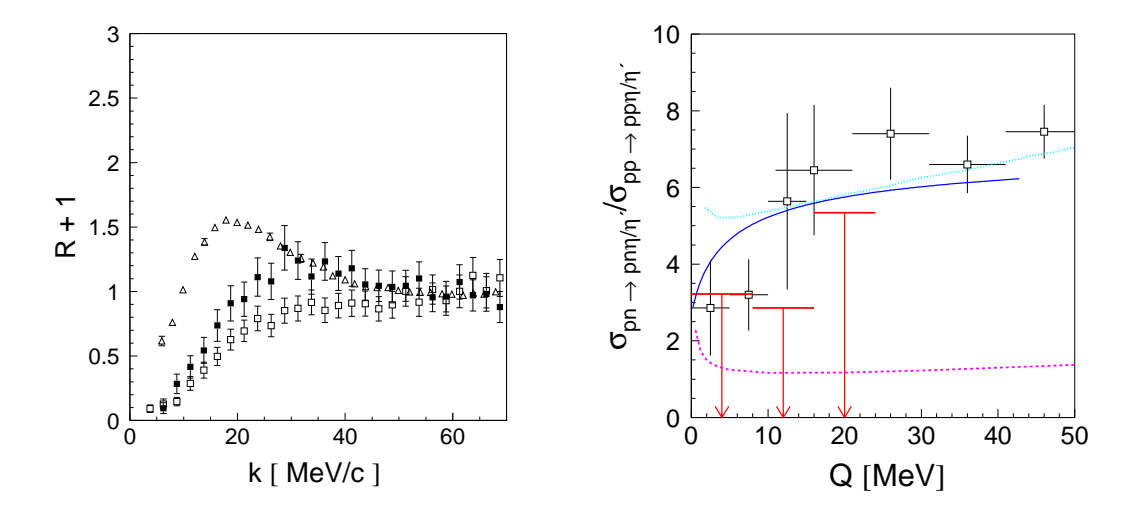


Figure 2: (Left panel) The two-proton acceptance corrected correlation functions normalized to the corresponding simulated correlation function for a point-like source. Results for the $pp \to pp\eta$ (full squares) and $pp \to pp + pions$ (open squares) are compared to the two-proton correlation function determined from heavy ion collisions (triangles). (Right panel) Upper limit of the ratio $(R_{\eta'})$ of the total cross sections for the $pn \to pn\eta'$ and $pp \to pp\eta'$ reactions (arrows) in comparison with the ratio (R_{η}) determined for the η meson (open squares). The superimposed solid line indicates a result of a fit to the R_{η} data taking into account the final state interaction of nucleons. The dotted line presents the result of calculations performed under assumption of a dominance of the $S_{11}(1535)$ resonance in the production process and the dashed line denotes the result obtained within a covariant effective meson-nucleon theory including meson and nucleon currents with the nucleon resonances $S_{11}(1650)$, $P_{11}(1710)$ and $P_{13}(1720)$.

DIRECT DETERMINATION OF THE η' MESON WIDTH

E. CZERWIŃSKI* for the COSY-11 Collaboration[†]

In the review by the Particle Data Group (PDG) [1], two values for the total width of the η' meson are given. One of these values, $(0.30\pm0.09)~{\rm MeV/c^2}$, results from the average of two measurements [2, 3], though only in one of these experiments was $\Gamma_{\eta'}$ extracted directly based on the mass distribution [3]. The second value $(0.205\pm0.015)~{\rm MeV/c^2}$, recommended by the PDG, is determined by fit to altogether 51 measurements of partial widths, branching ratios, and combinations of particle widths obtained from integrated cross sections [1]. The result of the fit is strongly correlated with the value of the partial width $\Gamma(\eta' \to \gamma \gamma)$, which causes serious difficulties when the total and the partial width have to be used at the same time, like e.g. in studies of the gluonium content of the η' meson [4, 5]. This encourage us to perform precise direct measurement of the total width of the η' meson.

The reaction $pp \to pp\eta'$ measured at five different beam momenta using COSY-11 detector setup [6] was used for the determination of the total width of the η' meson, which was directly derived from the mass distributions independently of other properties of this meson, like e.g. partial widths or production cross sections. The η' meson was produced in proton-proton collisions via the $pp \to pp\eta'$ reaction and its mass was reconstructed based on the momentum vectors of protons taking part in the reaction. The schematic view of the COSY-11 detector setup is presented in Fig. 1. The reader interested in the description of the detectors and analysis

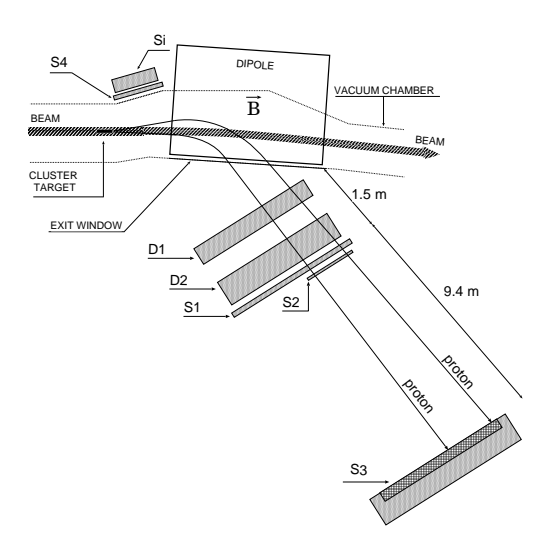


Figure 1: Schematic view of the COSY-11 detector setup (top view). S1, S2, S3 and S4 denote scintillator detectors, D1 and D2 indicate drift chambers and Si stands for the silicon-pad detector.

procedures can find detailed informations in Ref. [7, 8]. The momentum of the COSY beam [9] and the dedicated zero degree COSY-11 facility enabled the measurement at an excess energy of only a fraction of an MeV above the kinematic threshold for the η' meson production. This was the most decisive factor in minimizing uncertainties of the missing mass determination, since at threshold the partial derivative of the missing mass with respect to the outgoing proton momentum

^{*}Institute of Physics, Jagiellonian University, 30-059 Cracow, Poland and Institute for Nuclear Physics and Jülich Center for Hadron Physics, Research Center Jülich, 52425 Juelich, Germany and INFN, Laboratori Nazionali di Frascati, 00044 Frascati, Italy, e-mail address: eryk.czerwinski@lnf.infn.it

[†]The COSY–11 Collaboration: E. Czerwiński, R. Czyżykiewicz, D. Gil, D. Grzonka, B. Kamys, A. Khoukaz, J. Klaja, P. Klaja, W. Krzemień, P. Moskal, W. Oelert, J. Ritman, T. Sefzick, M. Siemaszko, M. Silarski, J. Smyrski, A. Täschner, M. Wolke, J. Zdebik, M. Zieliński, W. Zipper

tends to zero. In addition, close to threshold the signal-to-background ratio increases due to the more rapid reduction of the phase space for multimeson production than for the η' .

Based on the η' meson mass spectra reconstructed for 2300 events with the experimental resolution of 0.3 MeV/c² the total width of the η' meson was determined. The systematic error was estimated by studying the sensitivity of the result to the variation of parameters describing the experimental conditions in the analysis and in the simulation [7, 8]. The final missing mass spectra are presented in Fig. 2. The total width of the η' meson was extracted from the missing-mass

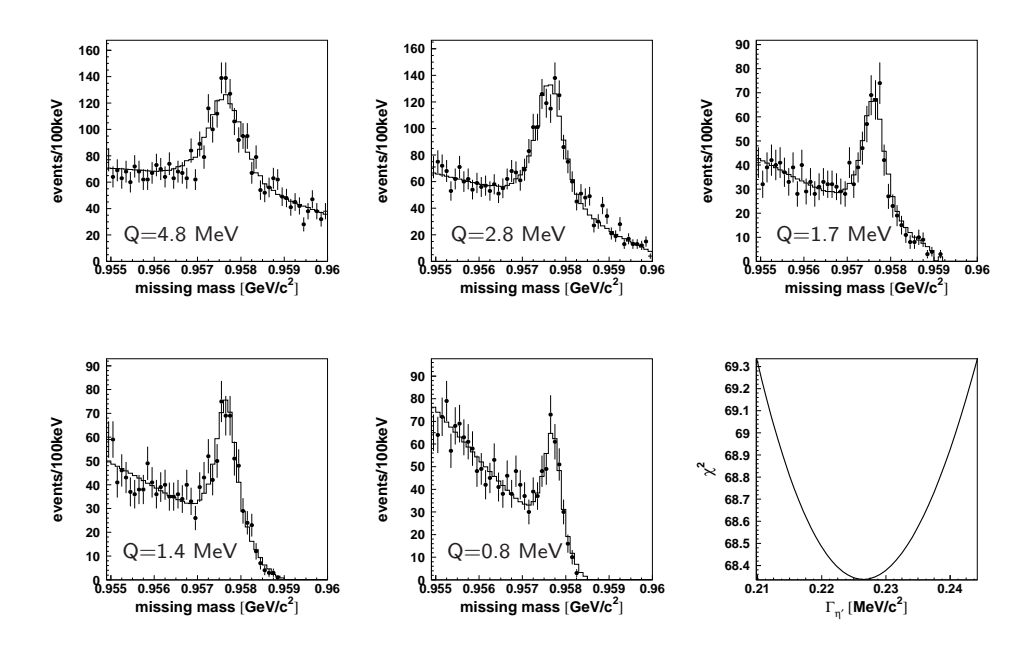


Figure 2: The missing-mass spectra for the $pp \to ppX$ reaction. The η' meson signal is clearly visible. The experimental data are presented as points, while in each plot the line corresponds to the sum of the Monte Carlo generated signal for the $pp \to pp\eta'$ reaction with $\Gamma_{\eta'} = 0.226 \text{ MeV/c}^2$ and the background obtained from another energy. The plot at the bottom right of the figure presents χ^2 as a function of the $\Gamma_{\eta'}$.

spectra and amounts to $\Gamma_{\eta'} = 0.226 \pm 0.017 ({\rm stat.}) \pm 0.014 ({\rm syst.}) \ {\rm MeV/c^2}$. The result does not depend on knowing any of the branching ratios or partial decay widths. The extracted $\Gamma_{\eta'}$ value is in agreement with both previous direct determinations of this value [3, 2], and the achieved accuracy is similar to that obtained by the PDG [1].

- [1] C. Amsler et al., Phys. Lett. **B667**, 1 (2008).
- [2] R. Wurzinger et al., Phys. Lett. **B374**, 283 (1996).
- [3] D. M. Binnie et al., Phys. Lett. **B83**, 141 (1979).
- [4] B. Di Micco, Acta. Phys. Pol. Proc. Suppl. B2, 63 (2009).
- [5] F. Ambrosino et al., J. High Energy Phys. 07 (2009) 105.
- [6] S. Brauksiepe et al., Nucl. Instrum. Methods Phys. Res. A376, 397 (1996).
- [7] E. Czerwiński, PhD dissertation, Jagiellonian University, 2009; arXiv:0909.2781.
- [8] E. Czerwinski, P. Moskal et al., Phys. Rev. Lett. 105, 122001 (2010).
- [9] R. Maier et al., Nucl. Instrum. Methods Phys. Res. A390, 1 (1997).

SOME OPEN ISSUES IN η AND η' PHOTOPRODUCTION

KANZO NAKAYAMA, F. Huang, M. Döring, and H. Haberzettl

The current knowledge of most of the nucleon resonances comes primarily from the study of πN scattering and pion photoproduction reactions. In recent years, the study of other meson production reactions has intensified in search of so-called missing resonances. These are resonances that are predicted by quark models but not observed in the existing experimental data. Since it is conceivable that these resonances escape detection in the usual pion-production channels simply because they couple only weakly to the pion but might otherwise couple more strongly to other mesons, it is important to study such competing meson-production reactions in the hope of revealing at least some of the "missing" resonances. In this contribution, some of the open issues in both the η' and η photoproduction reactions are discussed. The theoretical model adopted here for describing these meson photoproduction reactions is based on an effective Lagrangian approach, whose details are given in Ref. [1]. It includes the nucleonic, mesonic and nucleon resonance currents and is fully gauge invariant as demanded by the generalized Ward-Takahashi identity.

Until recently, not many data existed for η' photoproduction, but this situation is now changing rapidly as the new high-precision data on the free proton as well as on the quasi-free proton and neutron processes are being measured. The theoretical model of Ref. [1] reproduces extremely well $(\chi^2/N \cong 0.5)$ the very-high-precision angular-distribution data measured recently [2] in the energy range from threshold to W = 2.35 GeV with a minimum set of four resonances. The new high-precision cross-section data certainly impose a more stringent constraint on the resonance parameters than compared to earlier cross-section data, however, they are not sufficient to determine these parameters uniquely. For that one still requires spin observables. Apart from the insufficient number of observables (measured experimentally), some of the features that contribute to our current inability to fix the resonance parameters in η' photoproduction are: (a) the phase of the $\eta'N$ scattering is not known, (b) no known resonance couples to η' . Also, as compared to the more widely studied π and/or η photoproductions, here, there is nothing to help fix the phase of the dominant threshold amplitude, such as Watson's theorem in π photoproduction, or a dominant resonance like $S_{11}(1535)$ in η photoproduction. Furthermore, there is an ambiguity as to how one should treat the dominant background contribution: in the MAID model [3], the reggeized ρ and ω t-channel contributions have a destructive interference between them, while in the model of Ref. [1], the ρ and ω meson-exchange contributions are constructive. This phase difference in the background contribution — which is non-negligible — certainly leads to a difference in the extracted resonance parameters from the two models. Data at higher energies beyond the resonance region may help fix the relative sign of these two contributions when they become available. Experimentally, on the other hand, there is a noticeable discrepancy between the recent cross-section data sets from the CLAS [2] and CBELSA/TAPS [4] Collaborations, especially at high energies and backward angles.

Unlike η' photoproduction, the η photoproduction reaction has been studied extensively. Apart from the fact that this reaction serves as an isospin filter since the η meson is an isoscalar meson (as is the η' meson), it reveals most clearly the $S_{11}(1535)$ resonance which couples strongly to the ηN channel. Our model reproduces the recent differential cross section and beam asymmetry data [5] with a very reasonable fit quality ($\chi^2/N \cong 1.8$). Unlike in η' photoproduction, here the resonance parameters are much better constrained. Neither the present model nor other existing

^{*}Department of Physics and Astronomy, University of Georgia, Athens, GA 30602, U.S.A. and Institut für Kernphysik and Jülich Center for Hadron Physics, Forschungszentrum Jülich, 52425 Jülich, Germany (Email: nakayama@uga.edu).

[†]Department of Physics and Astronomy, University of Georgia, Athens, GA 30602, U.S.A.

 $^{^{\}ddagger}$ Institut für Kernphysik and Jülich Center for Hadron Physics, Forschungszentrum Jülich, 52425 Jülich, Germany.

[§]Center for Nuclear Studies, Department of Physics, The George Washington University, Washington, DC 20052, U.S.A.

models can describe the measured target asymmetry [6], especially at energies close to threshold. Unlike the beam asymmetry, which involves the real part of a product of spin matrix elements, the target asymmetry (T) involves the imaginary part of a product of spin matrix elements. Therefore, the latter observable is expected to be more sensitive to the final-state interaction. Unfortunately, so far, no calculation exists that explicitly includes the final-state interaction. The recoil-nucleon polarization (P) involves the same expression in terms of the spin matrix elements as T, except for one of the additive terms which has a different sign than T. In attempting to describe P, we, therefore, expect difficulties similar to those found when describing T. In this regard, the combinations $T \pm P$ may help isolate the source of the problem with the current models in describing T.

In recent years, the η photoproduction reaction has received renewed attention because of an observed bump structure around $\sqrt{s} \approx 1.67$ GeV in the ratio of the total cross sections, $\sigma_n/\sigma_p \equiv \sigma(\gamma n \to \eta n)/\sigma(\gamma p \to \eta p)$ in the quasi-free processes [7]. This bump structure was interpreted as a potential signal of a non-strange member of anti-decuplet pentaquarks. Here, we address this issue within an SU(3) coupled-channel chiral unitary approach. Within this approach, the bump structure arises naturally as a result of coupled-channel effects due to the strong coupling to the intermediate $K\Lambda$ and $K\Sigma$ channels [8]. In the quasi-free proton case, the photon can couple to the charged Kaon in the intermediate $K^+\Lambda$ state, while in the quasi-free neutron case, this contribution is absent, for the corresponding intermediate state is $K^0\Lambda$ and the photon does not couple to a neutral Kaon. This coupled-channel effect is a direct consequence of the dynamics driven by the Weinberg-Tomozawa interaction together with the strong coupling to $K\Lambda$ and $K\Sigma$ channels resulting from SU(3) symmetry. The present result does not rule out other explanations for the bump structure, such as narrow resonances. On the other hand, the prediction of our chiral unitary model for σ_n/σ_p in quasi-free $\gamma N \to K\Lambda$ processes on the deuteron does not exhibit any bump structure, unlike for η photoproduction. The measurement of σ_n/σ_p in $K\Lambda$ photoproduction, therefore, can shed light on the accuracy of our chiral unitary model. Furthermore, it is interesting to note that a measurement of the longitudinal spin transfer coefficient (L_z) in $\gamma N \to \eta N$, together with the corresponding unpolarized cross sections, is capable of disentangling the coupled-channel scenario discussed above from the narrow-resonance scenario in a model-independent way. Alternatively, measurements of the target and recoil polarizations with a circularly polarized photon beam can also distinguish between the two scenarios in a model-independent way. Of course, such measurements pose enormous experimental challenges.

- K. Nakayama and H. Haberzettl, Phys. Rev., C69, 065212, (2004); ibid., C73, 045211, (2006);
 K. Nakayama, Yongseok Oh, and H. Haberzettl, arXiv:0803.3169.
- [2] M. Williams et al., CLAS Collaboration, Phys. Rev., C80, 045213, (2009).
- [3] W.-T. Chiang et al., Phys. Rev., C68, 045202, (2003).
- [4] V. Crede et al., CBELSA/TAPS Collaboration, Phys. Rev., C80, 055202, (2009).
- [5] O. Bartalini et al., GRAAL Collaboration, Eur. Phys. J., A33, 169, (2007).
- [6] A. Bock et al., PHOENICS Collaboration, Phys. Rev. Lett., 81, 534, (1998).
- [7] V. Kuznetsov et al., GRAAL Collaboration, Phys. Lett., B647, 23, (2007).
- [8] M. Döring and K. Nakayama, Phys. Lett., **B683**, 145, (2010).

THE $pd o ^3 { m He} \eta \,\, \pi^0 \,\, { m REACTION}$ AT $T_p = 1450 \,\, { m MeV}$

KARIN SCHÖNNING* for the CELSIUS/WASA Collaboration

Recently, many important results on photo-production of the $\eta\pi^0$ system have appeared. Chrystal Ball/TAPS data from the $\gamma p \to \pi^0 \eta p$ reaction [1] were interpreted in terms of a dominant cascade decay of the $D_{33}\Delta(1700)$ isobar through the s-wave $\Delta(1700) \to \eta\Delta(1232)$ followed by the p-wave $\Delta \to \pi^0 p$ [2]. A similar interpretation is possible also for $\gamma d \to \pi^0 \eta d$ data [3].

To further investigate the role of resonances like $\Delta(1700)$, $\Delta(1232)$ and $N^*(1535)$ in $\pi^0\eta$ production and the competition between the ${}^3{\rm He}\pi^0$ and ${}^3{\rm He}\eta$ interactions, the $pd \to {}^3{\rm He}\eta\pi^0$ reaction has been studied with the WASA detector [4] at the CELSIUS storage ring in Uppsala, Sweden.

The experiment was carried out using a 1450 MeV proton beam impinging on a deuterium pellet target. The ³He ions were measured in a Forward Detector and the photons from the π^0 and η decays were in a central electromagnetic calorimeter. Only the $\eta \to \gamma \gamma$ decay channel was considered (BR=39.3%). Events with one identified ³He, four photons, one π^0 candidate and one η candidate were selected. Furthermore, the missing momentum of the ³He was required to match the total momentum of the four photons. Finally, all events where two good π^0 candidates could be formed from the four photons, were rejected. More details about the selection criteria are given in Ref. [5]. The background from $2\pi^0$ production is discussed in some detail in Ref. [6] and $3\pi^0$ production was studied in Ref. [7]. The $\eta\pi^0$ events were identified by the peak at the η mass in the ³He π^0 missing mass spectrum, see figure 1. The events fulfilling all selection criteria were background subtracted, using simulated phase space events from $2\pi^0$ and $3\pi^0$ production normalised to the cross sections given in Refs. [6, 7]. The data were then corrected for acceptance and normalised, all following the proceedure described in Ref. [5]. This resulted in a measured cross section of $23.6 \pm 1.6 \pm 2.2$ nb plus a normalisation uncertainty of 14%. Details about the normalisation proceedure can be found in [8].

Invariant mass distributions of the ${}^3{\rm He}\pi^0$, ${}^3{\rm He}\eta$ and $\eta\pi^0$ systems were reconstructed and are shown in figures 2-4. The ${}^3{\rm He}\pi^0$ invariant mass is strongly enhanced near $m_p + M_{\Delta(1232)}$ which indicates the importance of the $\Delta(1232)$ resonance. Since no microscopic model of $\eta\pi^0$ production in pd collisions exists as yet, the p-wave rise due to the $\Delta(1232)$ was simulated by weighting the phase space Monte Carlo data with the momentum squared k^2 of the π^0 in the ${}^3{\rm He}\pi^0$ rest system. These weighted MC data were found to reproduce the data well. The ${}^3{\rm He}\eta$ invariant mass is peaked near the $m_p + M_{N(1535)}$ sum, which suggest involvement of the $N^*(1535)$ resonance. However, it turned out that the weighted MC data reproduce also this behaviour. Thus, the low mass enhancement in the ${}^3{\rm He}\eta$ system may very well be an effect of the $\Delta(1232)$ in the ${}^3{\rm He}\pi^0$ interaction. The $\eta\pi^0$ invariant mass distribution show no sign of any "ABC-like" effect (see e.g Ref. [9]) nor any significant high mass enhancement due to the $a_0(980)$ resonance. The latter is not surprising since we are far below the nominal threshold of $a_0(980)$ production.

For the future it would be interesting with high statistics measurements by e.g. WASA at COSY, at both higher and lower beam energies. The influence from the $\Delta(1232)$ resonance should have an impact on the energy dependence of the cross section and also on the angular distributions of the final state particles. Some angular distributions were studied with the CELSIUS/WASA data presented here and they are consistent with isotropy, though with large error bars. It is also not clear from this data what the dynamical origin of the η meson is. Does it come from the $N^*(1535)$ in a two-step process or from the subsequent decay of the $\Delta(1700)$? It will be interesting to see what a new generation of measurements can tell us.

^{*}formerly at Uppsala University. Present email address: karin.schonning@cern.ch

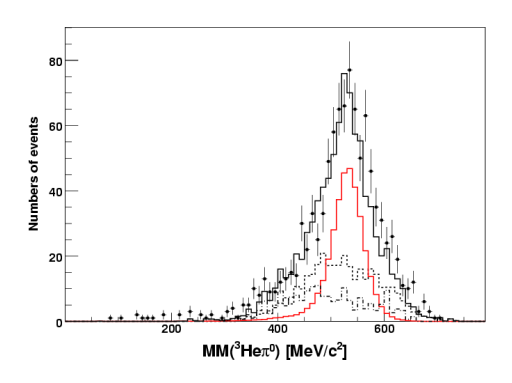


Figure 1: (colour online) The missing mass of the $^3{\rm He}\pi^0$ -system. The dots are data, the red histogram simulated $pd \to ^3{\rm He}\eta\pi^0$ events, the dashed histogram phase space $pd \to ^3{\rm He}2\pi^0$ MC data, the dashed-dotted phase space $pd \to ^3{\rm He}3\pi^0$ and the solid line shows the sum of all simulated events.

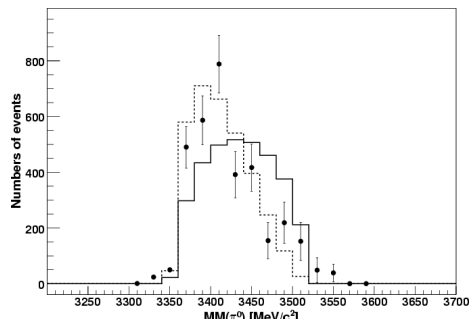


Figure 3: The missing mass of the π^0 , which is equivalent to the invariant mass of the ${}^3{\rm He}\eta\text{-system}.$

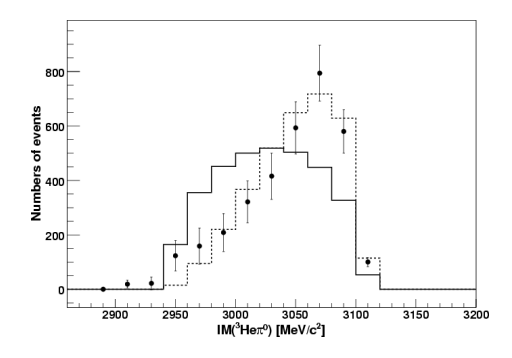


Figure 2: The invariant mass of the $^3{\rm He}\pi^0$ -system. The dots are background subtracted and acceptance corrected data. The solid line histogram phase space simulated $pd \to ^3{\rm He}\eta\pi^0$ events and the dashed histogram is phase space events weighted with the momentum squared of the π^0 in the $^3{\rm He}\pi^0$ rest system.

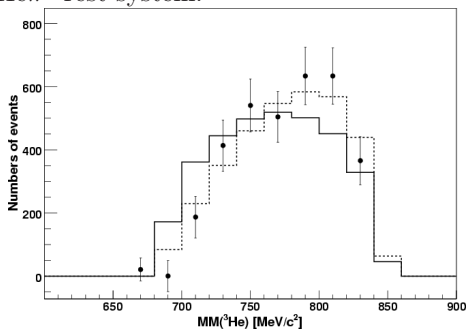


Figure 4: The missing mass of the ${}^{3}\text{He}$, which is equivalent to the invariant mass of the $\eta\pi^{0}$ system.

- [1] V. L. Kashevarov et al., Eur. Phys. J., A 42, 141, (2009).
- [2] M. Doring, E. Oset and D. Strottman Phys. Rev., C 73, 045209, (2006).
- [3] B. Krusche, I.Jaegle, Acta Phys. Polon. B Proc. Suppl., 2, 51, (2009).
- [4] Chr. Bargholtz et al., Nucl. Instr. Meth., A 594, 339, (2008).
- [5] K. Schönning et al. Phys. Lett., **B** 685, 33, (2010).
- [6] K. Schönning, Meson production in pd collisions, Ph. D. thesis, Uppsala University (2009).
- [7] K. Schönning et al., Eur. Phys. J., A 45, 11, (2010).
- [8] K. Schönning et al. Phys. Rev., C 79, 044002, (2009).
- [9] M. Bashkanov et al. Phys. Lett., B 637, 223, (2006).

Investigation of Double Pion Production in pp collisions at T_p =1400 MeV

TAMER TOLBA *, ** AND JAMES RITMAN * on behalf of the WASA-at-COSY Collaboration

1.1 Introduction

The reaction $pp \to pp\pi^0\pi^0$ was investigated using the WASA at COSY facility. The total and differential cross sections of the double pion production at a beam energy of 1400 MeV have been evaluated. Preliminary results [1] are presented here and compared to theoretical expectations. Recently, double pion production has been extensively studied in the $pp \to pp\pi\pi$ reaction from near threshold (T_p =775 MeV) up to T_p =1300 MeV [2, 3]. In contrast, experimental information on the double pion production in NN collisions is scarce at higher energies.

A full reaction model describing the double pion production in NN collisions has been developed by a theoretical group at the University of Valencia - Spain at the end of the 1990s [4]. The model involves chiral Lagrangian terms for nucleons and pions (non-resonant terms) plus amplitudes describing the $\Delta(1232)$ and Roper excitations at energy ranges from threshold up to 1400 MeV. This model was slightly modified by a group from Tübingen University - Germany [5] and denoted as Valencia model in the following.

Here we report on the total cross section and the reaction mechanism for the $pp \to pp\pi^0\pi^0$ reaction at $T_p = 1400$ MeV where no previous experimental information is available.

1.2 Experimental Setup and Data Analysis

The experimental data analyzed in this work were collected using the Wide Angle Shower Apparatus (WASA) [6] at the COSY accelerator in the Forschungszentrum Jülich, Germany. The detector provides nearly full solid angle coverage for both charged and neutral particles, and allows multi-body final state hadronic interactions to be studied with high efficiency.

The recoil protons are detected in the forward detector and identified using the Δ E-E method. The two π^0 are reconstructed in the central detector from their two-photon decays. The criterion used in the selection of the event sample demands 1 or 2 charged tracks in the forward detector and exactly 4 neutral clusters in the central detector with no restrictions on charged tracks in the central detector. With these constraints, the geometrical acceptance is found to be $\sim 45\%$.

1.2.1 Results

The total cross section of the neutral double pion production at $T_p=1400$ MeV is found to be $\sigma_{tot}=(324\pm61)~\mu$ b. The data were corrected for the detector acceptance generated by a Monte Carlo model tuned in order to match the experimental data (explained in detail in Ref. [1]). Figure 1.1 shows the new point determined in this work compared with the previous work at lower beam energies [2, 3] and the theoretical expectations calculated with the Valencia model [4]. Since previous experimental data do not exist for the $pp \to pp\pi^0\pi^0$ reaction at the proton beam energy used here, a direct comparison between this result and previous data is not possible. However, our result shows the same rising trend of the previous cross section values starting at \sim 1170 MeV. This new data is lower by factor of two compared to the total cross section calculated by the theoretical expectations from the Valencia model (the solid black line in Figure 1.1), but it matches very well their expected cross section for the double $\Delta(1232)$ process, i.e. in the case that the Roper excitation process is negligible (the dashed-dotted green line in Figure 1.1).

In order to study the double pion production mechanism, the differential cross section distribution for different kinematical variables describing the system have been determined. The results are compared to the expectations based on the uniform population of the available phase space

^{*}Institut für Kernphysik, Forschungszentrum Jülich, 52428 Jülich, Germany

 $^{{\}rm **T.Tolba@fz-juelich.de}$

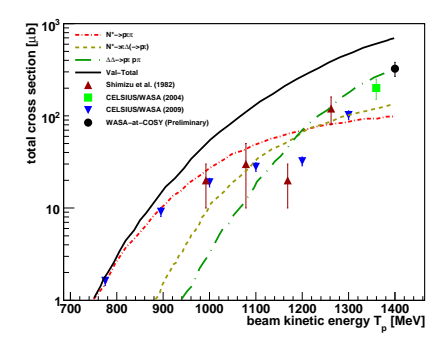


Figure 1.1: The total cross section for the $pp \to pp\pi^0\pi^0$ reaction as a function of beam kinetic energy. The result presented here at $T_p=1400$ MeV denoted by the black dot together with previous data and theoretical calculations: From near threshold up to 1300 MeV (blue inverted triangles) [3], at 1360 MeV (green square) [7], bubble chamber results (dark red triangles) [2] and the theoretical expectations [4] (where the long dashed dotted line represents the production via double $\Delta(1232)$, the dashed line represents the production via Roper decay $N^*(1440) \to D^*(1440) \to D^*(1440)$

(PS) and to the theoretical expectations. The theoretical models are normalized to the same total cross section as the data.

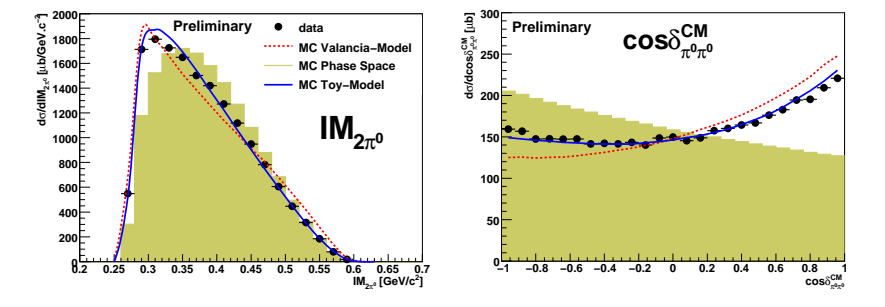


Figure 1.2: Comparison of the data (black dots) with theoretical expectations: phase space (shaded area), the Valencia model (red dashed line) and the tuned Monte Carlo model (blue solid line), for the differential cross section as functions of the $2\pi^0$ invariant mass (left plot) and the $2\pi^0$ opening angle (right plot).

From Figure 1.2 we see that the $2\pi^0$ invariant mass $(IM_{2\pi^0})$ distribution (left plot) shows a behavior similar to phase space with a systematic enhancement at low $IM_{2\pi^0}$. This indicates the tendency of the two pions to be emitted parallel in the overall center of mass frame. This can be clearly seen in the two pion opening angle distribution $\cos \delta^{CM}_{\pi^0\pi^0}$ (right plot), where the enhancement at $\cos \delta^{CM}_{\pi^0\pi^0} = 1$ corresponds to a small angle between the pions.

The upper left frame of Figure 1.3 shows the correlation of the pairs of the invariant mass square of the $p\pi^0$ system $(IM_{p\pi^0}^2)$. Evidence for the $\Delta(1232)$ resonance can be seen as a strong enhancement at $IM_{p\pi^0}^2=1.52~{\rm GeV^2}/c^4$, which is the square of the $\Delta(1232)$ mass. This observation is supported by the projection onto the $IM_{p\pi^0}^2$ axis (lower left plot) where the enhancement at m_Δ^2 is observed.

In contrast to the clear evidence of the $\Delta(1232)$, there is no significant evidence for the presence of the Roper resonance $N^*(1440)$ in the y-axis of the $IM^2_{p\pi^0}$ versus $IM^2_{p\pi^0\pi^0}$ distribution, as shown in Figure 1.3 (upper right plot). This observation is supported by the one-dimensional projection onto the $IM^2_{p\pi^0\pi^0}$ axis (lower right plot).

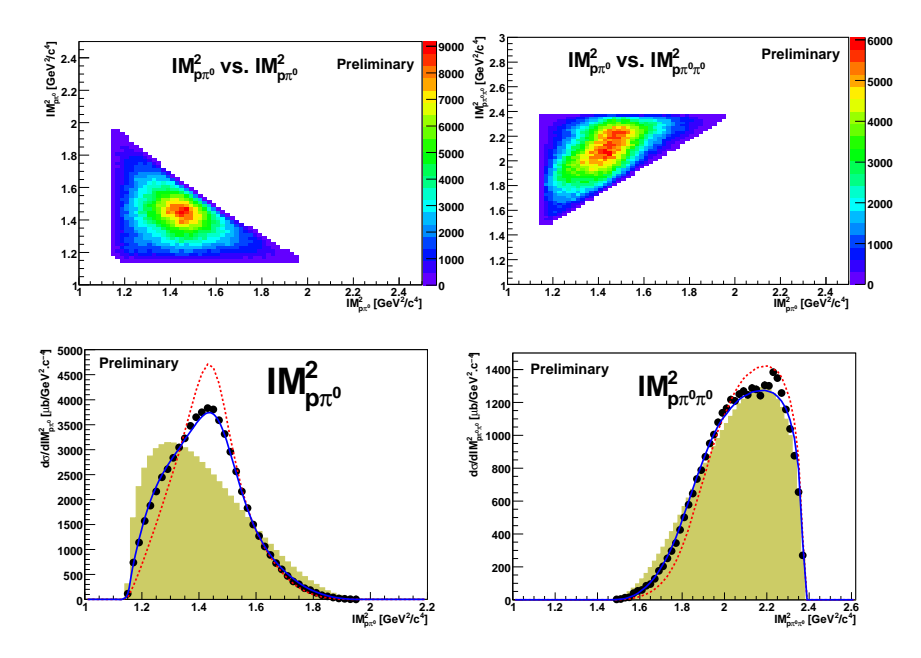


Figure 1.3: The same as Figure 1.2 except for differential cross section distributions as functions of $IM_{p\pi^0}^2$ versus $IM_{p\pi^0}^2$ (upper left, data only), $IM_{p\pi^0}^2$ versus $IM_{p\pi^0\pi^0}^2$ (upper right, data only), $IM_{p\pi^0}^2$ (lower left), and $IM_{p\pi^0\pi^0}^2$ (lower right).

1.3 Conclusion and Outlook

The total as well as the differential cross sections of the $pp \to pp\pi^0\pi^0$ reaction at $T_p=1400~{\rm MeV}$ have been determined and compared to the previous experimental data and theoretical expectations. The results show a good agreement with the expectations that the $\pi^0\pi^0$ production, at the energy studied here, is dominated by $\Delta\Delta$ excitations as the intermediate state, with no significant contribution from the Roper resonance.

The next step is to investigate the production of charged pions $(\pi^+\pi^-)$ in order to study the complete double pion production mechanisms, of which the vector mesons (e.g. $\rho^0(770)$) are expected to play an important role.

- [1] T. Tolba, PhD Thesis, Bochum University, (2010).
- [2] F. Shimizu et al., Nucl. Phys., A386, 571, (1982).
- [3] T. Skorodko et al., Phys. Lett., **B679**, 30, (2009).
- [4] L. Alvarez-Ruso et al., Nucl. Phys., A633, 519, (1998).
- [5] T. Skorodko, PhD Thesis, Tübingen University, (2009).
- [6] H. H. Adam et al., arxiv: nucl-ex/0411038.
- [7] I. Koch, PhD Thesis, Uppsala University, (2004).

$\gamma\gamma$ PHYSICS WITH THE KLOE EXPERIMENT

CECILIA TACCINI* for the KLOE Collaboration

The term " $\gamma\gamma$ physics" stands for the study of the reaction $e^+e^- \to e^+e^-\gamma^*\gamma^* \to e^+e^-X$, where X is some arbitrary final state allowed by conservation laws. $\gamma\gamma$ scattering at e^+e^- colliders can give access to states with $J^{PC}=0^{\pm+};2^{\pm+}$, not directly coupled to one photon ($J^{PC}=1^{--}$). These processes, of order α^4 , depend on the logarithm of the center of mass energy E, so that for E greater than a few GeV they dominate hadronic production at e^+e^- colliders. For quasi-real photons the number of produced events can be estimated from the expression

$$N = L_{ee} \int dW_{\gamma\gamma} \frac{dL}{dW_{\gamma\gamma}} \sigma(\gamma\gamma \to X)$$
 (1)

where L_{ee} is the e^+e^- luminosity, $W_{\gamma\gamma}$ the photon-photon center of mass energy $(W_{\gamma\gamma} = M_X)$, $dL/dW_{\gamma\gamma}$ the photon-photon flux and σ the cross section into a given final state. By neglecting single powers of $\ln(E/m_e)$, when the scattered leptons are undetected in the final state one has

$$\frac{dL}{dW_{\gamma\gamma}} = \frac{1}{W_{\gamma\gamma}} \left(\frac{\alpha}{2\pi} \ln \frac{E}{m_e}\right)^2 f(z) \qquad z = \frac{W_{\gamma\gamma}}{2E} \tag{2}$$

with f(z) (Low function) [1, 2] given by

$$f(z) = (2+z^2)^2 \ln \frac{1}{z} - (1-z^2)(3+z^2)$$
(3)

The two $\gamma\gamma$ processes studied with KLOE are $e^+e^- \to e^+e^-\eta$ and $e^+e^- \to e^+e^-\pi^0\pi^0$. DA Φ NE is an e^+e^- collider operating at $\sqrt{s} \simeq M_\phi = 1.02$ GeV. The KLOE detector consists of a large volume drift chamber surrounded by a lead and scintillating fibers calorimeter. Charged particle momenta are reconstructed with resolution $\sigma_p/p \simeq 0.4\%$ for large angle tracks. Calorimeter clusters are reconstructed with energy and time resolution of $\sigma_E/E = 5.7\%/\sqrt{E(\text{GeV})}$ and $\sigma_t = 57 \text{ ps}/\sqrt{E(\text{GeV})} \oplus 100 \text{ ps}$. The sample used for the analyses consists of data taken at $\sqrt{s} = 1 \text{ GeV}$, which allows reduction of the background from ϕ decays, with an integrated luminosity of 240 pb⁻¹. Data are processed with a dedicated $\gamma\gamma$ filter asking for at least two photons (prompt clusters not associated to tracks) with energy E > 15 MeV and polar angle $20^\circ < \theta < 160^\circ$, the most energetic with E > 50 MeV, the fraction of energy carried by photons $R = (\sum_{\gamma} E_{\gamma})/E_{cal} > 0.3$ and the total energy in the calorimeter $100 < E_{cal} < 900 \text{ MeV}$. The latter requirement rejects low energy background and the high rate processes $e^+e^- \to e^+e^-$, $e^+e^- \to \gamma\gamma$.

A search for the $e^+e^- \to e^+e^-\eta$ process is performed, with $\eta \to \pi^+\pi^-\pi^0$. The selection of these events asks for two photons constrained to originate from a π^0 decay and two tracks with opposite curvature coming from the collision point. The charged pion mass is assigned to the two tracks and a least squares function based on Lagrange multipliers imposes that $\pi^+\pi^-\pi^0$ come from an η decay. Therefore most background events are suppressed, except for the irreducible process $e^+e^- \to \eta\gamma \to \pi^+\pi^-\pi^0\gamma$, with the monochromatic photon, $E_{\gamma} = 350$ MeV, lost in the beam pipe. For these background events, however, the correlation between the squared missing mass, M_{miss}^2 , and the longitudinal momentum, p_L , of the $\pi^+\pi^-\pi^0$ system is rather different than for the signal. Further criteria are applied to suppress processes with photons and e^+e^- in the final state. The MC generator used for the signal [3] allows the full phase space generation of $e^+e^- \to e^+e^-\gamma^*\gamma^* \to e^+e^-\eta$ events. Fig. 1 (left) shows the distribution of M_{miss}^2 for data fitted with the superposition of MC shapes for signal and background. An independent fit is performed with the distribution of p_L . Both fits show the same yields for the background processes and more than 600 signal events. The cross section of the irreducible process $e^+e^- \to \eta\gamma \to \pi^+\pi^-\pi^0\gamma$ is evaluated using the same sample of data and asking for three photons in the final state. A kinematic fit is performed, requiring energy and momentum conservation, and the improved variables are used to fit the distribution of the energy of the recoil photon (center plot of Fig. 1), which yields

^{*}Università Roma Tre and INFN, Sezione Roma Tre

 $\sigma(e^+e^- \to \eta\gamma \to \pi^+\pi^-\pi^0\gamma, 1~{\rm GeV}) = (198 \pm 2_{\rm Stat})~{\rm pb.}$ Systematics are under evaluation. Finally, a search for $e^+e^- \to e^+e^-\pi^0\pi^0$ events is performed, motivated by the interest in the $\gamma\gamma \to \sigma$ dynamics [4]. The main requirements of the data analysis are: four photons originated from $2\pi^0$ decays, no tracks in the drift chamber, photon energy fraction R>0.75, transverse momentum $p_{T4\gamma}<80~{\rm MeV}$. Other cuts on the photon energies are applied to improve the signal to background ratio. The MC used allows for full phase space generation and treats the process $e^+e^- \to e^+e^-\pi^0\pi^0$ including a σ particle as a Breit-Wigner resonance [3]. The spectrum in the 4γ invariant mass compared with the expected backgrounds is shown in Fig. 1 (right). From the plot, an excess is evident at low $M_{4\gamma}$ values, consistent in shape with expectations from $e^+e^- \to e^+e^-\pi^0\pi^0$ events. This is the only new measurement of $\gamma\gamma \to \pi^0\pi^0$ reaction in the region of the σ meson after [5]. Systematic study of the cross section and understanding of the $\sigma \to \pi^0\pi^0$ contribution are in progress.

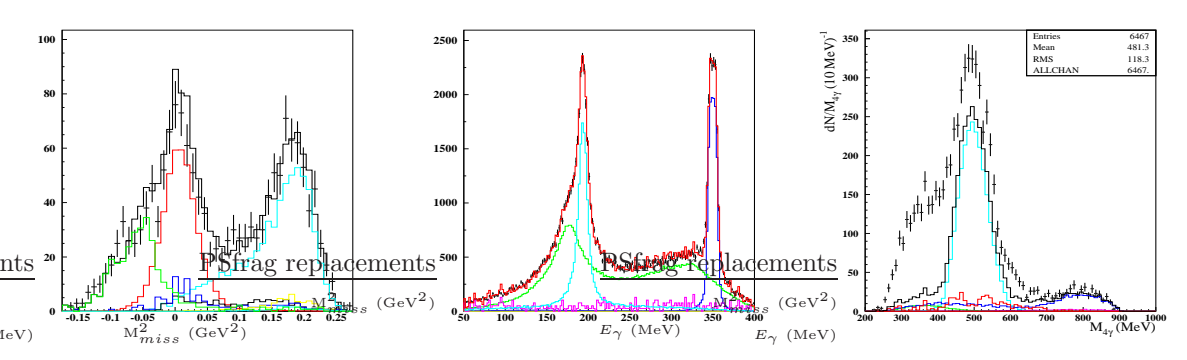


Figure 1: Left: fit of the M_{miss}^2 distribution for the $e^+e^- \to e^+e^-\eta$ analysis. Main contributions are: $e^+e^-\gamma$ (green) at negative M_{miss}^2 values due to the pion mass assigned to e^+e^- tracks, $\eta\gamma$ (red), signal events (ligt blue). Middle: fit of the recoil photon energy spectrum for the $e^+e^- \to \eta\gamma$ analysis. The $\eta\gamma$ peak (blue) and the $\omega\gamma$ peak (light blue) are visible; the broad distribution (green) is due to $\omega\pi^0$ events. Right: $M_{4\gamma}$ spectrum for events selected in the $e^+e^- \to e^+e^-\pi^0\pi^0$ data analysis, compared with the sum of the expected backgrounds from MC. Main background contributions are: $K_S \to \pi^0\pi^0$ (light blue), $\omega(\to \pi^0\gamma)\pi^0$ (blue) and $\gamma\gamma$ (red).

These results are encouraging in view of the forthcoming data taking campaign of the KLOE-2 project [6], when analyses of the on-peak sample will be possible with the information coming from two different tagging detectors: the low energy taggers (LET), located in the region between the two quadrupoles inside KLOE (about 1 m from the IP), and the high energy taggers (HET), located at the exit of the first bending magnet (about 11 m from the IP). The energy range covered will be (160-230) MeV for LET and (425-490) MeV for HET.

- [1] S. J. Brodsky, T. Kinoshita and H. Terazawa, Phys. Rev. D 4, 1532 (1971);
- [2] F. Low, Phys. Rev. 120, 582 (1960);
- [3] F. Nguyen, F. Piccinini and A. D. Polosa, Eur. Phys. J. C 47, 65 (2006);
- [4] C. Amsler, T. Gutsche, S. Spanier and N. A. Törnqvist "Note on Scalar Mesons" in K. Nakamura et al. (Particle Data Group), J. Phys. G 37, 075021 (2010);
- [5] H. Marsiske et al. (Crystal Ball Collaboration), Phys. Rev. D 41, 3324 (1990);
- [6] G. Amelino-Camelia et al., Eur. Phys. J. C 68, 619 (2010)

A COVARIANT FORMALISM FOR THE $\gamma^*N \to N^*$ TRANSITIONS

GILBERTO RAMALHO*†

CFTP, Instituto Superior Técnico, Lisbon, Portugal

In the covariant spectator quark model the $\gamma^*N \to B$ transition current is determined by the (constituent) quark current and by the covariant wave functions Ψ_N for the nucleon and Ψ_B for the baryon B [1, 2]. The quark current is parameterized using vector meson dominance and the wave functions Ψ_B represented in terms of the quark and diquark (quark pair) states of flavor, spin, orbital angular momentum and radial excitations, corresponding to the quantum numbers defining each baryon [1].

Our goal was to study the role of the valence quark degrees of freedom and also the effect of the meson cloud effects, in particular for the inelastic reactions. In general, one can decompose the form factor G_X as $G_X = G_X^B + G_X^{mc}$, where G_X^B is the bare contribution (from valence quarks) and G_X^{mc} the meson cloud contribution [1].

The first application of the model was for the case B=N, the nucleon elastic form factors, where the nucleon was taken as a quark-diquark S-wave system [2]. In that study the quark current and nucleon scalar wave function were calibrated by the experimental data, defining the nucleon wave function and the quark current for future applications. In the nucleon case no pion cloud structure was considered. The parametrization proved to be consistent also with lattice QCD simulations, once the model was extended for the lattice QCD regime where meson cloud mechanisms are negligible [3].

The next application was for the case $B=\Delta$, where the wave function is represented by an admixture of the dominant S-wave with two distinct smaller D-wave components [4, 5]. The calibration of the Δ wave function was done using lattice QCD data, and an excellent fit was achieved [5]. To describe the physical data, a phenomenological pion cloud contribution for the magnetic dipole transition form factor and a pion cloud contribution for the quadrupole form factors based on large N_c limit [5], were added to the extrapolation of lattice to the physical region. The final result is in agreement with the experimental data [5].

The covariant spectator model can also be applied for the radial excitations of the nucleon and $\Delta(1232)$ systems [6, 7]. Because in those cases the wave function of the radial excited state is defined in terms of the lower order states, nucleon or $\Delta(1232)$, there are no additional parameters involved. For the nucleon radial excitation N(1440), also known as Roper resonance, no explicit meson cloud was added. The results are consistent with the experimental data for large Q^2 ($Q^2 > 1.5 \text{ GeV}^2$) [6]. [See the top of Fig. 1]. As for the $\Delta(1600)$, by considering valence quark degrees of freedom only overshoots the data for low Q^2 . However, a simple estimation of the pion cloud effects based on the analogy between the reaction with $\Delta(1232)$ and $\Delta(1600)$, makes the results closer to the data [7] [See the bottom of Fig. 1].

^{*}gilberto.ramalho@cftp.ist.utl.pt

[†]In collaboration with Franz Gross (Thomas Jefferson National Accelerator Facility, Virginia, USA and College of William and Mary, Virginia, USA), M.T. Peña (CFTP, Instituto Superior Técnico, Lisbon, Portugal) and K. Tsushima (CSSM, School of Chemistry and Physics, University of Adelaide, Australia)

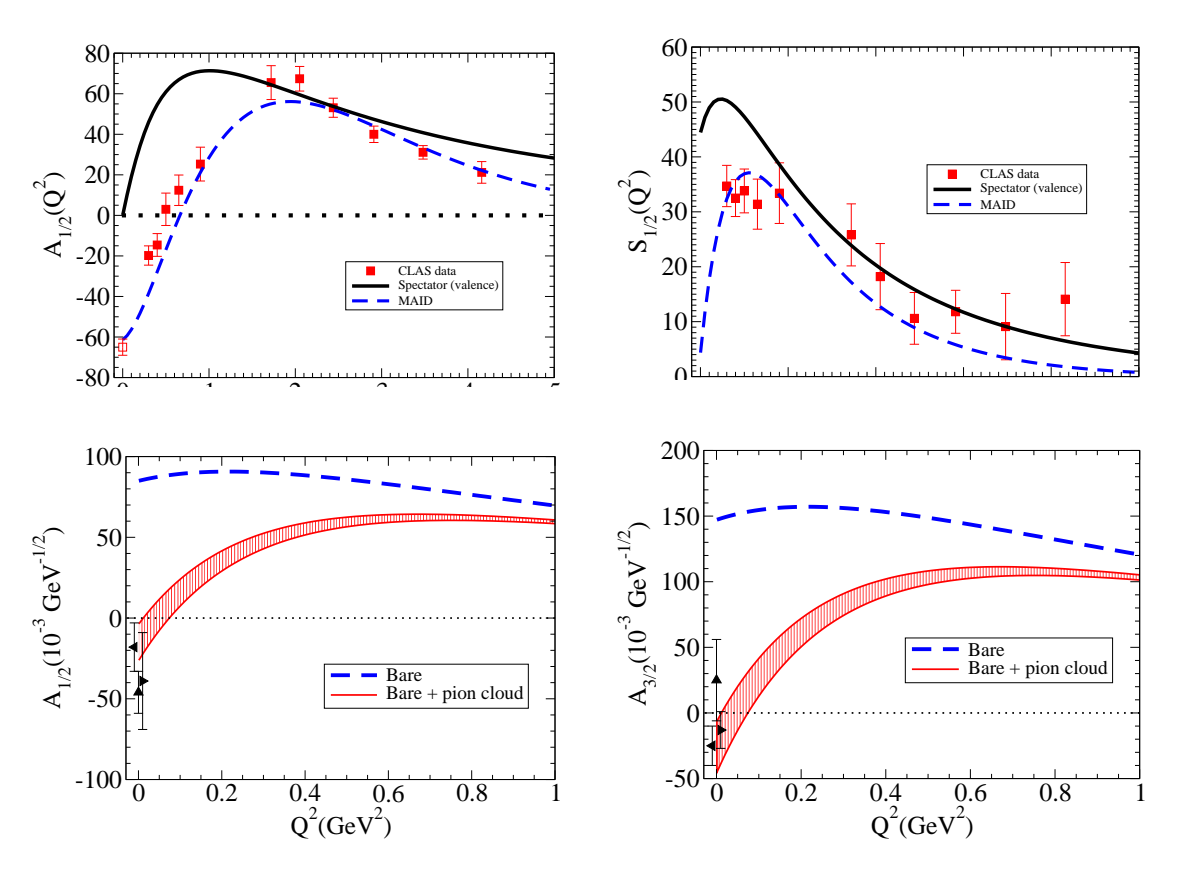


Figure 1: Helicity amplitudes for the $\gamma^*N \to N(1440)$ [6] (top); and $\gamma^*N \to \Delta(1600)$ [7] (bottom) reactions, determined with the spectator quark model. For the $\Delta(1600)$ the pion cloud contribution is also represented.

Other possible applications of the covariant spectator quark model are the determination of the octet and decuplet electromagnetic form factors [8, 9, 10]. A reaction of particular interest for the Workshop corresponds to the B = N(1535), the S11 resonance. The calculation of the $\gamma^* N \to N(1535)$, transition form factors is in progress [11].

- [1] G. Ramalho, F. Gross, M. T. Peña and K. Tsushima, arXiv:1008.0371 [hep-ph].
- [2] F. Gross, G. Ramalho and M. T. Peña, Phys. Rev. C 77, 015202 (2008).
- [3] G. Ramalho and M. T. Peña, J. Phys. G 36, 115011 (2009).
- [4] G. Ramalho, M. T. Peña and F. Gross, *Phys. Rev. D* 78, 114017 (2008).
- [5] G. Ramalho and M. T. Peña, Phys. Rev. D 80, 013008 (2009).
- [6] G. Ramalho and K. Tsushima, Phys. Rev. D 81, 074020 (2010).
- [7] G. Ramalho and K. Tsushima, arXiv:1008.3822 [hep-ph], to appear in Phys. Rev. D.
- [8] F. Gross, G. Ramalho and K. Tsushima, Phys. Lett. B 690, 183 (2010).
- [9] G. Ramalho, K. Tsushima and F. Gross, Phys. Rev. D 80, 033004 (2009).
- [10] G. Ramalho, M. T. Peña and F. Gross, Phys. Rev. D 81, 113011 (2010).
- [11] G. Ramalho and M. T. Peña, work in progress.

WHAT DO WE LEARN FROM THE ABC?

HEINZ CLEMENT* for CELSIUS-WASA and WASA-at-COSY Collaborations

1.1 Introduction

The ABC effect, an intriguing low-mass enhancement in the $\pi\pi$ invariant mass spectrum, is known from inclusive measurements [1] of the production of an isoscalar pion pair in fusion reactions to light nuclei. Its nature has been a puzzle now for 50 years.

In an effort to solve this long-standing problem by exclusive and kinematically complete highstatistics experiments, we have measured the fusion reactions to d and 4 He with WASA at COSY [2]. These measurements cover the full energy region, where the ABC effect has been observed previously in inclusive reactions. They also complement the systematic measurements of nucleon-nucleon induced two-pion production [3, 4, 5, 6, 7, 8, 9, 10, 11, 12] carried out at CELSIUS-WASA.

1.2 Experimental Results

From the present data base covering all **pp** induced two-pion production channels – including the fusion processes $pp \to d\pi^+\pi^0$ to the deuteron and to quasi-bound $^2{\rm He}$ – we find that the t-channel Roper, $\Delta\Delta$ and $\Delta(1600)$ excitations are the dominant processes and sufficient for explaining all data for the two-pion production in **isovector** NN collisions.

The situation changes dramatically for the **isoscalar** NN channel. The most basic fusion reaction in this channel $pn \to d\pi^0\pi^0$ – measured as quasifree process in pd collisions – exhibits not only a pronounced ABC effect, *i.e.* a low-mass enhancement in the $\pi\pi$ invariant mass spectrum, but in correlation with it also a sharp Lorentzian-shaped structure in the total cross section (Fig. 1). Its peak energy is about 80 MeV below the nominal $\Delta\Delta$ threshold of 2 m_{Δ} and its width of only 70 MeV is much less than the width of $2\Gamma_{\Delta}\approx 230$ MeV expected from the conventional t-channel $\Delta\Delta$ process. At the same time the peak cross section is about five times larger than that of the t-channel $\Delta\Delta$ process.

The Dalitz plots of the data exhibit at all energies within this Lorentzian-shaped structure the ABC effect, *i.e.* the low-mass enhancement in $M_{\pi\pi}$, but simultaneously also the excitation of the $\Delta\Delta$ system, though this excitation is below the nominal $\Delta\Delta$ threshold of 2 m_{Δ} . At energies above the Lorentzian-shaped structure the Dalitz plot changes to what is expected from the conventional t-channel $\Delta\Delta$ process.

From the angular distributions we tentatively assign the quantum numbers $I(J^P) = 0(3^+)$ to this structure in the total cross section. At present no conventional process is known, which could at least qualitatively explain this phenomenon. We note, however, that quark-model calculations, notably those of Ref. [16] predict a state with exactly these quantum numbers at about this mass. However, the estimated width is too large by far.

In a second experiment at COSY we have measured the double pionic fusion to ${}^{4}\text{He}$ over the full energy region of the ABC effect by use of the reaction $dd \rightarrow {}^{4}\text{He}\pi^{0}\pi^{0}$ in the range $T_{d} = 0.8$ - 1.4 GeV [15].

Our findings for the double-pionic fusion to $^4{\rm He}$ are in accordance with the observations for the basic $pn \to d\pi^0\pi^0$ reaction pointing to the same fundamental mechanism. In both reactions we observe the ABC effect to be correlated with a peak in the energy dependence of the total cross section exhibiting a peak cross section about 90 MeV below the mass of $2m_\Delta$ and a width, which is several times smaller than that of the conventional $\Delta\Delta$ process. If attributed to a resonance in pn and $\Delta\Delta$ systems, then it apparently is robust enough to survive even in nuclei. In the $^4{\rm He}$ case the peak structure in the total cross section is considerably broader than in the deuteron case. This is consistent with both Fermi motion of the basic pn system and collision broadening - as is well-known, e.g. from excitations of the Δ resonance in nuclei.

^{*}Physikalisches Institut, University of Tübingen, Germany; clement@pit.physik.uni-tuebingen.de

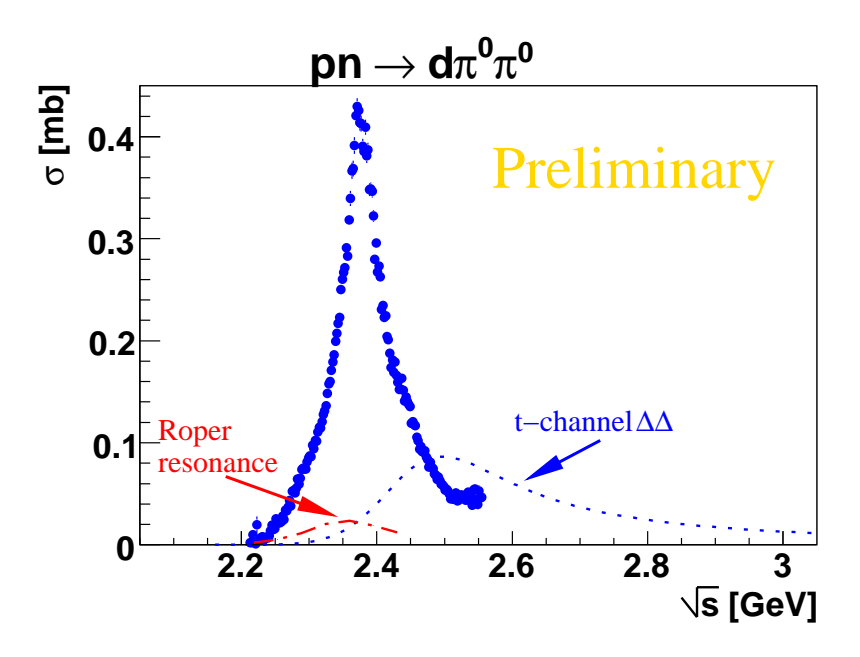


Figure 1.1: Preliminary results [13, 14] from WASA-at-COSY for the total cross section of the $pn \to d\pi^0\pi^0$ reaction in comparison to the **conventional** contributions originating from the excitation of the Roper resonance and of the $\Delta\Delta$ system (t-channel process).

1.3 Acknowledgments

We acknowledge valuable discussions with E. Oset, A. Sibirtsev and C. Wilkin on this issue. This work has been supported by BMBF (06TU9193), COSY-FFE (Forschungszentrum Jülich) and DFG (Europ. Graduiertenkolleg 683).

- [1] N. E. Booth, A. Abashian, K. M. Crowe, Phys. Rev. Lett. 7, 35 (1961); 6, 258 (1960)
- [2] H. H. Adam et al., arxiv: nucl-ex/0411038
- [3] T. Skorodko et al., submitted for publication; arxiv:1007.0405 [nucl-ex]
- [4] T. Skorodko et al., Phys. Lett. B 679, 30 (2009)
- [5] T. Skorodko et al., Eur. Phys. J. A 35, 317 (2008)
- [6] W. Brodowski et al., Phys. Rev. Lett. 88, 192301 (2002)
- [7] J. Pätzold et al., Phys. Rev. C 67, 052202(R) (2003)
- [8] J. Johanson et al., Nucl. Phys. A 712, 75 (2002)
- [9] M. Bashkanov et al., Phys. Rev. Lett. 102, 052301 (2009); arXiv: 0806.4942 [nucl-ex]
- [10] F. Kren et al., Phys. Lett. B 684, 110 (2010)
- [11] M. Bashkanov et al., Phys. Lett. B 637, 223 (2006); arXiv: nucl-ex/0508011
- [12] S. Keleta *et al.*, Nucl. Phys. **A 825**, 71 (2009)
- [13] M. Bashkanov et al., Proc. PANIC08, Elsevier 239 (2009); arXiv: 0906.2328 [nucl-ex]
- [14] M. Bashkanov et al., Proc. MESON10, Int. J. Mod. Phys., in press
- [15] A. Pricking et al., Proc. MESON10, Int. J. Mod. Phys., in press
- [16] J. L. Ping et al., Phys. Rev. C 79, 024001 (2009)

Interaction of η and η' with Nucleons and Nuclei including η bound states

USE OF $\pi^+d \to \eta pp$ TO STUDY THE ηN AMPLITUDE NEAR THRESHOLD

HUMBERTO GARCILAZO*AND M. T. PEÑA†

1.1 Introduction

The ηN scattering length $a_{\eta N}$ is not well known since it must be obtained indirectly from the combined analysis of $\pi N - \pi N$ and $\pi N - \gamma N$ together with the available differential and total cross sections data of $\pi N \to \eta N$. Although for the various analyses [1, 2, 3, 4, 5] the imaginary part of the ηN scattering length comes out quite stable at ~ 0.26 fm, basically as a consequence of the optical theorem, the values for Re $a_{\eta N}$ run from 0.4 to 1.07 fm. A recent approach [6] using the process $np \to \eta d$ with a three-body treatment of the final state concluded that $0.4 \le \text{Re } a_{\eta N} \le 0.6$ fm.

In this study we follow a suggestion by Fujioka and Itahashi [7] who pointed out that the process $\pi d \to \eta pp$ at incident pion momentum $p_{lab} = 903$ MeV/c ($T_{lab} = 776$ MeV) allows for the η and one of the protons to be at rest in the laboratoy frame and therefore the rescattering process $\eta p \to \eta p$ near threshold could give an important contribution to the cross section. The model of $\pi d \to \eta pp$ that we will use includes single- and double-scattering terms and it has been described in Refs. [8, 9]. The dominant diagram is the single-scattering term where the neutron in the deuteron undergoes the elementary process $\pi^+ n \to \eta p$ while the proton remains as spectator. The double-scattering term where a nucleon is exchanged which leads to the NN final-state-interaction (FSI) will not be considered here. This term is important only when the relative momentum of the two final nucleons is close to zero, i.e., when the η gets the maximum energy and the two nucleons recoil with equal momenta so that the NN relative momentum is zero [8]. In the kinematical region of the ηN FSI the η and one nucleon are left at rest while the other nucleon moves with maximal energy so that the NN relative momentum is very large.

1.2 Results

We calculated the differential cross section $d\sigma/d\Omega$ in the backward direction ($\theta=180^{\circ}$) without the ηN FSI as well as with three models of the ηN amplitude that have been proposed in the literature, namely, Re $a_{\eta N}=0.407$ fm [5], Re $a_{\eta N}=0.717$ fm [1], and Re $a_{\eta N}=1.07$ fm [3]. The results for the differential cross section using these four models are, respectively 0.67 μ b, 1.43 μ b, 2.65 μ b, and 4.33 μ b. Thus, in the backward direction the ηN FSI can increase the cross section by a factor of 6.5 for the model with Re $a_{\eta N}=1.07$ fm and by factors of 4 and 2 for the other two models.

As we have shown the ηN FSI can produce large effects in the $\pi d \to \eta pp$ cross section in the backward direction at $p_{lab} = 903 \; \mathrm{MeV/c}$. Therefore, a measurement of it will allow us to determine the ηN scattering length.

^{*}Escuela Superior de Física y Matemáticas, Instituto Politécnico Nacional, Edificio 9, 07738 México D.F., Mexico; email: humberto@esfm.ipn.mx

[†]Instituto Superior Técnico, Centro de Física Teórica de Partículas, and Department of Physics, Av. Rovisco Pais, 1049-001 Lisboa, Portugal; email: teresa.pena@ist.utl.pt

- M. Batinić, I. Šlaus, A. Švarc, and B. M. K. Nefkens, Phys. Rev. C 51, 2310 (1995); M. Batinić,
 I. Dadić, I. Šlaus, A. Švarc, B. M. K. Nefkens, and T.-S. H. Lee, Physica Scripta 58, 15 (1998).
- [2] A. M. Green and S. Wycech, Phys. Rev. C 55, R2167 (1997).
- [3] A. M. Green and S. Wycech, Phys. Rev. C 60, 035208 (1999).
- [4] A. Sibirtsev, S. Schneider, Ch. Elster, J. Haidenbauer, S. Krewald, and J. Speth, Phys. Rev. C 65, 044007 (2002).
- [5] A.M. Gasparian, J. Haidenbauer, C. Hanhart, Phys.Rev.C 68 045207,(2003).
- [6] H. Garcilazo and M. T. Peña, Eur. Phys. J. A. 38 209 (2008).
- [7] H. Fujioka and K. Itahashi, arXiv:1002.0201 [nucl-ex].
- $[8]\,$ H. Garcilazo and M. T. Peña, Phys. Rev. C ${\bf 59}$ 2389 (1999).
- [9] H. Garcilazo and M. T. Peña, Phys. Rev. C 62 011002 (2000).

SEARCH FOR η -MESIC NUCLEI AT J-PARC

HIROYUKI FUJIOKA*

1.1 Introduction

The J-PARC facility, whose construction was completed recently, supplies secondary particles by bombarding $30\,\mathrm{GeV^1}$ protons accelerated by the main ring onto a production target. Whereas strangeness nuclear physics with intense kaon beam is one of the main issues, experiments with pion beam are also possible.

Looking back at past experimental search for η -mesic nuclei, the (π^+, p) reaction was already investigated by Chrien et~al.~[1], who reported non-observation of any narrow peak from η -mesic nuclei. However, we consider the experimental conditions have room for improvement. The momentum transfer in their measurement was as large as $\sim 200\,\mathrm{MeV}$ because of finite scattering angle they adopted, which can be almost zero by choosing the proper beam momentum around the magic momentum and detecting scattered particles in very forward direction. Furthermore, the detection of the decay particles of η -mesic nuclei will improve the signal-to-noise ratio drastically, as demonstrated by recent observations by TAPS/MAMI [2] and COSY-GEM [3].

1.2 Search for η -mesic nuclei

1.2.1 (π, N) reaction on nuclei

Among already approved experiments at J-PARC, the E15 experiment aims to search for antikaonnuclear bound states, K^-pp , by use of the (K^-, n) reaction on ³He target [4]. Since its experimental principle can be applied to η -mesic nuclei search, the case when we will use its setup with a small modification after the experiment is discussed here. For details, please refer to Refs. [5, 6].

The E15 experiment will use the K1.8BR beamline, which can provide secondary particles with their momenta up to $1.1\,\mathrm{GeV}/c$. It should be noted that the magic momentum for the η -mesic nuclei with the (π,N) reaction on a heavy nucleus is around $0.7-1.0\,\mathrm{GeV}/c$, which depends on the binding energy of an η meson. In addition, the scattered neutron and proton² in forward direction (up to 6° degrees) can be detected by TOF counters. Therefore, the missing-mass spectroscopy for the (π^-, n) or (π^+, p) reaction can be performed there.

As for the coincidence measurements, the E15 experiment is preparing a Cylindrical Detector System to detect charged particles from a K^-pp system ($K^-pp \to p + \Lambda \to p + p + \pi^-$). An η -meson and an nucleon in an η -mesic nucleus couple strongly with the $N^*(1535)$ resonance, and the η -mesic nucleus can emit a back-to-back pair of proton and π^- in its decay. An exclusive measurement will be feasible by detecting these charged particles by the Cylindrical Detector System.

By the way, a theoretical study related with this experimental plan has been developed by Nagahiro et al. [8] They argue that a possible change of the property of in-medium $N^*(1535)$ resonances would affect η -nucleus interaction. In the chiral doublet model, which assumes the resonance as the chiral partner of the nucleon, their mass gap is expected to reduce as a function of nuclear density, while the mass of $N^*(1535)$ will not change largely according to the chiral unitary model.

1.2.2 Pilot experiment with deuteron target

Even after the coincidence of the decay particles, some of events which do not associate with an η meson will survive as a background, and it might be too huge to observe a peak structure from η -mesic nuclei production.

^{*}Kyoto University (fujoka@scphys.kyoto-u.ac.jp)

¹It will be upgraded to 50 GeV in near future.

²As well as the (K^-, n) reaction, the (K^-, p) reaction will be measured simultaneously in the E15 experiment [7].

In order to estimate the background level, a pilot experiment using deuteron target is under consideration. The signal corresponds to the following reaction:

$$\pi^+ + d \to p + p^*(1535) \to p + p + \eta.$$
 (1.1)

It should be emphasized that the final state of this reaction is the same as that of a quasi-free reaction $(\pi^+ + "n" \to p + \eta)$ with a proton spectator, but the former can be distinguished from the latter by detecting two protons fast enough $(\gtrsim 200\,\mathrm{MeV/c})$. The reaction (1.1) is a two-step process: $\pi^+ + "n" \to p + \eta$, followed by $\eta + "p" \to p^*(1535) \to p + \eta$. The rescattering in the second step can be seen as low-energy ηN scattering, which is difficult to investigate experimentally in a direct way.

It is interesting to compare the cross section of this reaction $(p+p+\eta)$ final state) with that of a different reaction with $p+p+\pi^0$ final state. Since not only $N^*(1535)$ but also other resonances $(N^*$ and $\Delta^*)$ can decay into $p+\pi^0$, this channel corresponds to "signal+background". If its cross section is much larger, it may be difficult to observe signals from η -mesic nuclei in a coincidence measurement. of the (π, N) reaction on finite nuclei.

1.2.3 $(p, {}^{3}\text{He})$ reaction

Inspired by the result by the COSY-GEM collaboration [3], an experimental plan to utilize the SKS spectrometer, constructed for hypernuclear spectroscopy, at the K1.8 beamline, and the ENSTAR detector for detection of decay particles. One of the candidate of the target could be lithium-6, which can be regarded as an α -d cluster, to produce the $^4\text{He} - \eta$ system.

- [1] R. E. Chrien et al., Phys. Rev. Lett. 60, 2595, (1988).
- [2] M. Pfeiffer et al., Phys. Rev. Lett. 92, 252001, (2004).
- [3] A. Budzanowski et al., Phys. Rev. C 79, 012201(R), (2009).
- [4] M. Iwasaki, T. Nagae *et al.*, J-PARC E15 proposal (2006). (http://j-parc.jp/NuclPart/pac_0606/pdf/p15-Iwasaki.pdf)
- [5] K. Itahashi, H. Fujioka, S. Hirenzaki, D. Jido, and H. Nagahiro, Letter of Intent for J-PARC (2007). (http://j-parc.jp/NuclPart/pac_0707/pdf/LoI-itahashi.pdf)
- [6] H. Fujioka, Acta Physica Polonica B 41, 2261, (2010).
- [7] H. Fujioka et al., J-PARC P28 proposal (2009).(http://j-parc.jp/NuclPart/pac_0907/pdf/Fujioka.pdf)
- [8] H. Nagahiro, D. Jido, and S. Hirenzaki, Phys. Rev. C 80, 025205, (2009).

SEARCH FOR η BOUND STATES IN NUCLEI

 $\begin{array}{c} HARTMUT\ MACHNER^*\\ for\ the\ COSY\text{-}GEM\ collaboration \end{array}$

1.1 Introduction

The existence of bound states between η mesons and nuclei via the strong interaction was predicted by Liu and coworkers [1]. Their finding that nuclei with mass number A>12 can bind was later extended to even lighter nuclei [2]. While there a a lot of theoretical predictions concerning the binding energy and the width of such a state, experimental evidence is scarce. Here we will concentrate on searches performed at COSY in Jülich, mainly by the GEM collaboration.

1.2 Recoil Free Production

It was shown in the study of hypernuclei and pionic atoms that recoil free meson production is essential to see a signal of the bound state. This means that in a transfer reaction a particle carries away all the beam momentum and the meson (or hyperon) is produced at rest. Then the meson wave function has maximal overlap with the nuclear wave function. This condition was not obeyed in previous searches. The $(d,^3\text{He})$ reaction transfers only one nucleon and has large cross section. On the contrary the cross section for deuteron break up is large and the break-up protons habe the same magnetic rigidity as the ^3He ions, thus making the identification of a state almost impossible. We, therefore, choose the $(p,^3\text{He})$ reaction. Although the cross section for the two nucleon transfer reaction is small, the background is much, much smaller than in the previous case. In summary we searched for the bound state in a two step process:

$$p + ^{27} Al \rightarrow^{3} He + X \tag{1.1}$$

$$X \to \pi^- + p + Y. \tag{1.2}$$

Suppose $X = \eta \bigotimes^{25} \text{Mg}$. Then the chain $\eta + N \rightleftharpoons N^*(1535) \to \pi + N$ will occur. This is the elementary process of step (1.2). The $(d,^3\text{He})$ ions were detected at forward angles by the magnetic spectrograph Big Karl [3] while the proton and pion were detected by the detector ENSTAR [4]. The details of the measurements were given in [5]. The data are shown in Fig. 1.1 as cross sections in the laboratory system. A peak was found with

$$BE + i\sigma = (-13.13 \pm 1.64) + i(4.35 \pm 1.27) \text{ MeV}.$$
 (1.3)

Its significance is 5σ . The rather small width was attributed by Haider and Liu [6] due to an interference between the resonant and the non-resonant process leading to the same final state. Another possibility might be that the peak is not the 1s state but the 1p state. Then the 1s state is deeper bound. A fit with two Gaussians and phase space behavior for the unbound part is also shown in Fig. 1.1. Of course only the narrow peak is statistical significant.

1.2.1 Search in Two Body Final States

The usual approach is to factorize the s-wave reaction amplitude, f_s , near threshold in the form

$$f_s = \frac{f_B}{\frac{1}{a} + \frac{r_0}{2}p^2 - ip} \tag{1.4}$$

where p is the η c.m. momentum, a the complex scattering length and r_0 the effective range. The unperturbed production amplitude f_B is assumed to be slowly varying and is often taken to be constant in the near-threshold region.

^{*}Fachbereich Physik, Universität Duisburg-Essen, Duisburg, Germany, h.machner@fz-juelich.de

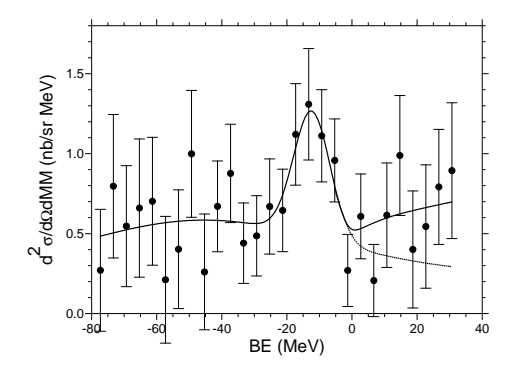
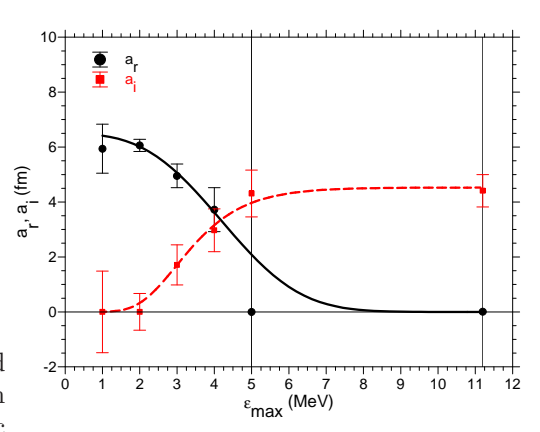


Figure 1.1: Missing mass spectrum converted to binding energy BE of a bound system $^{25}Mg \otimes \eta$ as measured with the magnetic spectrograph. All cuts and background sub- Figure 1.2: Real and imaginary part of the sians and a phase space behavior for the un- of the energy bin width. bound system. Dotted curve: same as solid curve but without phase space contribution.



traction have been applied. The solid curve is scattering length for the η^3 He interaction as a fit with a constant background, two Gaus- deduced from the data of ref. [10] as function

Unitarity demands that the imaginary part of the scattering length be positive, i.e., $a_i > 0$. In addition, to have binding, there must be a pole in the negative energy half-plane, which requires that[8]

$$|a_i|/|a_r| < 1. (1.5)$$

Finally, in order that the pole lie on the bound-rather than the virtual-state plane, one needs also $a_r < 0$. In a recent experiment [7] the $dd \to \eta \alpha$ reaction was studied employing a tensor polarized beam. Therefore, the s-wave amplitude could be extracted. From these results, assuming $r_0 = 0$ in Eq. 1.4, a scattering length could be deduced

$$a_{^4He\eta} = [\pm (3.1 \pm 0.5) + i \cdot (0.0 \pm 0.5)] \text{ fm}.$$
 (1.6)

yielding a pole position

$$|Q_{^4He\eta}| \approx 4 \text{MeV}.$$
 (1.7)

We now want to compare this result with the scattering length for the $pd \to \eta^3$ He reaction. Although there are high precise data close to threshold [9], [10] their results differ to to different analysis methods. In addition both experiments found a s-p interference close to threshold. Therefore, we have reanalyzed the data from [10] applying the same formalism as in the $dd \to \eta \alpha$ case. In order to study where the onset of the interference starts the analysis is performed by truncating the data above ϵ_{max} . The results are shown in Fig. 1.2. For $\epsilon_{max} > 2$ MeV the real part starts to decrease while the imaginary part stars to increase. Therefore, we stick to the range below and have

$$a_{3He\eta} = \left[\pm (6.06 \pm 0.22) + i \cdot (0.0 \pm 0.7) \right] \text{ fm}$$
 (1.8)

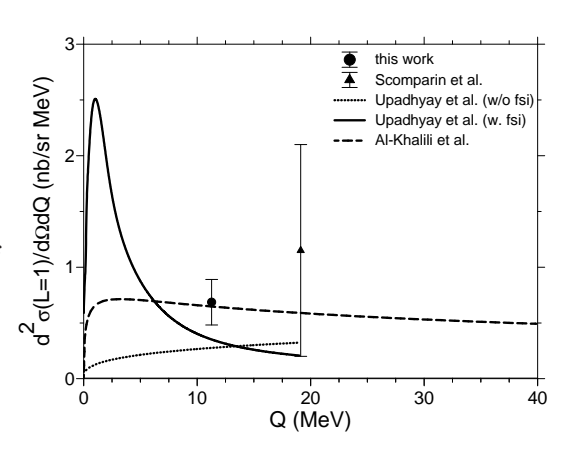
quite similar to the $dd \to \eta \alpha$ case. This gives

$$|Q_{^3Hen}| \approx 1 \text{MeV}.$$
 (1.9)

These above-threshold data are, of course, insensitive to the sign of a_r so that they could never tell whether the system is quasi-bound or virtual. Since $|Q_{^3He\eta}| < |Q_{^4He\eta}|$ indicates that $^3\text{He}\eta$ is indeed quasi-bound.

GEM has the extended the study to heavier systems. In the $p^6 \text{Li} \rightarrow \eta^7 \text{Be}$ reaction the recoiling Be was measured at 11.3 MeV above threshold [11]. A differential cross section of $\frac{d\sigma}{d\Omega} = (0.69 \pm$ $0.20(\text{ stat.}) \pm 0.20(\text{ syst.}))$ nb/sr for the ground state plus the $1/2^-$ was measured. Assuming isotropic emission yield a total cross section shown in Fig. 1.3 and compared with a previous measurement and two model calculations. The quality of the data is not sufficient to extract a scattering length. More measurements closer to threshold are necessary.

Figure 1.3: Excitation function of the reaction $p + ^6$ Li $\rightarrow \eta + ^7$ Be with Be in its ground state and first excited state. The data are the GEM measurement [11] (full dot) and the for these states corrected result from [12] (triangle). The calculations based on the model of [13] are shown as dashed curve. Those performed by [14] for the total cross section were divided by 4π . The calculation with a strong fsi is shown as solid curve while the one without fsi is shown as dotted curve.



- Q. Haider and L. C. Liu, Phys. Lett. B 172, 257 (1986); R. S. Bhalerao and L. C. Liu, Phys. Rev. Lett. 54, 865 (1985).
- [2] S. A. Rakityansky, S. A. Sofianos, M. Braun, V. B. Belyaev, and W. Sandhas, Phys. Rev. 53 R2043 (1996); S. Wycech, A. M. Green and J. A. Niskanen, Phys. Rev. C 52 544 (1995).
- [3] M. Drochner et al., Nucl. Phys. A 643, 55 (1998).
- [4] M.G. Betigeri et al., Nucl. Instr. Methods in Phys. Research A 578, 198 (2007).
- [5] A. Budzanowski et al. (COSY-GEM Collaboration), Phys. Rev. C 79, 061001(R) (2009).
- [6] Q. Haider and L. C. Liu, Acta Phys. Polon. B41, 2231 (2010).
- [7] A. Budzanowski et al. (The GEM Collaboration), Nucl. Phys. A 821, 193 (2009).
- [8] Q. Haider, L. C. Liu Phys. Rev., C 66, 045208 (2002).
- [9] J. Smyrski et al., Phys. Lett. B 649, 258 (2007), arXiv:nucl-ex/0702043.
- [10] T. Mersmann et al., Phys. Rev. Lett. 98, 242301 (2007).
- [11] A. Budzanowski et al. (The GEM Collaboration), accepted by Phys. Rev. C as rapid communication.
- [12] E. Scomparin et al., J. Phys. G 19, L51 (1993).
- [13] J. S. Al-Khalili, M. B. Barbaro, and C. Wilkin, J. Phys. G 19, 403 (1993).
- [14] N. J. Upadhyay, N. G. Kelkar, and B. K. Jain, Nucl. Phys. A 824, 70 (2009).

SEARCH FOR η -MESIC 4 He WITH WASA-AT-COSY

 $WOJCIECH\ KRZEMIE\'N\ ^*$ on behalf of the WASA-at-COSY Collaboration

1.1 Introduction

Recently, the progress in the spectroscopy of pionic and kaonic atoms, as well as pionic and kaonic nuclei has permitted to obtain deeper insights on the meson-nucleus interaction and the in-medium behaviour of spontaneous chiral symmetry breaking [1].

Analogically to the other exotic nuclear systems, the investigation of the η -mesic nuclei would provide many interesting informations about the η -N interaction, N* in-medium properties [2] and would deepen our knowledge of the fundamental structure of η meson [3]. The η meson is electrically neutral, therefore such a system can be formed only via the strong interaction which distinguishes it qualitatively from pionic atoms where the binding is the effect of the sum of the attractive electromagnetic force and the repulsive strong interaction.

The search of the η - mesic nucleus was performed in many experiments in the past [4, 5, 6, 7, 8, 9] and is being continued at COSY [10], JINR [6], J-PARC [11] and MAMI [9]. Many promising indications where reported, however, so far there is no direct experimental confirmation of the existence of mesic nucleus. In the region of the light nuclei systems such as η -He or η -T, the observation of the strong enhancement in the total cross-section and the phase variation in the close-to-threshold region provided strong evidence to the hypothesis of the existence of a pole in the scattering matrix which can correspond to the bound state [12]. However, as it was stated by Liu [13], the theoretical predictions of width and binding energy of the η -mesic nuclei is strongly dependent on the not well known subtreshold η -nucleon interaction. Therefore, the direct measurements which could confirm the existence of the bound state, are mandatory.

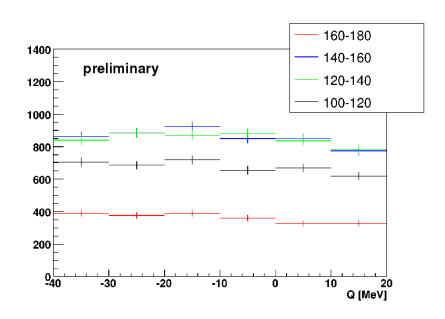
1.2 Experiment

In June 2008 we performed a search for the $^4{\rm He}-\eta$ bound state by measuring the excitation function of the $dd\to^3{\rm He}p\pi^-$ reaction near the eta production threshold using the WASA-at-COSY detector. During the experimental run the momentum of the deuteron beam was varied continuously within each acceleration cycle from 2.185 GeV/c to 2.400 GeV/c, crossing the kinematic threshold for the η production in the $dd\to^4{\rm He}\,\eta$ reaction at 2.336 GeV/c. This range of beam momenta corresponds to the variation of $^4{\rm He}-\eta$ excess energy from -51.4 MeV to 22 MeV. The experimental method is based on measuring the excitation function for chosen decay channels of the $^4{\rm He}-\eta$ system and a search for a resonance-like structure below the $^4{\rm He}-\eta$ threshold. The relative angle between the outgoing $p-\pi^-$ pair which originates from the decay of the N*(1535) resonance created via absorption of the η meson on a nucleon in the $^4{\rm He}$ nucleus, is 180° in the N* reference frame and is smeared by about 30° in the center-of-mass frame due to the Fermi motion of the nucleons inside the $^4{\rm He}$ nucleus. The center-of-mass kinetic energies of the p and π^- originate from the mass difference $m_\eta-m_\pi$ and are around 50 MeV and 350 MeV, respectively.

The Figure 1.1 presents the preliminary excitation function in 20 degrees intervals in $\Theta_{cm}(p-\pi)$ angle.

The figure indicates no structure in the angular range close to the 180 degree where the signal is expected. The ratio of excitation functions from various angular ranges is also constant as indicated in the right panel of Fig. 1.1. Therefore, taking into account the luminosity and the detector acceptance we preliminary estimated that an upper limit for the η -mesic production via the $dd \to (\eta^4 {\rm He})_{b.s.} \to {}^3{\rm He}\,p\,\pi^-$ reaction is equal to about 20 nb on a one σ level.

^{*}wojciech.krzemien@if.uj.edu.pl, Institute of Physics, Jagiellonian University, Cracow, Poland.



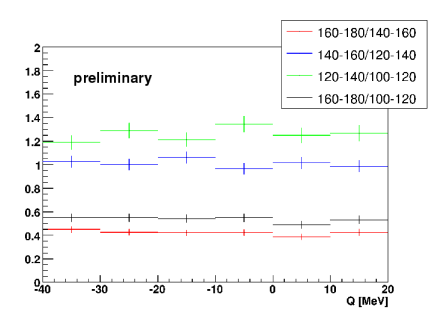


Figure 1.1: (left) Excitation function for the $dd \to {}^3{\rm He}p\pi$ reaction measured in the 20 degrees intervals of the $\Theta_{cm}(p-\pi)$ angle. (Right) Ratio of excitation functions angular ranges as indicated in the figure.

1.3 Outlook

The research program of η -mesic He with WASA-at-COSY will be continued. A two-week measurement with WASA-at-COSY for the $dd \to {}^3{\rm He}p\pi^-$ channel is scheduled for November 2010. After two weeks of measurement with a luminosity of $4 \cdot 10^{30}~{\rm cm}^{-2}~{\rm s}^{-1}$, we expect a statistical sensitivity of a few nb (σ) . A non-observation of this signal would significantly lower the upper limit for the existence of the bound state.

- [1] S. Hirenzaki, Prog. Theor. Phys. Suppl. 168, 458-465 (2007).
- [2] D. Jido, H. Nagahiro, S. Hirenzaki, Phys. Rev. C66, 045202 (2002).
- [3] S. D. Bass, A. W. Thomas, Acta. Phys. Pol. B 41, (2010), 2239.
- [4] B. J. Lieb et al., Proc. Int. Nucl. Phys. Conf., Sao Paulo, Brazil (1989).
- [5] G. A. Sokol et al., arXiv:nucl-ex/9905006 (1999)
- [6] M. Kh. Anikina et al., arXiv:nucl-ex/0412036 (2004).
- [7] A. Gillitzer, Acta Phys. Slovaca 56, 269 (2006).
- [8] A. Budzanowski et al., Phys. Rev. C79, 061001(R) (2009).
- [9] B. Krusche, F. Pheron, Y. Magrbhi Acta. Phys. Pol. B 41, (2010), 2249.
- [10] P. Moskal, J. Smyrski, Acta. Phys. Pol. B 41, (2010), 2281.
- [11] H. Fujioka, K. Itahashi, Acta. Phys. Pol. B 41, (2010), 2261.
- [12] C. Wilkin Acta. Phys. Pol. B 41, (2010), 2191.
- [13] Q. Haider, L.C. Liu, Phys. Rev. C66, 045208 (2002).

List of Participants

Name	Affiliation	Contribution
Adlarson, Patrick	Uppsala University	Page 17
Bashkanov, Mikhail	University Tuebingen	
Berlowski, Marcin	Soltan Institute Nuclear Studies	
Bijnens, Johan	Lund University	
Chatterjee, Banhi	Forschungszentrum Juelich	
Clement, Heinz	Physikalisches Institut, Univ. Tuebingen	Page 59
Coderre, Daniel	Forschungszentrum Juelich	
Colangelo, Gilberto	University of Bern	Page 14
Czerwinski, Eryk	Jagiellonian University Cracow	Page 46
Denig, Achim	University Mainz	Page 25
Ditsche, Christoph	HISKP, Bonn University	
Escribano, Rafel	Universitat Autònoma Barcelona	
Fransson, Kjell	Uppsala University	
Froehlich, Ingo	Goethe University Frankfurt	
Fujioka, Hiroyuki	Kyoto University	Page 65
Garcilazo, Humberto	Instituto Politecnico Nacional	Page 63
Gauzzi, Paolo	Sapienza Universitá di Roma / INFN	
Giovannella, Simona	INFN Frascati	Page 5
Goldenbaum, Frank	Forschungszentrum Juelich	
Hodana, Malgorzata	Jagiellonian University Cracow	
Höistad, Bo	Uppsala University	
Jany, Anna	Jagiellonian University Cracow	
Jany, Benedykt	Jagiellonian University Cracow	
Kampf, Karol	Lund University	Page 11
Klaja, Joanna	Forschungszentrum Juelich	Page 27
Klaja, Pawel	Forschungszentrum Juelich	Page 44
Krusche, Bernd	University of Basel	Page 37
Krzemien, Wojciech	Jagiellonian University Cracow	Page 70
Kubis, Bastian	HISKP, Bonn University	Page 20
Lanz, Stefan	Bern University	Page 15
Leupold, Stefan	Uppsala University	Page 22
Machner, Hartmut	Forschungszentrum Juelich	Page 67
Masjuan, Pere	University Vienna	Page 9
Nakayama, Kanzo	University of Georgia	Page 48
Ostrick, Michael	University Mainz	
Passeri, Antonio	INFN Roma	presentation only
Peña, Teresa	Instituto Superior Técnico	D 00
Petri, Thimo	Forschungszentrum Juelich	Page 29
Pricking, Annette	Physikalisches Institut, Univ. Tuebingen	D **
Ramalho, Gilberto	Instituto Superior Técnico	Page 57
Ramstein, Beatrice	Institut de Physique Nucleaire d Orsay	Page 42
Redmer, Christoph	Uppsala University Dhysikaliashas Institut, Univ. Tushingan	Page 31
Rio, Elena Perez del	Physikalisches Institut, Univ. Tuebingen	
Roy, Ankhi	Indian Institute of Technology Indore	
Schadmand, Susan Schneider, Sebastian	Forschungszentrum Juelich HISKP, Bonn University	Page 12
Schönning, Karin	Uppsala University	~
<u> </u>	University of California	Page 50
Starostin, Aleksandr Stepaniak, Joanna	Soltan Institute Nuclear Studies	Page 8
Taccini, Cecilia	INFN Roma	Page 55
Tengblad, Ulla	Uppsala University	1 age 00
Tolba, Tamer	Forschungszentrum Juelich	Page 52
Unverzagt, Marc	University of Mainz	Page 40
Wilkin, Colin	University College London	Page 35
Wirzba, Andreas	Forschungszentrum Juelich	150 00
Wurm, Patrick	Forschungszentrum Juelich	
Zdráhal, Martin	Charles University Prague	
24141141, 1114111111	- Indian officially i insuc	<u> </u>